LBL-136
c.2

VAPORIZATION KINETICS OF MAGNESIUM NITRIDE

Roy Tom Coyle
(Ph.D. Thesis)

January 1972

AEC Contract No. W-7405-eng-48

LBL-136
c.2

DISCLAIMER

VAPORIZATION KINETICS OF MAGNESIUM NITRIDE

Contents

VAPORIZATION KINETICS OF MAGNESIUM NITRIDE

Roy Tom Coyle

Inorganic Materials Research Division, Lawrence Berkeley Laboratory and Department of Materials Science and Engineering, College of Engineering; University of California, Berkeley, California

ABSTRACT

The vaporization of magnesium nitride in a torsion-effusion apparatus in the range 1050K to 1300K has revealed several unusual features, which are explained in this work. The Knudsen pressure was measured as a function of time, temperature, orifice area, sample size, and specific surface area of powder; Langmuir pressures were measured and the surface studied microscopically. The Knudsen pressure versus time experiments showed three stages: (1) the pressure rises to a maximum due to the rupturing of a magnesium oxide protective film; (2) the pressure decreases according to a logrithmic law $1/P_K = k_1 + k_2 \log t$; and (3) the pressure drops more rapidly than predicted by the logrithmic law after 70% vaporization because of a reduction in the specific surface area of the sample.

The vaporization behavior observed in most of the experiments was due to the processes occurring in the logrithmic stage. A diffusion barrier of magnesium oxide that reforms after the first stage of vaporization or some barrier intrinsic to the nitride is thought to be the cause of this stage. The activation energy for growth of the layer and for diffusion through it was 37.5 kcal/mole of vapor.

The Motzfeldt-Whitman technique for finding equilibrium pressures from nonequilibrium data was found to fail because the product of the evaporation coefficient and the effective vaporization area in the Motzfeldt-Whitman equation varied with orifice area. Apparent equilibrium

pressures lower by a factor of 170 than true equilibrium were observed because of the diffusion barrier on the surface of the particles. The temperature dependency of the apparent vapor pressures gave an enthalpy of vaporization, 354 kcal/mole that was much greater than the equilibrium value, 210 kcal/mole. This was explained by the activation energy for diffusion and the temperature dependency of the layer thickness. The equilibrium pressure was determined from an inflection point in the pressure versus time curve when the Knudsen cell was cooled from a high temperature, from the maximum in the pressure versus time curve for a cell with a 0.15 mm diameter orifice, from a Motzfeldt-Whitman extrapolation at constant weight loss of nitride, and from pressure versus temperature measurements using a 0.15 mm diameter orifice. The equilibrium vapor pressure was found to be higher than calculated from enthalpies and entropies for the reactants and products in the vaporization reaction. A new estimate was made for the entropy at 298K of magnesium nitride, 17.5 eu, as against previous estimates of 21 and 22.4 eu.

I. INTRODUCTION

Studies of the vaporization of magnesium nitride have revealed unusual behavior. Several workers[1-3] have measured the vapor pressure (the total pressure above the solid) for the reaction

$$Mg_3N_2(s) \longrightarrow 3Mg(g) + N_2(g) \qquad (1)$$

by a method that was expected to yield equilibrium values[2,3] and have found it to be markedly lower than pressures calculated from independent thermochemical data (see Fig. 1). An examination of the data on which the calculated pressures are based and a review of the vapor pressure measurements will be helpful in fully appreciating this discrepancy.

The calculated vapor pressure is obtained from the enthalpy and entropy of formation at 298K for the reactant and products in Eq. (1) and their high temperature heat capacity data. Table 1 shows the results of of several measurements of the enthalpy of formation of magnesium nitride. The values found by Lebedev and Nefedova[4] and by Mitchell[5] are in good agreement even though they were obtained by very different methods and the values by Neuman, et al.,[6] Brenner,[7] and Neuman, et al.[8] show good support for these. The early data of Matignon[9] and of Moser and Herzner[10] appear to be in error. A value of 110.2 can be accepted as a weighted average that is probably in error by no more than 1 kcal/mole.

Mitchell[5] reported heat capacity data for the nitride in the range 462K to 1273K. This combined with Satoh's[12] data in the range 273K to 691K gives good data at high temperatures, however the low temperature measurements needed for establishing the entropy at 298K have not been made. Mitchell[5] has estimated this entropy to be 22.4 eu by using a

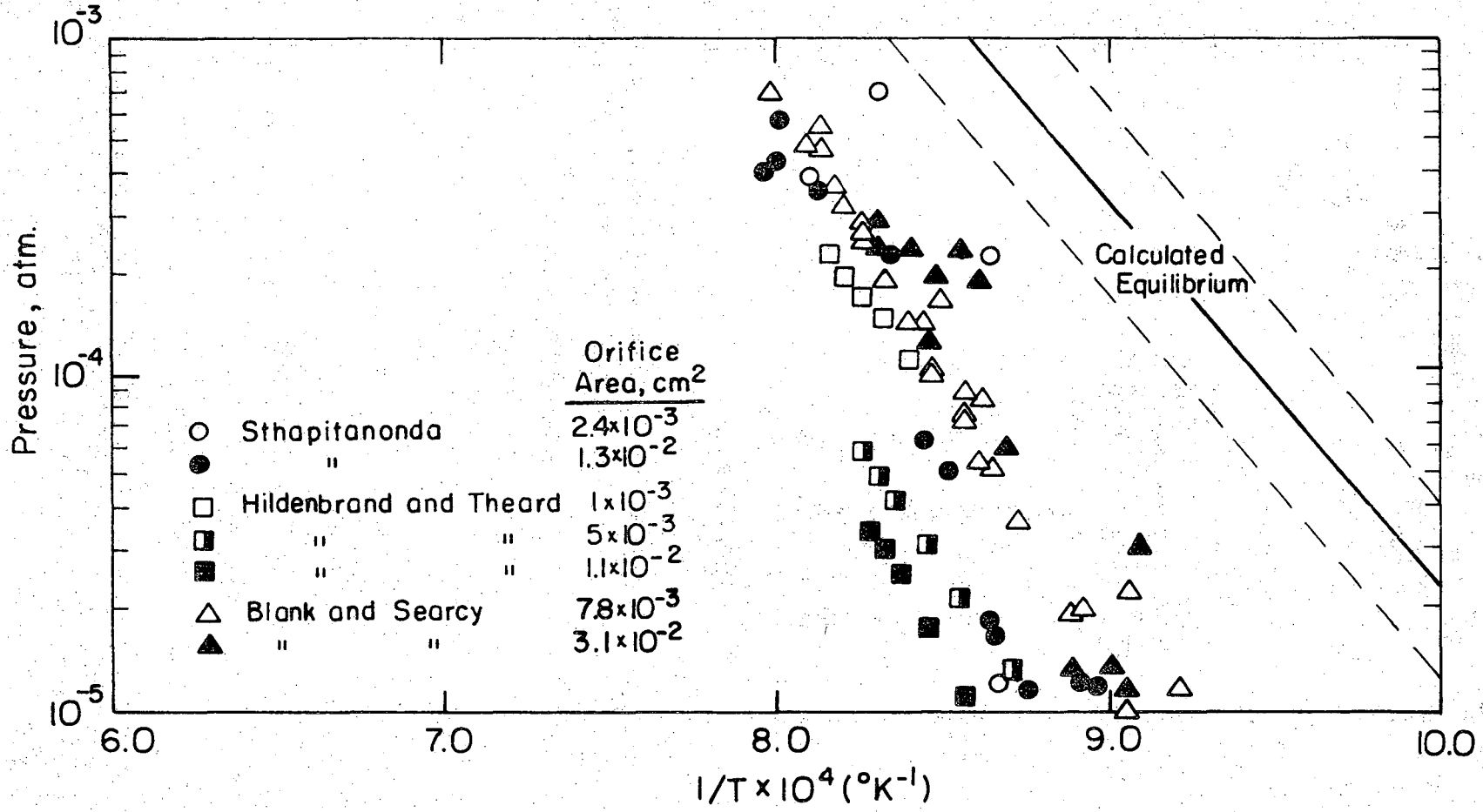

XBL 719-7250

Fig. 1 Knudsen effusion vapor pressures measured for magnesium nitride.

Table I. Enthalpy of formation of magnesium nitride.

Worker	Method	ΔH° 298 Kcal/mole
Lebedev and Nefedova[4]	Bomb (PbN_6 + Mg)	-110.7
Mitchell[5]	Solution (H Cl)	-110.2
Neuman, et al.[6]	Solution (H Cl)	-112*
Brunner[7]	Solution (H_2O)	-109*
Neuman, et al.[8]	Bomb (Mg + N_2)	-116*
Matignon[9]	Solution (H_2SO_4)	-137*
Moser and Herzner[10]	Solution (H_2SO_4)	-127*

*These are corrected with more accurate supplementary data by Bichowski.[11]

modified form of Latimer's rule for estimating the entropy of oxides; the reliability of this value is almost certainly better than ±5 eu.

The data for elemental magnesium are well established. Hultgren, et al.[13] have selected 35.0 ± 0.3 kcal/mole for the enthalpy of vaporization and 35.50 eu for the entropy of vaporization, both at 298K, and have also selected heat capacity values for the vapor. Heat capacity and entropy data for N_2 are provided by Stull and Sinke.[14]

Figure 1 shows the vapor pressure above magnesium nitride that is calculated from these data. The dashed lines shown in the figure allow ±5 eu for the uncertainty in the entropy of formation of the nitride. That the true vapor pressure of magnesium nitride is included within these boundaries is virtually certain.

The results of several vapor pressure studies on magnesium nitride are shown in Figs. 1 and 2. Figure 1 shows measurements made by Knudsen effusion techniques while Fig. 2 shows measurements made by the transpiration technique and includes some of the Knudsen data for comparison. Sthapitanonda[1] measured vapor pressures by both methods, and examined the vapors over the compound spectroscopically at temperatures in the range 1573K to 1673K. He detected $Mg_2(g)$ and presented data that indicate a very low $Mg_2(g)/Mg(g)$ ratio (0.001) above the nitride at 1600K with the ratio decreasing at lower temperatures, thus showing that the dimer is of little importance in the products of vaporization. He attributed his relatively high transpiration results to the reaction of small amounts of oxygen in the nitrogen flow gas with Mg(g) and explained the low

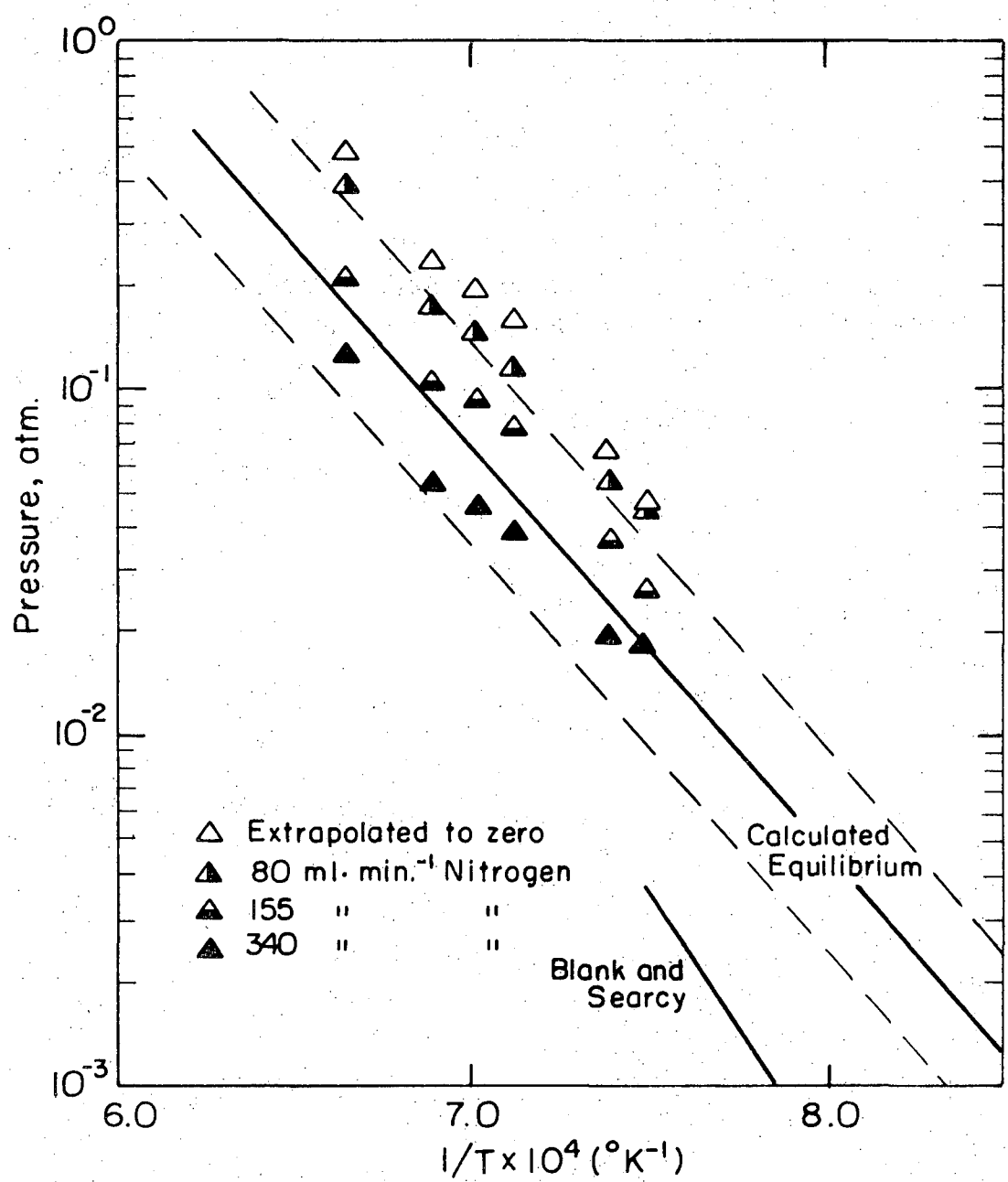

Fig. 2 Vapor pressures measured for magnesium nitride by the transpiration technique.

Knudsen values by suggesting that the evaporation coefficient* is low.

Hildenbrand and Theard[2] employed the torsion effusion technique with three different orifice sizes to measure vapor pressures; they used magnesium nitride that they analysed to be better than 99% pure. Their results show a marked dependency on orifice area which led them to use a simplified form of the Motzfeldt-Whitman equation,[22,23]

$$P_E = P_K\left(1 + \frac{W_B B}{\alpha A'}\right) \quad , \tag{2}$$

to obtain equilibrium pressures from their data; where P_E is the equilibrium pressure, P_K is the measured pressure, W_B is the orifice Clausing factor,[24-26] B is the effusion cell orifice area, α is the evaporation coefficient, and A' is the effective sample surface area.[21] Equation (2) assumes that the evaporation coefficient and effective sample areas are independent of orifice area and predicts that extrapolations of plots of measured pressures against orifice area to zero area yield the equilibrium vapor pressure. Hildenbrand and Theard calculated apparent equilibrium pressures in rough agreement with Sthapitanonda's[1] large orifice data and calculated an upper limit to the evaporation coefficient of 5×10^{-3}. The equilibrium pressures obtained in this way are lower by more than a factor of ten than pressures calculated from the thermochemical data discussed above and show a markedly different temperature dependence. Pressures obtained by extrapolation of Eq. (2) have usually agreed with

---

*The evaporation coefficient in vacuo is the ratio of the measured flux in Langmuir vaporization[15-17] to the flux that could strike the surface in the equilibrium vapor and is calculated by using the Hertz-Langmuir-Knudsen equation.[15-20] It is usually assumed that the evaporation coefficient is independent of the vapor pressure above the vaporizing material[21] and that it is equal to the condensation coefficient.

pressures calculated from reliable thermochemical data to within a factor of 3 and have shown temperature dependencies close to those from the thermochemical calculation.

Hildenbrand and Theard concluded that either the heat of formation of $Mg_3N_2(s)$ is in error, or the rate of vaporization is limited by a secondary process which leads to false apparent equilibrium pressures when Eq. (2) is applied. They favored the second explanation, largely because thermodynamic quantities calculated from their data were inconsistent with apparently reliable values calculated from the independent thermochemical data. They noted that Kay and Gregory[27] have reported that Eq. (2) used with effusion data for the reaction $Mg(OH)_2(s) = MgO(s) + H_2O(g)$ yields apparent equilibrium pressures far lower than the known equilibrium pressure.

Blank and Searcy[3] have made a torsion-effusion and a torsion-Langmuir[15-17,28] study of magnesium nitride using two orifice sizes; they observed no significant orifice area dependence, but their measured pressures were in good agreement with the extrapolated pressures of Hildenbrand and Theard. The range of evaporation coefficients, 2×10^{-2}, at 1000K to 3×10^{-3} at 1250K, calculated by Blank and Searcy from the ratio of their Langmuir (free surface) pressures to their Knudsen pressures has an average near the value which Hildenbrand and Theard calculated by means of Eq. (2). Blank and Searcy express doubt, however, on the basis of the independent thermochemical data, that equilibrium pressures and valid evaporation coefficients had been measured in their work; placing particular stress on the observation that the apparent entropy calculated

for Eq. (1) from the effusion data differs by 54 eu from the expected value.

Blank and Searcy also observed that when the background pressure of the system was raised by as much as a factor of 10 over the normal background pressure of about 10^{-8} atm by introduction of either nitrogen or argon there was no measurable effect on the rate of evaporation of magnesium nitride Langmuir samples. At higher pressures, however, the introduction of either argon or nitrogen reduced sublimation rates markedly; nitrogen appeared to have a slightly greater retarding effect than argon on the evaporation. The fractional reduction in pressure that resulted from a given pressure of either gas increased with increasing temperature. They concluded that the rate of free surface sublimation is probably limited by the adsorption of gas molecules on surface sublimation sites. Also, since argon had nearly an marked as effect as nitrogen on the sublimation rate, and since argon would not be expected to strongly adsorb at the temperatures of the study, they concluded that water or oxygen impurities are probably the main adsorbing species.

Another aspect of the behavior of magnesium nitride is illustrated in Table II where it is seen that for the effusion and free surface data there is a large difference between second law* and third law** values of the enthalpy of sublimation. This is not unusual for Langmuir experiments but is rare in Knudsen effusion experiments.

---

*The second law method[29] of calculating the enthalpy of vaporization uses the van't Hoff equation;[30] it involves the determination of the slope of a plot of the logarithm of the pressure versus the reciprocal of the temperature.

**The third law method[30] uses free energy functions, which are determined by using the third law of thermodynamics, to calculate an enthalpy of vaporization for each pressure measurement.

Table II. Comparison of second and third law enthalpies of vaporization for magnesium nitride.

Worker	Container	Orifice Area Cm^2	Average Third Law ΔH° 298 Kcal/mole	Second Law ΔH° 298 Kcal/mole
Equilibrium, Calculated	--	--	215	
Sthapitanonda				
Transpiration	Porcelain	--	206	224
Effusion	MgO	2.30×10^{-3}	229	(only 2 points)
Effusion	MgO	1.26×10^{-2}	246	343
Hildenbrand and Theard				
Effusion	Graphite	1×10^{-3}*	244	309
Blank and Searcy				
Effusion	Graphite	7.9×10^{-3}	245	296
Free Surface	Graphite	--	290	219

*These data were extrapolated using the Motzfeldt-Whitman equation and this was the smallest orifice used.

Sthapitanonda's suggestion that a low evaporation coefficient, α, is responsible for the discrepancy between pressures measured by effusion methods and pressures calculated from thermochemical or transpiration data can be checked by using Eq. (2) to estimate a value for α. Assuming one gram of nitride in an effusion cell with a surface area of 1×10^{4} cm^2/gm, an orifice area of 1×10^{-3} cm^2/gm, using P_E/P_K equal to 10, and assuming W is equal to 1 gives $\alpha = 10^{-8}$. This compares with Hildenbrand and Theards' $\alpha = 5 \times 10^{-3}$ from their orifice area dependence and with Blank and Searcy's $\alpha = 10^{-3}$ from the difference between free surface and thermochemical data. This shows a discrepancy in α of five orders of magnitude which is an unexpected variation between the two techniques.

The reason for this unusual behavior has not been explained by the previous workers. Hildenbrand and Theard pointed out the similarities in discrepancies found for magnesium nitride and those found for magnesium hydroxide by Kay and Gregory.[27] However, Kay and Gregory were unable to explain their hydroxide results except to say that there must be some unusual surface behavior which they termed a pseudo-equilibrium surface. Blank and Searcy, on the basis of their free surface experiments in nitrogen and argon suggested that this pseudo-equilibrium surface might be associated with the adsorption of gases on the vaporization sites, however they were unable to make a more detailed argument.

This investigation was undertaken with the spirit that often in research a phenomenon is first understood in a system where the physical circumstances make for a large deviation from expectations based on previous ideas.[31] Magnesium nitride appears to be such a system. This

dissertation reports a study for magnesium nitride of Knudsen effusion and free surface vaporization as functions of temperature and time. The vapor phase was studied with a quadrapole mass filter and the solid phase was studied by x-ray diffraction techniques to establish Eq. (1) as the vaporization reaction. The vaporization behavior for magnesium nitride was discussed and a model involving a diffusion barrier was developed.

II. EXPERIMENTAL

A. Torsion Effusion

The torsion effusion technique was used for measuring the vapor pressure of magnesium nitride. A detailed description of the technique has been given by Freeman[32] and several workers have described its use in this laboratory.[33-35]

1. Torsion-Effusion Apparatus

A photograph of the torsion-effusion apparatus is shown in Fig. 3 and a diagram is shown in Fig. 4. The furnace was housed in a water cooled stainless steel vacuum chamber; it had thirteen 0.031 cm diameter tungsten hairpin heating elements (arranged to form an 11.5 cm diameter circular cylinder) which were surrounded by tantalum heat shields. Power was supplied to the heating elements through two water cooled copper electrodes by a low voltage source capable of delivering 48 kVA. A vacuum of 2×10^{-6} torr was maintained by an oil diffusion pump and a liquid nitrogen trap. The tantalum heat shields were perforated near the copper electrodes to facilitate the exchange of gases between the vacuum chamber and the furnace; and the variable leak valve allowed the introduction of gases to the vacuum chamber. A quadrapole mass filter and a shutter between it and the effusion cell were mounted as shown in Fig. 4 so that analyses of the gases in the vacuum system could be obtained.

Four different effusion cells--three made of graphite* and one

*Spectrographic grade, 99.999%, from the Ultra Carbon Corporation.

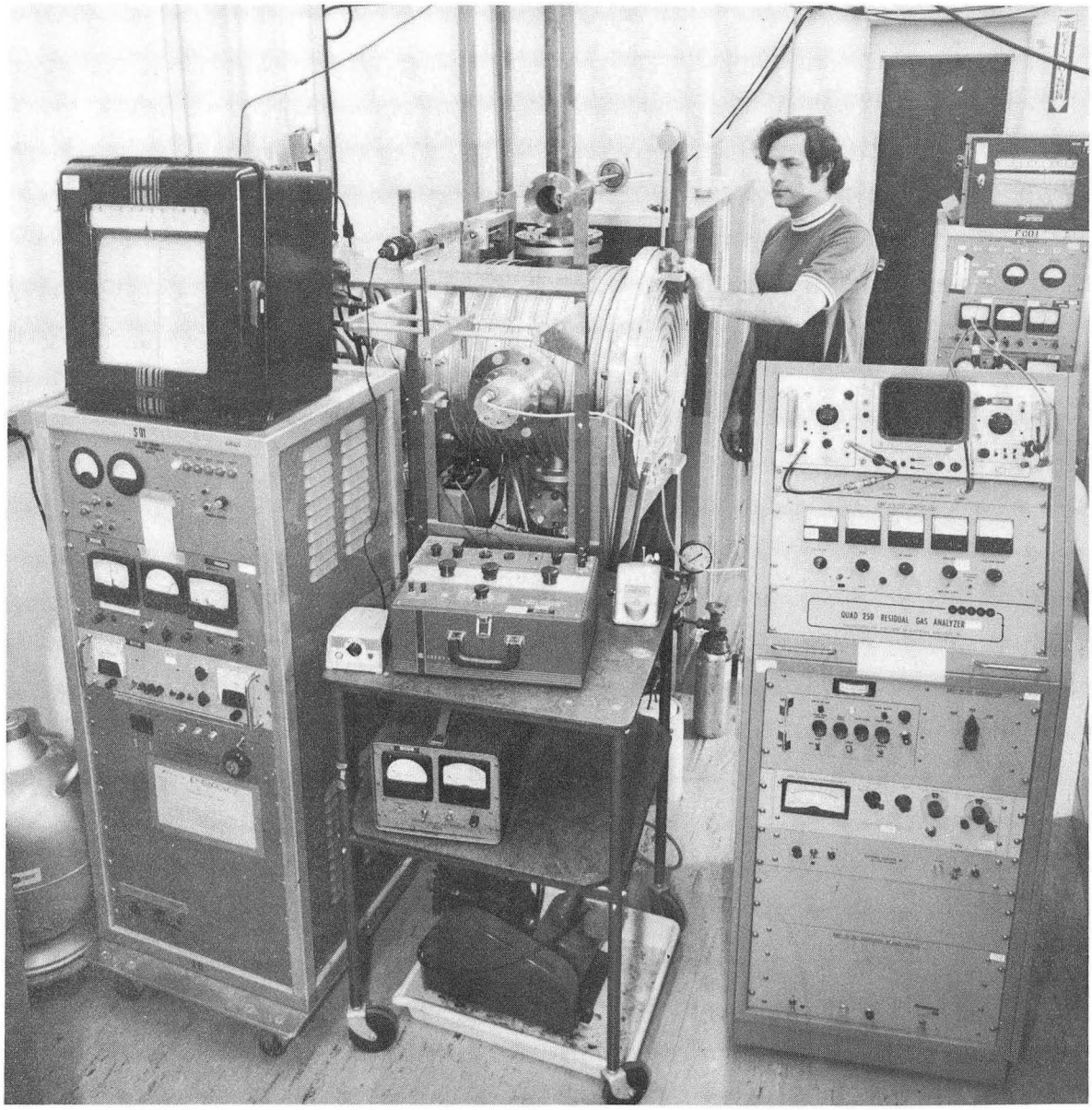

XBB 7110-5092

Fig. 3 Torsion effusion apparatus with quadrapole mass filter.

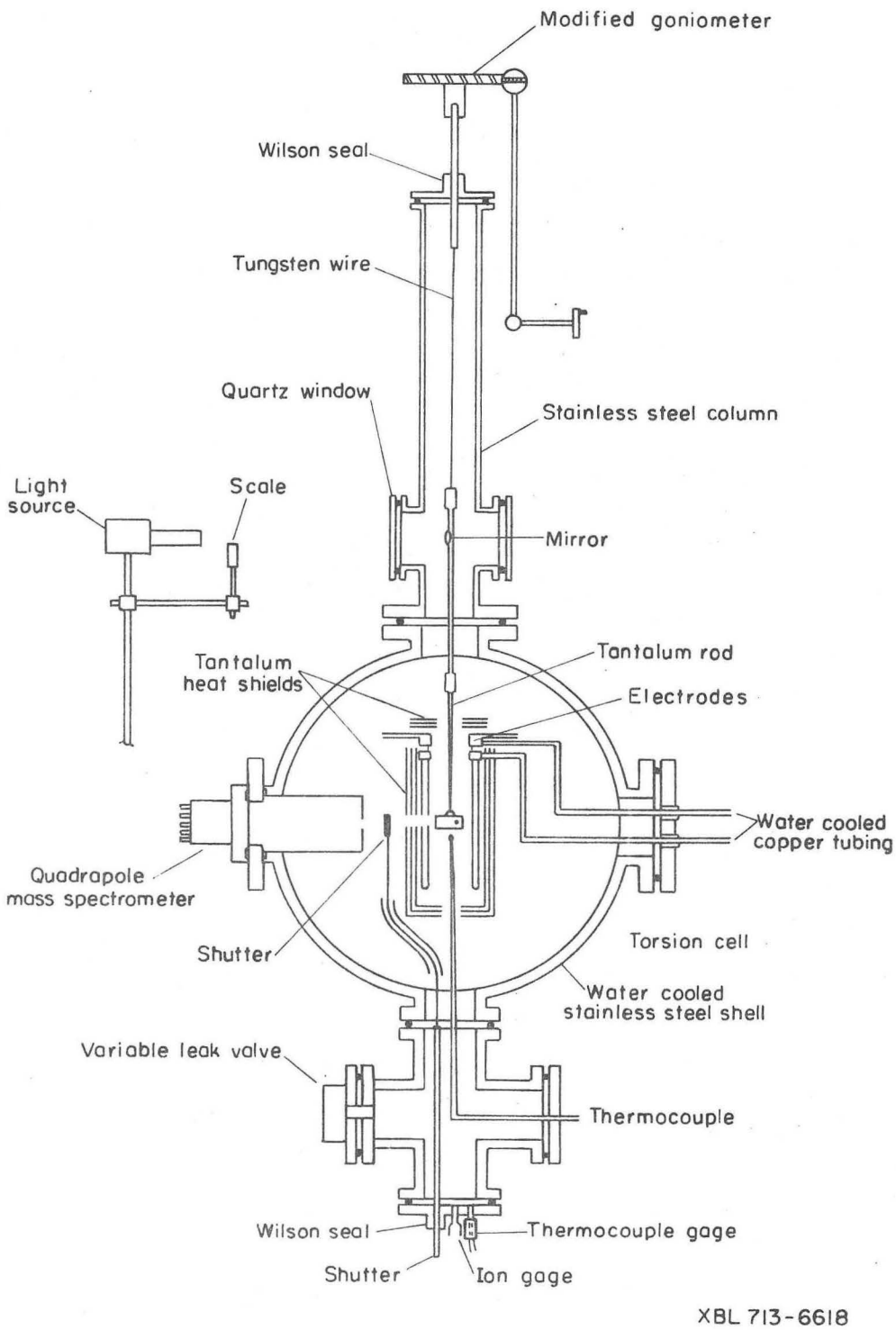

Fig. 4 Schematic diagram of the torsion effusion apparatus.

made of nickel**--were used in this work; they are shown schematically in Figs. 5 and 6. The type "A" cell in Fig. 5 was used for both Knudsen and Langmuir experiments; the assembly of cell parts for these two uses is shown in the bottom part of the figure.

A cell was suspended by a tungsten wire from a modified goniometer at the top of the apparatus; this arrangement allowed the effusion cell to rotate in response to effusion torques. Wires with diameters of 0.0025 cm, 0.0038 cm, and 0.0051 cm and lengths of about 44 cm were used in this work. The goniometer was used to measure the cell rotation, or angle of deflection and the mirror, light source, and scale served to sense the rotation of the cell.

2. Temperature Measurement

The temperature of the effusion cell was measured with a platinum/platinum-10 rhodium thermocouple (the probe thermocouple) placed 6 mm below the cell as shown in Fig. 4. The effusion cell was positioned in a zone of the furnace, 5 cm in length, where the temperature is constant within 2°K; the positioning was done with reference to a mark on one copper electrode of the furnace by using a cathetometer.

The temperature measured by the probe thermocouple was corrected to give the temperature in the effusion cell. This correction was determined by measuring the difference in temperature between a thermocouple placed in the effusion cell and the probe thermocouple as a function of the temperature of the probe thermocouple; there was never more than a 7K difference in the two temperatures for the range 1050K to 1300K. Separate

* Nickel 200, 99.5% including Cobalt, from the International Nickel Company.

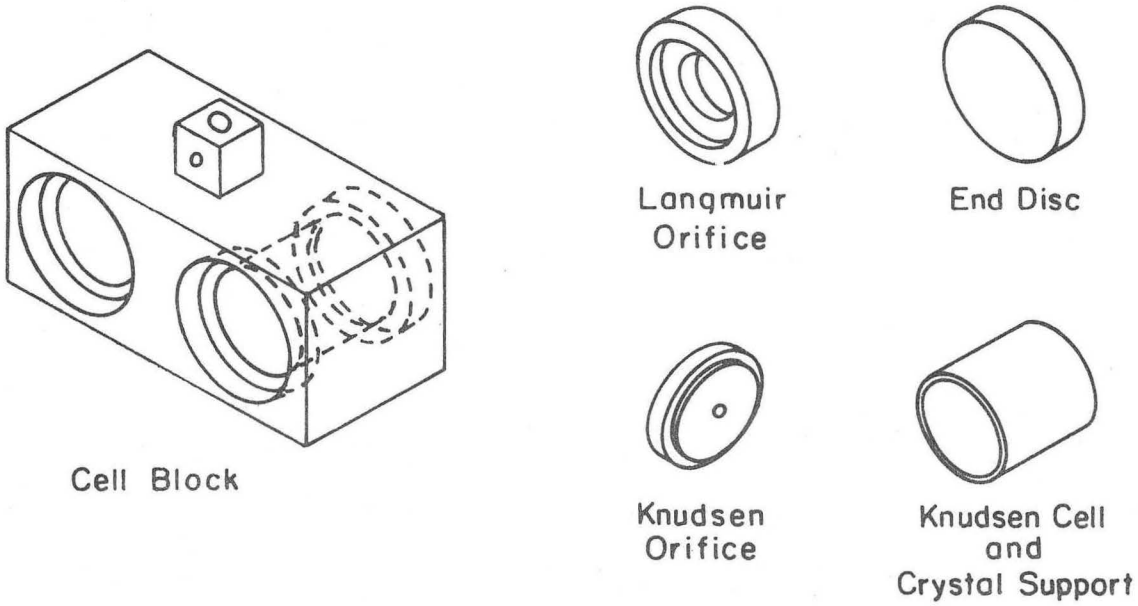

Fig. 5 Isometric diagram of the type A effusion cell parts (full scale) and cross section of the assembled parts for Knudsen and Langmuir experiments.

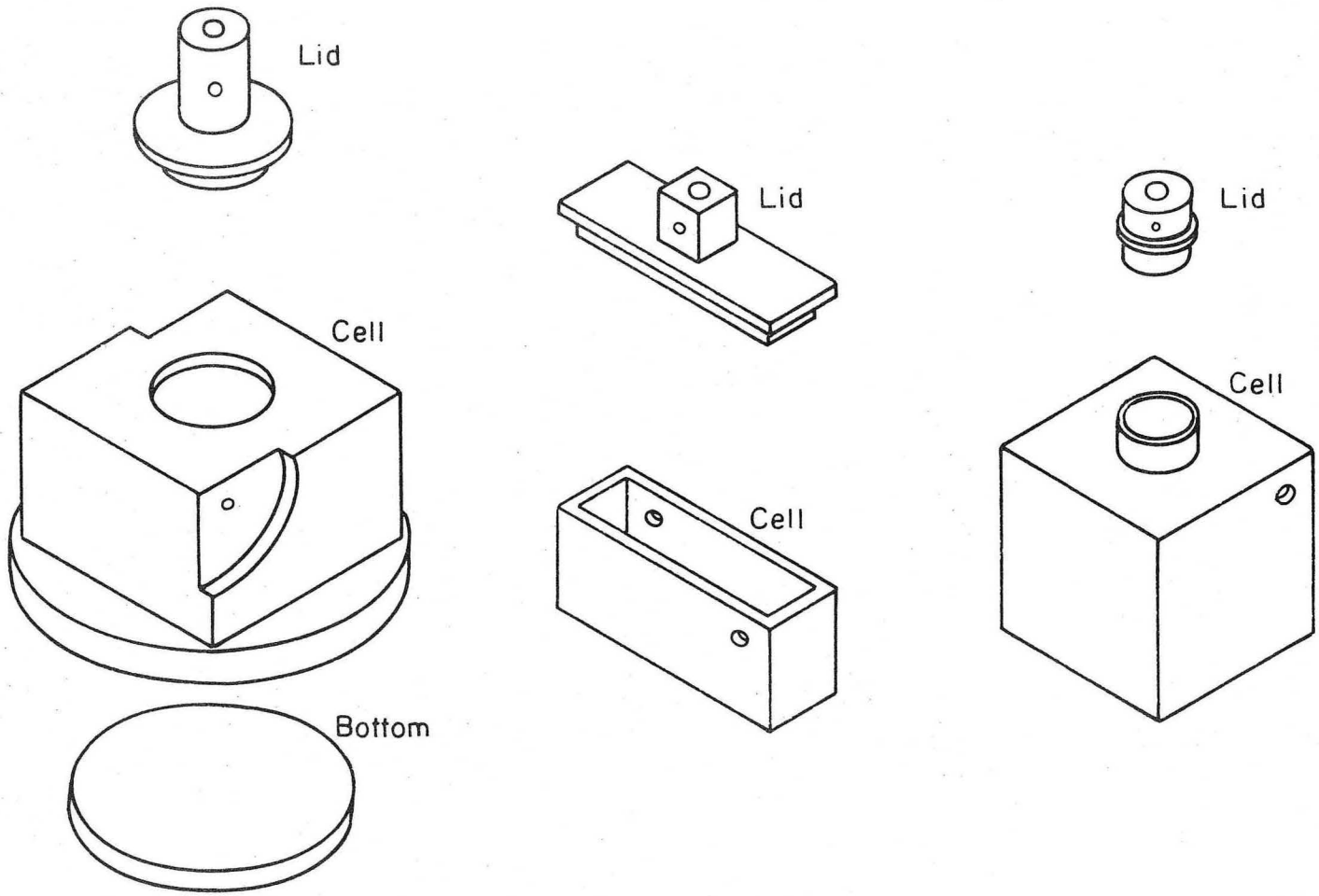

XBL714-6717

Fig. 6 Isometric diagram of effusion cell parts for type B, type C, and type D cell (full scale).

calibrations were done for the "A", "B", and "D" cells, but the results agreed within 6K. Calibrations were checked periodically throughout the investigation, and the results never changed by more than 5K. The thermocouples were calibrated by measuring the melting point of copper in a graphite crucible.

3. Experimental Procedure

Since magnesium nitride readily reacts with water vapor (a three gram sample is completely converted to the hydroxide when held 250 hours in the open air (the nitride was loaded into the effusion cell inside a dry box that contained a phosphorous pentoxide desiccant. The sample was then transferred to the torsion effusion furnace in a closed weighing dish and was mounted in the furnace through a glove box assembly over the furnace opening (the furnace was purged with dry nitrogen before and during this operation). Even with these precautions there was still significant outgassing of water vapor in the early stages of heating.

The vapor pressure in the effusion cell was calculated by means of the relationship:

$$P = \frac{2D\theta}{\Sigma\, q_i\, A_i\, f_i} \qquad (3)$$

where θ is the angle of deflection, q_i is the distance from the center of orifice i to the axis of cell rotation, A_i is the area of orifice i, and f_i is the correction factor for the nonideality of orifice i.[26,36,37] The measurements of q_i and of the orifice diameter (for calculating a_i) were made with a traveling microscope,* and the length of the orifice

*Gaertner Traveling Microscope.

(for calculating f_i) was measured with a micrometer. D is the torsion constant of the suspension system which was calculated from

$$D = \frac{4\pi^2 I_m}{t_m^2 - t_s^2} \qquad (4)$$

where I_m is the moment of inertia of a calibration disc and t_m and t_s are periods of rotational oscillation for the suspension system with the disc mounted and for the suspension system alone.

The angle of deflection in Eq. (3) was determined by using a null point technique with the goniometer used to keep the light beam at the null position on the scale--the null position was the beam position when the effusion torque was negligible. Several minutes are required for making a measurement in this way, however during some of the vapor pressure measurements on magnesium nitride the pressure changed rapidly with time and a new dynamic technique was used for measuring the angle of deflection. The essential feature of this technique is to relate the range swept out by the light beam to the angle of deflection from the null point--for example, at the null point the beam sweeps from 10 right to 10 left and at a deflection of 1° the beam sweeps from 14.7 right to 10 left. Plotting the angle of deflection versus the scale difference, the sweep to the right minus the sweep to the left, gives a straight line which was used in this work. With this technique a pressure can be determined every twenty seconds when a 0.0038 cm diameter tungsten wire is used.

Pressures were calculated on the assumption that the deflections were due entirely to effusion of vapor from the orifices; to insure that extranious deflections were not significant, cells "B" and "D"--the ones

with the smallest orifice areas--were heated with full magnesium nitride charges but with no orifice. For the "B" cell, deflections measured with no orifices amounted to 4% of the deflections measured when the smallest orifices, 0.15 mm, were present. For the "D" cell deflections with no orifices were 0.5% of the deflections with 0.02 mm orifices, the smallest used. In the free surface sublimation experiments a hole was drilled in the top of the cell block (see Fig. 5) to allow vapor from the rear face of the sample to escape without contributing to the deflection.

In the Motzfeldt-Whitman equation[22,23] it is important to use an orifice area which reflects the total flux from the effusion cell; this is called the effective orifice area and is determined as summarized in Table III. First a reduced orifice area is calculated from the geometrical properties of the orifices--this is the orifice area corrected for the molecules that are reflected back into the effusion cell by the nonideal orifice. Then an effective pore area is determined which takes into account the vapor that escapes from the cell through pores in the cell walls or through the interfaces between cell parts. The effective orifice area is calculated by the addition of the reduced orifice area and the effective pore area; physically it is the size of orifice required to account for the mass loss if there were no other losses than through the orifice. The method for determining the effective pore area is discussed in Appendix A.

Table III. Calculation of effective orifice area.

Effusion Cell	B 0.15	B 0.5	B 1.0	C 0.5	D 0.25	A 2.0	B 0.25	A 1.0
Diameter D_1	0.15 mm	0.515	1.043	0.531	0.234	2.131	0.257	1.082
Diameter D_2	0.15 mm	0.512	1.056	0.525	0.246	2.035	0.257	1.080
Length L_1	0.508 mm	1.237	1.237	0.159	0.254	1.57	1.237	1.68
Length L_2	0.508 mm	1.295	1.295	0.164	0.254	1.70	1.295	1.69
Channel $(2L/D)_1$	6.7733	4.832	2.3674	5.9887	2.171	1.473	9.626	3.113
Channel $(2L/D)_2$	6.7733	5.059	2.4526	6.2286	2.065	1.665	10.077	3.133
Clausing Factor W_1	0.25086	0.31636	0.47521	0.2738	0.4955	0.5860	0.19228	0.4120
Clausing Factor W_2	0.25086	0.30698	0.46697	0.2663	0.5072	0.5575	0.1881	0.4106
Orifice Area A_1	1.767×10^{-4} cm^2	2.083×10^{-3}	8.577×10^{-3}	2.212×10^{-3}	4.301×10^{-4}	3.56×10^{-2}	5.187×10^{-4}	9.195×10^{-3}
Orifice Area A_2	1.767×10^{-4} cm^2	2.059×10^{-3}	8.757×10^{-3}	2.1648×10^{-3}	4.753×10^{-4}	3.25×10^{-2}	5.187×10^{-4}	9.161×10^{-3}
$(WxA)_1$	4.433×10^{-5} cm^2	6.390×10^{-4}	4.076×10^{-3}	6.056×10^{-4}	2.131×10^{-4}	2.086×10^{-2}	9.974×10^{-5}	3.788×10^{-3}
$(WxA)_2$	4.433×10^{-5} cm^2	6.321×10^{-4}	4.089×10^{-3}	5.765×10^{-4}	2.411×10^{-4}	1.812×10^{-2}	9.757×10^{-5}	3.762×10^{-3}
Reduced Orifice Area $(WxA)_1+(WxA)_2$	8.866×10^{-5} cm^2	1.291×10^{-3}	8.165×10^{-3}	1.1821×10^{-3}	4.542×10^{-4}	3.898×10^{-2}	1.9731×10^{-4}	7.550×10^{-3}
Effective Pore Area P	1.4×10^{-4} cm^2	1.4×10^{-4}	1.4×10^{-4}	1.4×10^{-4}	1.4×10^{-4}	negligible	1.4×10^{-4}	negligible
Effective Orifice Area $P+[(WxA)_1+(WxA)_2]$	2.3×10^{-4} cm^2	1.43×10^{-3}	8.31×10^{-3}	1.32×10^{-3}	5.9×10^{-4}	3.9×19^{-2}	3.4×10^{-4}	7.6×10^{-3}

B. Gas Analysis

A quadrapole mass filter* and an ionization gauge** were used to determine the composition of the residual gases in the vacuum system and to sample the vapors streaming out of the Knudsen effusion cell. Figure 4 shows the position of both instruments in the vacuum system; the mass filter has been aligned with the orifice in the Knudsen cell. The partial pressure for each constituent of the residual gas was calculated from its mole fraction, which was obtained from the mass filter, and from the total pressure which was registered by the ionization gauge.

The determination of a mole fraction from the intensity measurement of the mass filter requires knowledge of the transmission probabilities and ionization cross section for the molecules. To measure the transmission probability of a molecule in the mass filter, n-butane† at 3.3×10^{-5} torr was introduced and the resulting fragmentation pattern, for 70 eV, was compared with a standard fragmentation pattern.[38] Figure 7 shows the results of these measurements. Ionization cross sections from Otvos and Stevenson[39] were used for all molecules except the value determined by Reed[40] was used for water vapor.

The ionization gauge was calibrated by comparing it to a McLeod gauge†† at various pressures of nitrogen. For other gases the relative sensitivities given by Dushman and Lafferty[41] were used with the nitrogen data to achieve calibration.

---

* EAI Quad 250 Residual Gas Analyzer.

** ETI Type VGIA/2.

† 99.99 mole percent Phillips Petroleum Research Grade.

†† CVC CM100 McLeod Gauge.

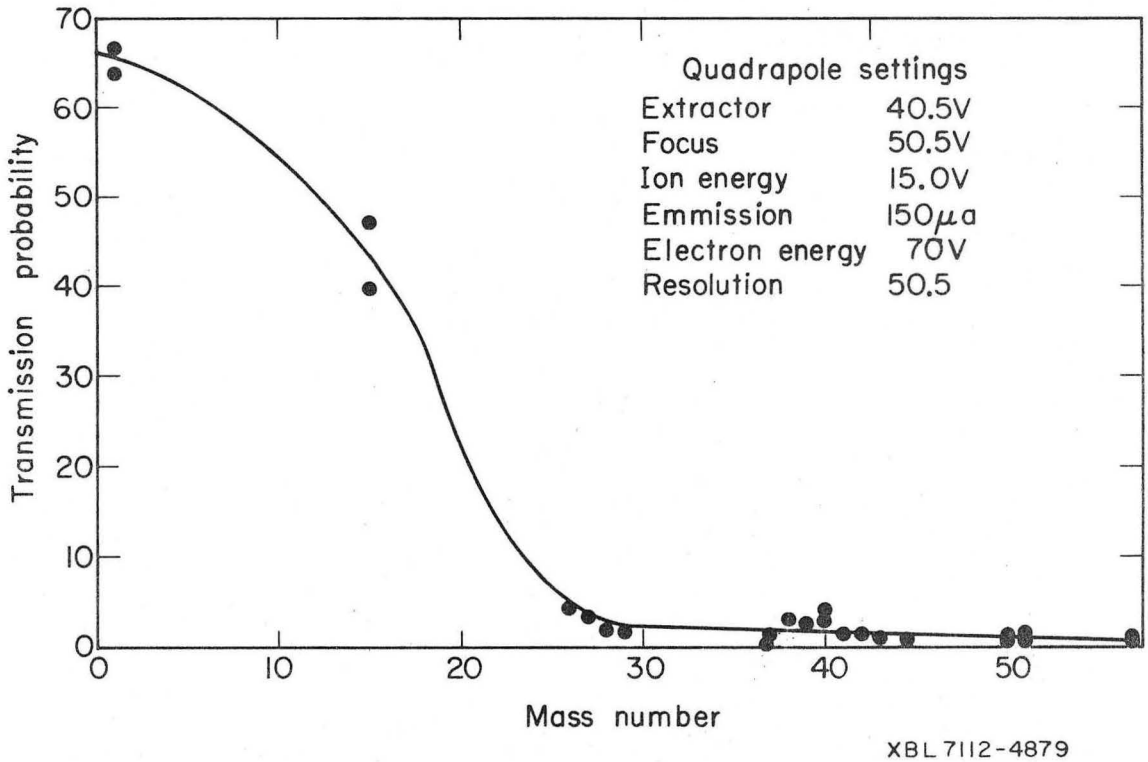

Fig. 7 Transmission probabilities for molecules in a quadrapole mass filter from the fragmentation of n-butane.

C. Sample Preparation

The magnesium nitride used in this work was obtained from three different commercial suppliers who estimated a purity of 99% on the basis of the purity of their starting materials. All of these materials were analysed for magnesium oxide by evaporating the magnesium nitride in a graphite cricible at 1250K and then weighing the residual material which was found by x-ray diffraction to be magnesium oxide; these results are shown in the first four rows of Table IV. Calculations showed that reaction with the residual water vapor and oxygen in the vacuum system can account for an oxide content of less than one-tenth percent. Thus all of the starting materials have significant amounts of magnesium oxide as a contamination. Loss of oxide by the reaction $MgO + C \longrightarrow CO(g) + Mg(s)$ was shown by experiment to be negligible.

In an effort to obtain high purity magnesium nitride, a sample of the material from Hall Labs was distilled in a 90K temperature gradient at about 1370K; the resulting material (last entry, Table IV) was about 99% magnesium nitride. The method is described below in detail with respect to its use in preparing samples for Langmuir studies.

X-ray diffraction patterns* of the above materials showed that magnesium nitride is the major phase,[42] but magnesium oxide peaks were also produced by some samples. Estimates of the oxide content from the diffraction patterns are also given in Table IV; estimates were made by the method described by Cullity.[43] Equal adsorption coefficients were assumed for the oxide and the nitride. The relative oxide contents estimated from the x-ray data support the contents calculated from the more accurate evaporation results.

*Picker Model 3488 X-ray Diffractometer.

Table IV. Analyses of magnesium nitride for magnesium oxide.

Source	Weight Percent MgO	
	Evaporation	X-Ray Diffraction
Ventron	4.1	Not detected
Hall Labs	19.4	7
Metal Hydrides	8.9	2
B and S*	25.0	6
This Laboratory	1.2	Not detected

*Metal Hydrides magnesium nitride used by Blank and Searcy after storage in a desiccator.

To obtain further information on the purity of the magnesium nitride a semi-quantitative--within 50%--spectrographic analysis for metallic elements was obtained; the results are presented in Table V. The nitride formed by purification in graphite is seen to be 99.99% pure according to this analysis while all of the others are 99%. Purification in stainless steel introduces a considerable amount of iron and manganese into the material; and the materials supplied by Metal Hydrides and Hall Labs are high in silicon and aluminum, respectively (these elements were possibly introduced by a grinding operation).

The magnesium nitride Langmuir samples prepared in this laboratory were made from the Hall Labs material by an evaporation and condensation technique using the apparatus shown in Fig. 8. About 35 grams of the nitride was placed in one end of a 304 stainless steel tube with a diameter of 1.5 in. and a length of 9 in. To avoid reaction of the nitride with oxygen and water vapor, the furnace chamber was pumped to a pressure of 10 microns and backfilled with dry nitrogen while the furnace was at a low temperature; this procedure was repeated three times. Samples were heated in a 3 psig nitrogen atmosphere to a temperature of 1420K. The nitride distilled to the other end of the tube, at a temperature of 1330K, where deposition occurred. In each run a piece of polycrystalline magnesium nitride that was 90% of theoretical density and was about an eighth of an inch thick was formed at the deposition end of the tube. Some work was done using a tube made of spectroscopic grade graphite, however, the yield was very low and the nitride deposited in the form of a fiberous mat.

XBB 7111-5658

Fig. 8 Vapor transport apparatus for preparing Langmuir specimens of magnesium nitride.

Table V. Spectrographic analysis* of magnesium nitride.

Element	Purified from Hall Labs Matl. Stainless Steel	Graphite	Metal Hydride	Hall Labs
Mg	Principal constituent in each sample.			
Fe	0.12%**	0.01%**	0.035%**	0.04%**
Ni	.007	.003	.025	.003
Co	<0.002% in each sample. Not detected.			
Cr	.03	<.005	.005	.0005
Si	.07	.015	.3	.02
Mn	.3	.015	.015	.05
Al	.04	.035	.015	.18
Cu	.002	.0005	.002	.002
Cd	.02	---	---	---
Ti	---	---	.003	---
Ag	---	---	---	.001
Zr	---	---	.05	.015
Ca	.004	.002	.05	.06
Ba	.001	---	.001	.005
Sr	<.005	<.005	<.005	<.005

*Done by American Spectrographic Laboratories, Inc.

**Weight percent.

Many of the effusion experiments were made with the Metal Hydrides powdered magnesium nitride. To insure that each effusion sample had the same distribution of particle sizes and the same surface area, all of the Metal Hydrides material was repeatedly split to yield seperate 5.3 gram samples by means of the particulate material sampler shown in Fig. 9.

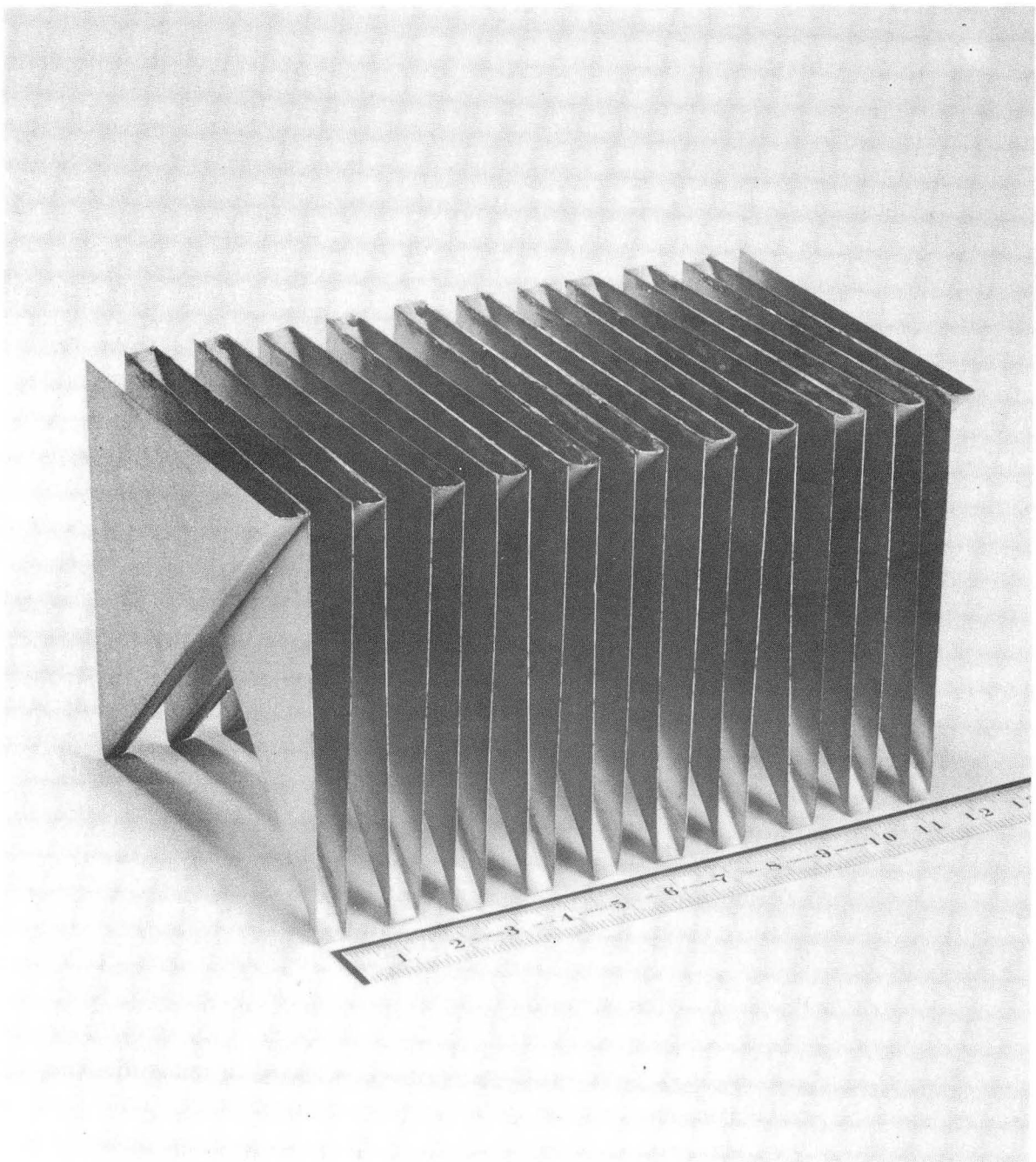

XBB 7110-5093

Fig. 9 Particulate material sampler for obtaining uniform samples of magnesium nitride powder for Knudsen effusion studies.

D. Lattice Parameter Measurements

In order to determine if the stoichiometry and/or impurity levels in the magnesium nitride changed during the effusion experiments, measurements of the lattice parameter were made by the Debye-Scherrer x-ray diffraction technique.[44,45] The magnesium nitride sample was placed in 12 mil diameter tubing made of Lindemann glass--this was done in a dry box. The specimen was then centered within a camera* and the film was mounted in the manner described by Straumanis.[44,46] The K_α radiation of copper was used with a nickel filter and the spacings between lines on the film was measured to 0.05 mm.**

E. Weight Loss Measurements

Weight loss experiments were used to measure the amount of magnesium nitride which escaped from the effusion cell during the vapor pressure measurements. For the B cells the torsion effusion furnace shown in Fig. 3 was used. After being heated the effusion cell was cooled to 330K and the vacuum was broken with dry nitrogen. The effusion cell was placed in a weighing dish and was left for 10 minutes to equilibrate in the balance room. The balance lamp was left on for 10 minutes prior to weighing† to establish thermal equilibrium; these procedures allowed an accuracy of within 50 micrograms. For "A" cells the procedure was altered because these experiments were done in the vapor transport

---

*A Norelco Type 52056 Debye-Scherrer 57.3 mm camera was used with the Norelco Type E58001/12031 x-ray diffraction unit.

**Norelco Type 52022/1 Film Illuminator and Measureing Device.

†Mettler H20T Semimicro balance.

apparatus shown in Fig. 8. The crucibles were removed from the hot zone of the furnace, dry nitrogen was introduced to break the vacuum, and after 1 minute the effusion cell was removed to a desiccator to cool. The cell was then placed in a weighing bottle and weighed after equilibration of the balance and the weighing dish as described above.

III. RESULTS

A. Investigation of the Evaporation Reaction

In order to confirm that the vaporization of magnesium nitride proceeds according to reaction (1) an investigation of the vapor phase was undertaken with a quadrapole mass filter and lattice parameter measurements were made of the solid phase.

The vapor species effusing from the Knudsen cell were identified by monitoring the partial pressures of the gases in the vacuum system. Data for several samples at several temperatures are shown in Table VI. On heating, the partial pressures of H_2, H_2O, and N_2 plus CO (these two gases cannot be distinguished) increased for both the silver and the magnesium nitride experiments. The increases must reflect desorption of these gases from the vacuum chamber and reaction of $H_2O(g)$ with the graphite Knudsen cell to give $H_2(g)$ and $CO(g)$. The $NH_3(g)$ in the magnesium nitride experiments was probably produced by the reaction of $H_2O(g)$ (from the $Mg(OH)_2$ in the nitride sample) with the nitride.

Magnesium vapor was released from the nitride samples in appreciable amounts at 800K. This low temperature of magnesium evolution and the fact that the peak was shutterable, while the nitrogen peak was not, indicated that the nitride sample had some unreacted magnesium metal.

Above 1100K, the expected range of magnesium nitride vaporization, $N_2(g)$ and $Mg(g)$ effused as evidenced by the shutter effects of these molecules. A check of mass 38 for $MgN(g)$ gave no shutter effect; thus the vapor phase in equilibrium with the nitride is $Mg(g)$ and $N_2(g)$, which is consistent with (1).

Table VI. Partial Pressures of Vacuum System Gases

Residual Gases	Pressure x 10^{10} (atm) H_2	NH_3	H_2O	Mg^2	N_2 & CO	O_2	Hydro-Carbons[3]	Total
298K (Aver. of 4)		---	8	---	8	4	4	24
Ag								
980K Initial	140	---	430	---	430	10	---	1000
1350K After 150 min.	61	---	61	---	61	<10	---	180
Metal Hyd. Mg_3N_2 Sample I								
570K Initial	260	430	540	---	270	<20	---	1500
940K Initial	1000[1]	570	290	---	1140	<20	---	3000
940 After 5 mins.	500[1]	---	60	600	600	<10	---	1800
1250K Initial	50[1]	---	7	47	2700	<10	---	2800
1250K After 35 mins.	30[1]	---	4	3	420	<5	---	450
Metal Hyd. Mg_3N_2 Sample II								
800K Initial	200	1600	200	---	200[1]	--	---	2200
" " 20 mins.	37	---	1	19	45	<2	---	100
910K Initial	89	---	1	22	110	<2	---	220
1100K Initial	64	---	32	16	640	<1	---	750
1100K After 13 mins.	30	---	4	20	120	<1	---	170

1. Estimated.
2. It is assumed that Mg(g) condenses before reaching the ionization gauge.
3. Determined only in residual gases at 298K.

To insure that the magnesium nitride was not changed in composition as a result of selective vaporization or change in oxygen content, the lattice parameter was measured. Table VII shows the parameters for four different samples, the weight percent of magnesium oxide in the sample, and the experimental conditions. The first two measurements show that the reproducibility of the results was about 0.0005Å; thus it is seen that there were no detectable differences in the lattice parameter. This fact indicated that no change in composition occurred under the experimental conditions in this work. These data also suggest that the amount of magnesium oxide in solution in the nitride was less than 1.2%, the amount in the purified sample. Thus, the principle solid phase is magnesium nitride with a composition that was not measurably changed by partial vaporization, and reaction (1) is confirmed as the vaporization reaction.

B. Vapor Pressure of Silver

Silver* was used as a standard for determining the accuracy of the vapor pressure measurements. Figure 10 shows the results of vapor pressure measurements in torsion effusion cells of type "A", "B" and "D" and also lists the second law enthalpies derived from these measurements. Since the melting point of silver is 1234K--in the middle of the range of the pressure measurements--the datum points below 1234K have been adjusted by the difference in pressure between the solid and a supercooled liquid so that all of the data are for the reaction, Ag(l) = Ag(g). Also included in the figure are the vapor pressure data selected

*Engelhard type J-6 fine silver powder 99.99+% silver.

Table VII. Lattice Parameter Measurements on Magnesium Nitride

Source of Magnesium Nitride	% MgO	Conditions	a_o (A°)
1. Purified 1st Meas.	< 1.2	1.2 atm N_2 @ 1320K	9.9651
2. Purified 2nd Meas.	<1.2	"	9.9656
3. Metal Hydrides Residual	>9	Knudsen Cell @ 1180K for 100 hrs	9.9657
4. Residue from purification	30	1.2 atm N_2 @ 1400K	9.9657
5. Metal Hydrides as received	9	------	9.9649
		Average	9.9654

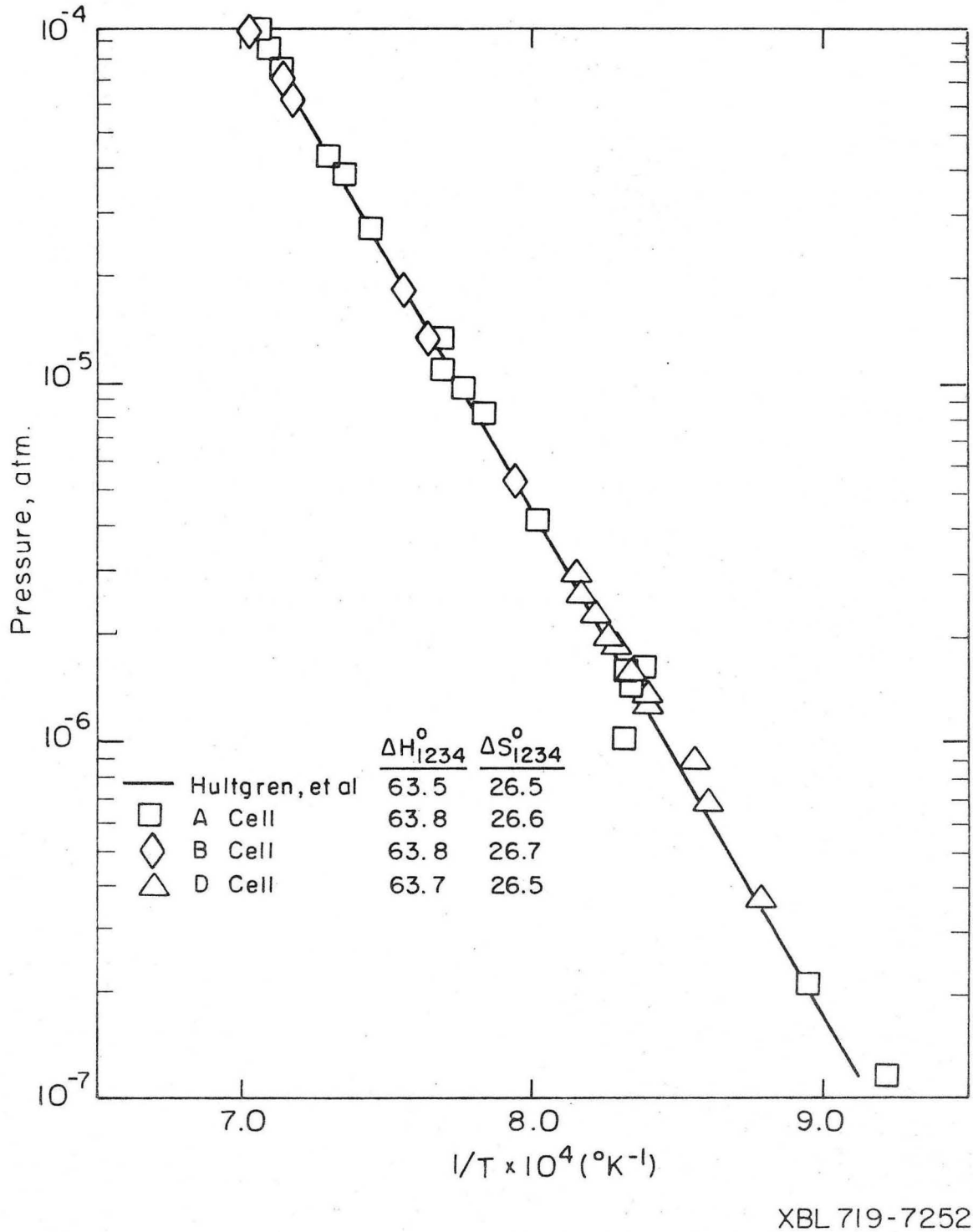

Fig. 10 Vapor pressures measured for silver by Knudsen effusion.

by Hultgren, et al.[13] for silver. It can be seen that almost all of the datum points were within 10% of the selected values. Other measurements of the vapor pressure of silver were made throughout the course of this work; the vapor pressures were within 20% and the second law heats of vaporization were within 5% of Hultgrens selected value, 63.5 kcal at 1234K.

C. Vapor Pressure Versus Time Experiments

Previous workers[1-3] have not reported a time dependency in their vapor pressure studies of magnesium nitride. However, in this work the vapor pressure of the magnesium nitride has been observed to increase to a maximum (near the calculated equilibrium value in some cases) in a period of about 15 minutes, to then decrease rapidly and after about 50 minutes to decrease slowly. This behavior is shown in Figs. 11 through 18 where vapor pressures versus the time elapsed from the start of heating at 950K are presented; the important parameters for each experiment are shown in Table VIII.

The table lists the nominal temperature of each experiment which is usually within five degrees of the actual temperature--there was cycling of the furnace temperature. Also listed in the table is the type of effusion cell (including the nominal orifice diameter), the effective orifice area of the cell, the charge of magnesium nitride in the cell, and the source of the nitride; notes about unusual conditions in the experiments are given in the last column. The data in the figures have been corrected to four temperatures; 1110K, 1150K, 1180K, and 1210K by using the equilibrium enthalpy of vaporization of magnesium nitride to adjust the measured vapor pressure to one of the above temperatures

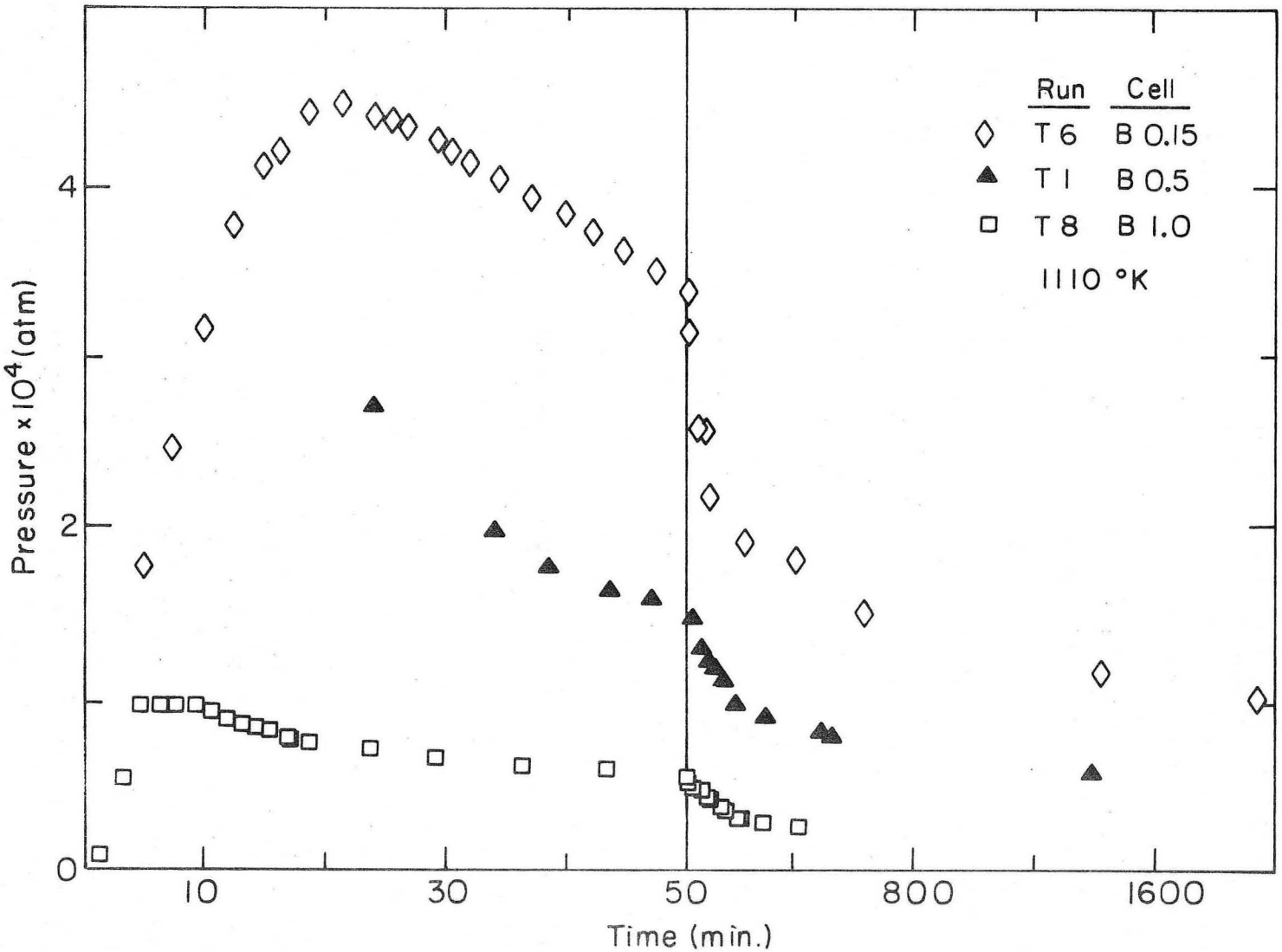

XBL 7110-7464

Fig. 11 Vapor pressure of magnesium nitride (M.H.S.) at 1110K for three different orifice areas in a B cell.

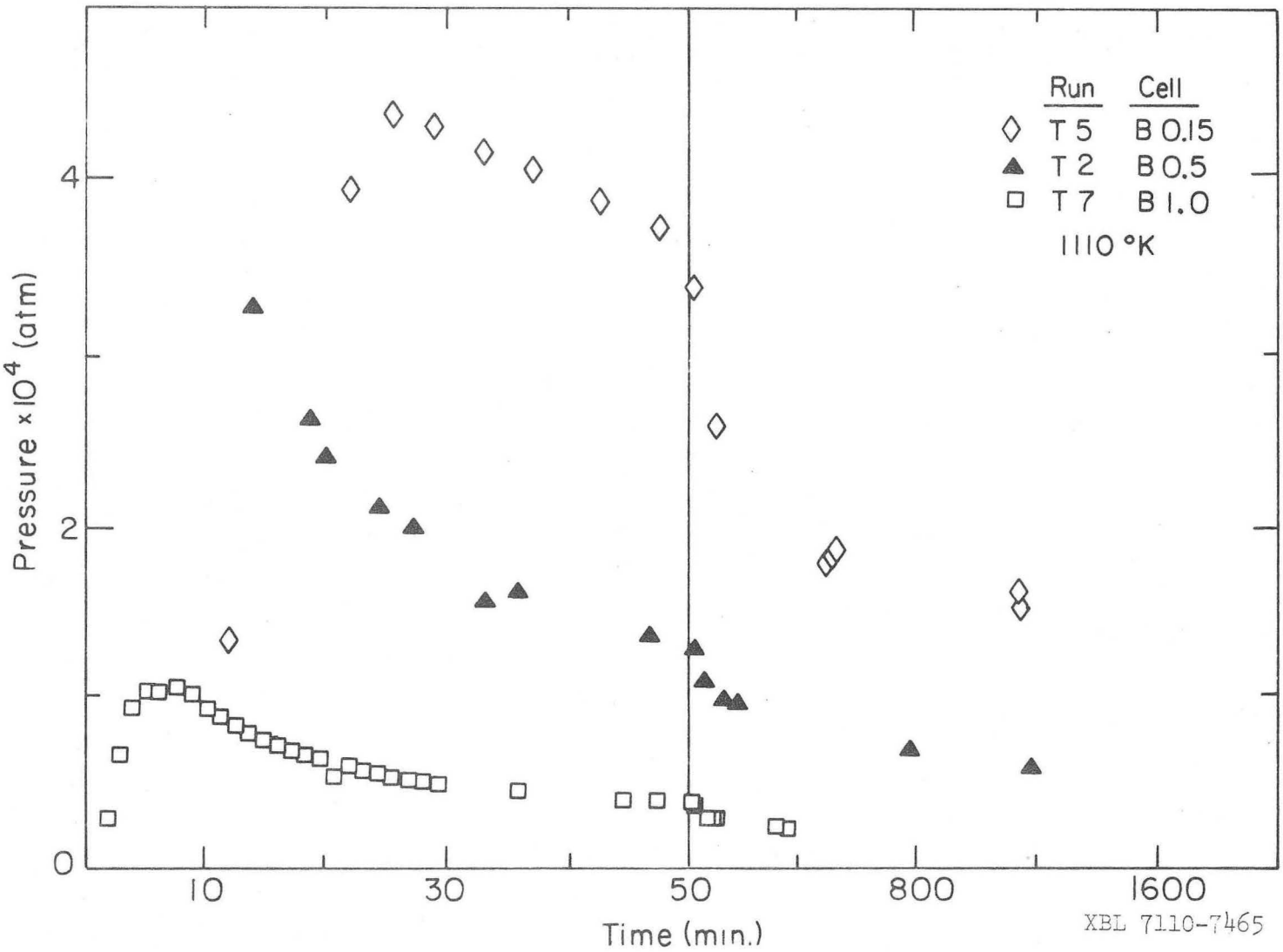

Fig. 12 Vapor pressure of magnesium nitride (M.H.S.) at 1110K for three different orifice areas in a B cell.

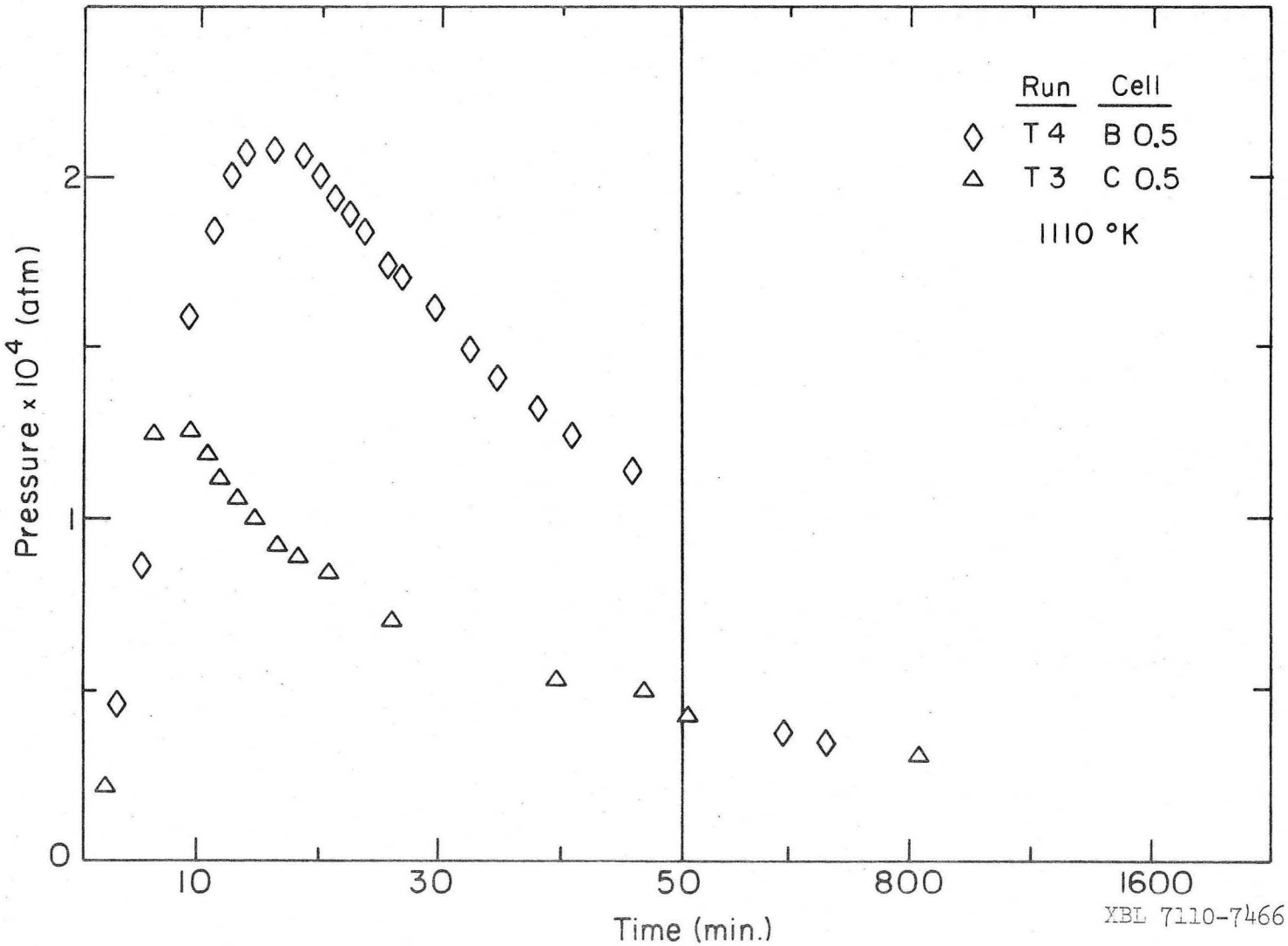

Fig. 13 Vapor pressure of magnesium nitride (M.H.S.) at 1110K for two different effusion cells with the same orifice.

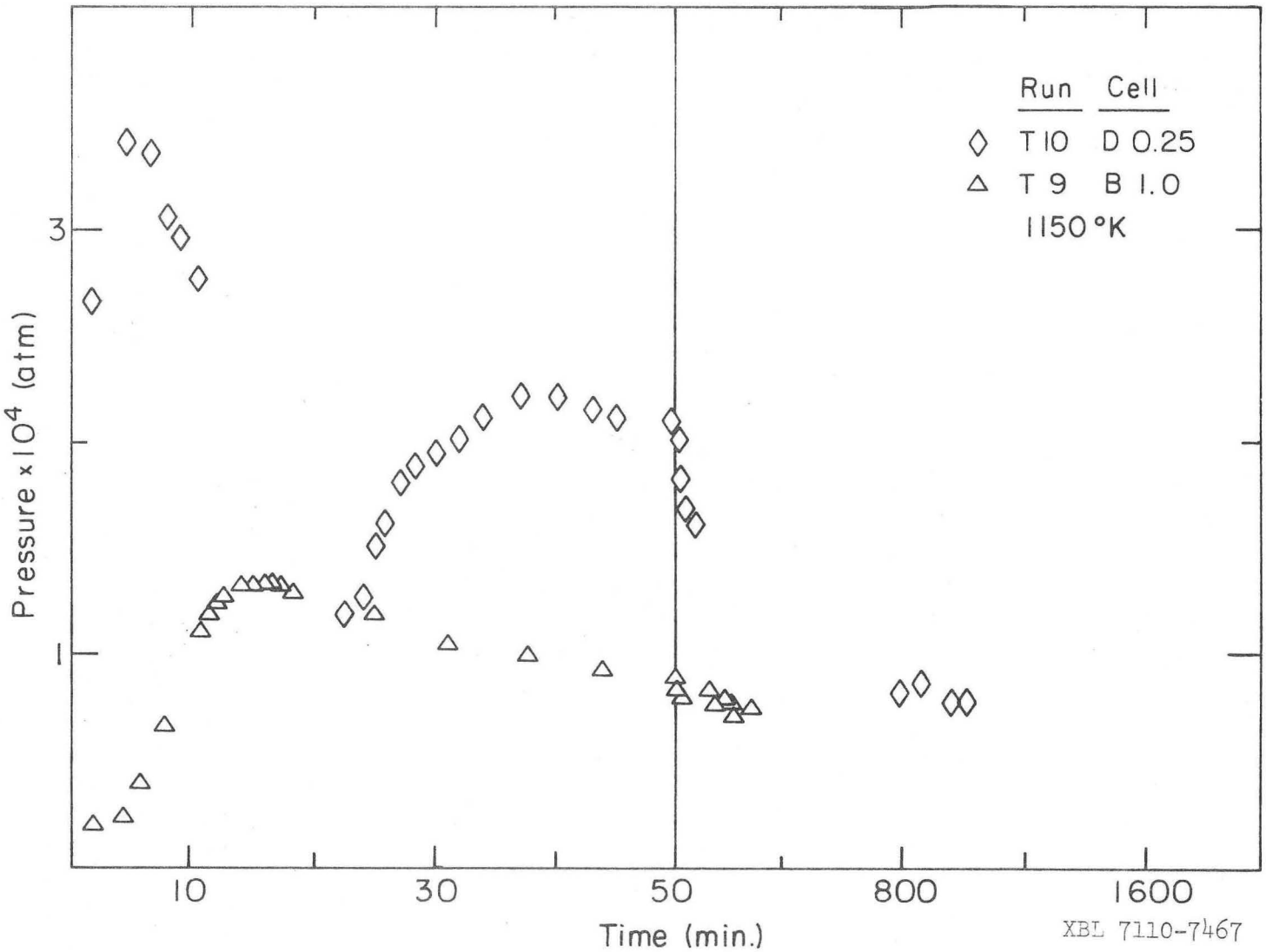

Fig. 14 Vapor pressure of magnesium nitride (M.H.S.) at 1150K for a nickel (D0.25) and for a graphite (B1.0) effusion cell. Experiment T10 interrupted at 11 minutes and resumed at 22 minutes.

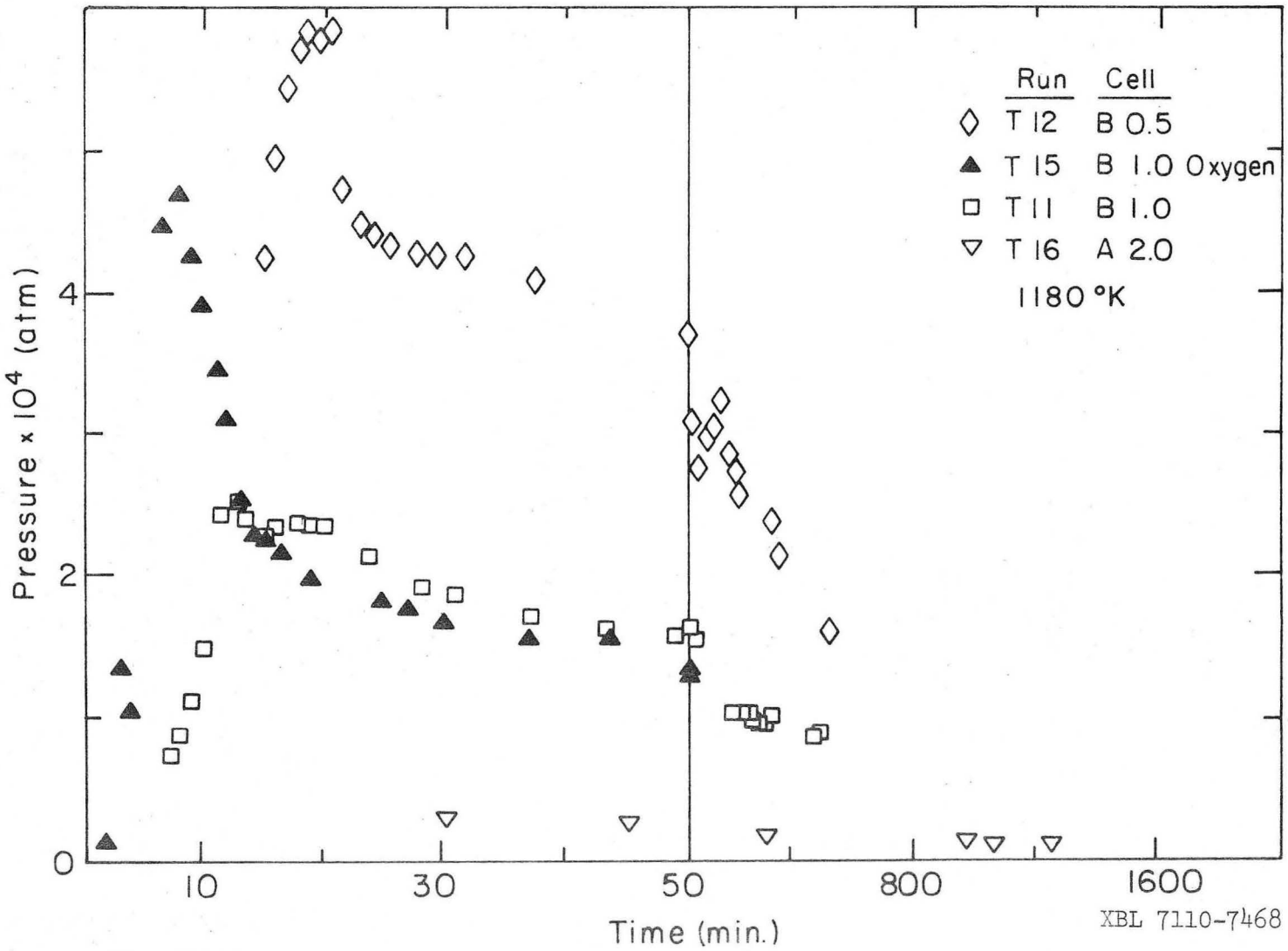

Fig. 15 Vapor pressure of magnesium nitride (M.H.S. except T16 Ventron) at 1180K. Run T15 with O_2 and T11 without.

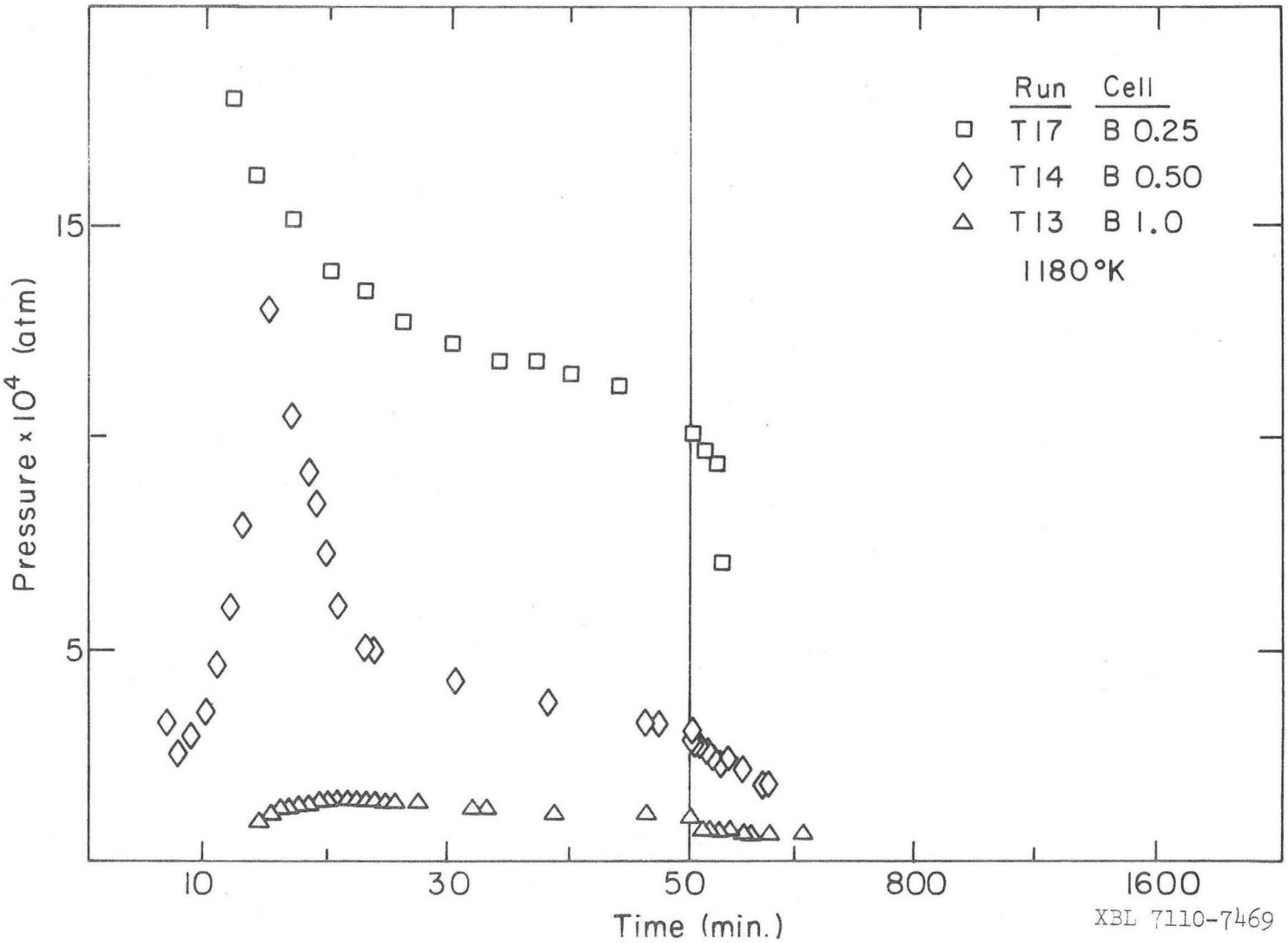

Fig. 16 Vapor pressure of magnesium nitride (M.H.S. except T17 Ventron) at 1180K.

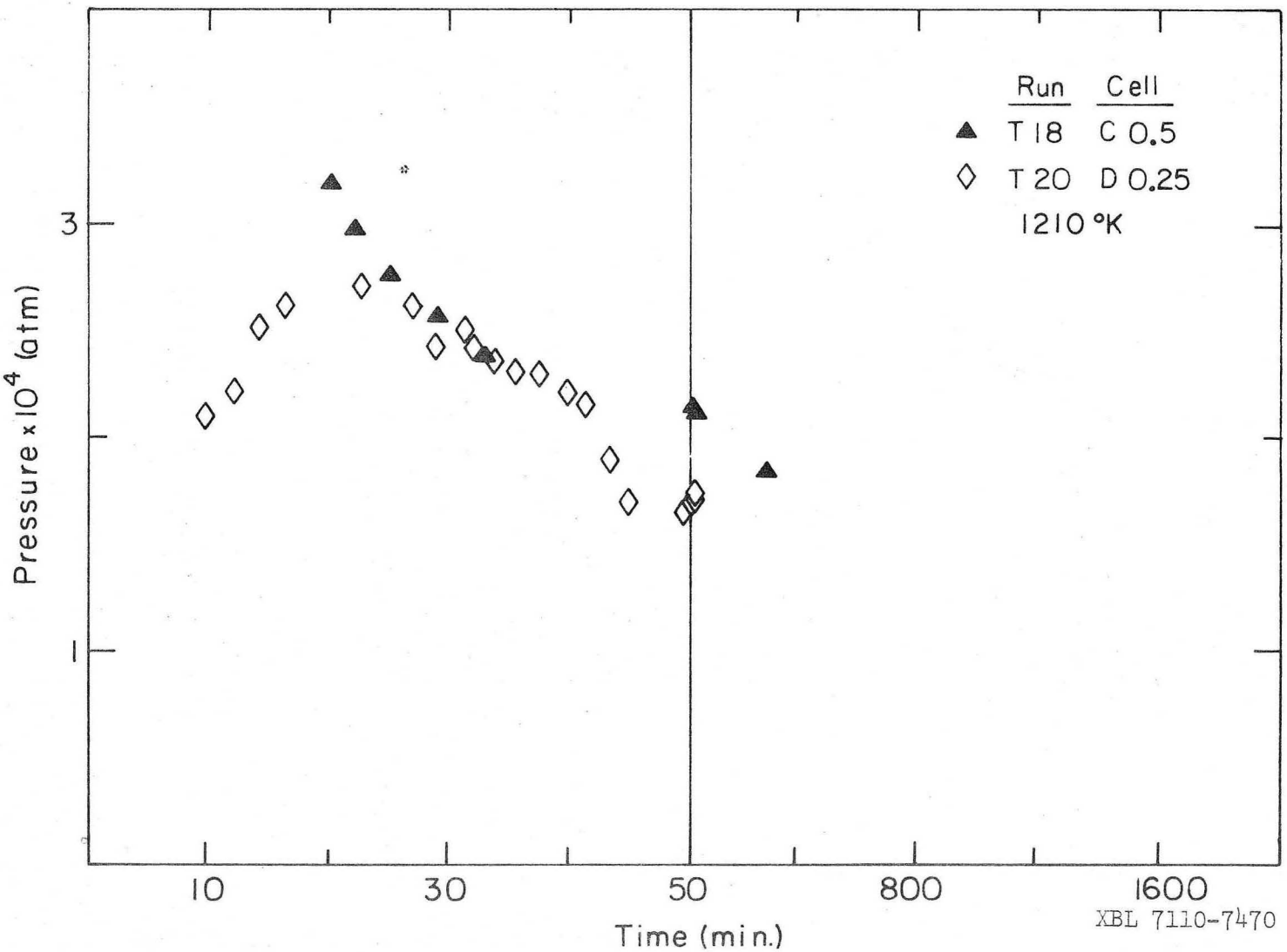

Fig. 17 Vapor pressure of 1.27 grams of Ventron magnesium nitride (T18) and of 6.0 grams of nitride prepared in this laboratory (T20).

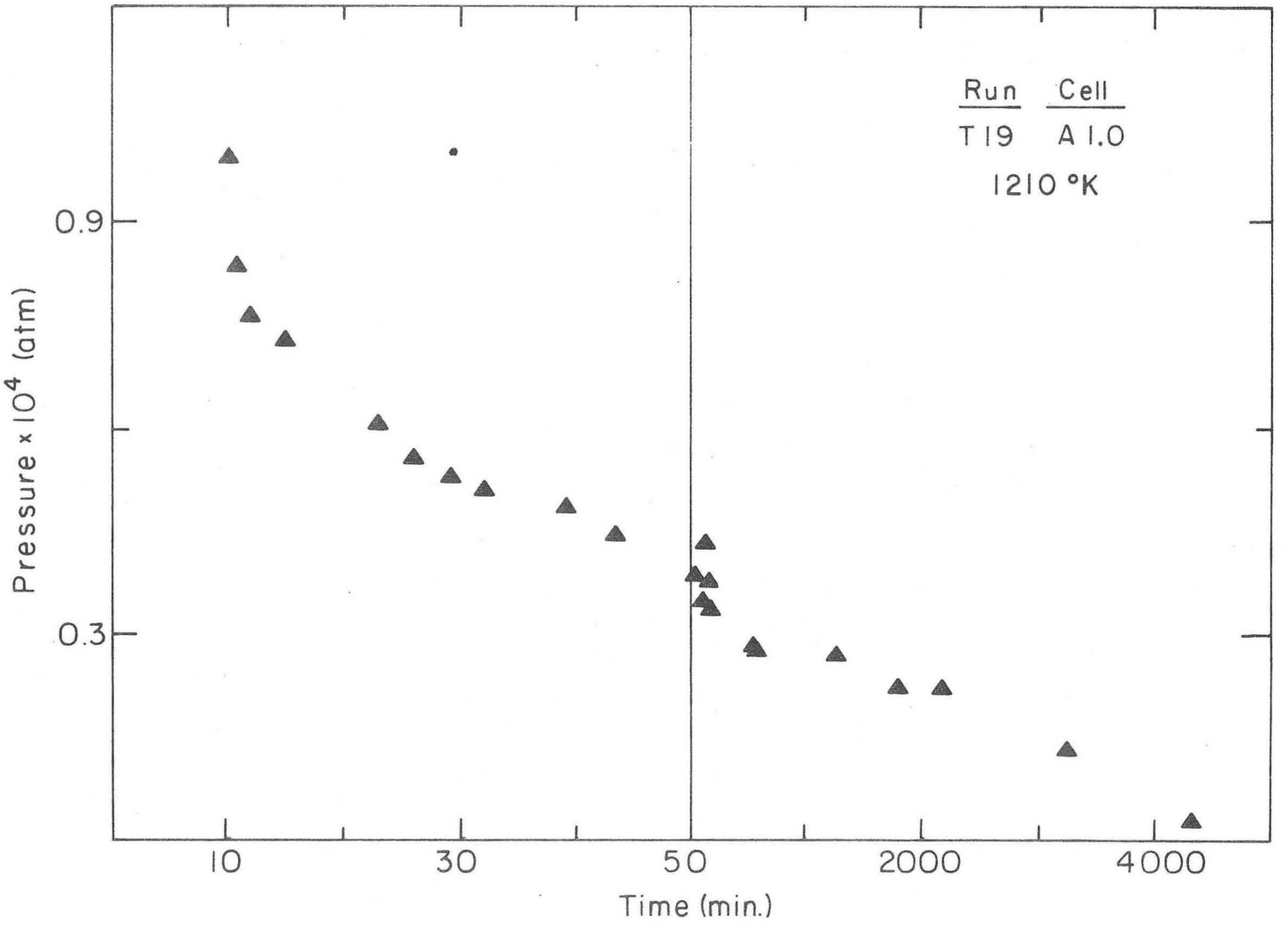

XBL 7110-7471

Fig. 18 Vapor pressure of magnesium nitride (Ventron). Experiment carried to exaustion.

Table VIII. Important parameters in pressure versus time experiments.

Run #	Nominal Temp °K	Cell Type	Effective Orifice Area $cm^2 x10^3$	Charge gm	Source	Notes
T1	1110	B 0.5	1.43	5.29	M.H.S.*	No Outgassing
T2	1103	B 0.5	1.43	5.36	"	
T3	1120	C 0.5	1.32	1.4	"	
T4	1093	B 0.5	1.43	5.50	"	
T5	1120	B 0.15	0.23	5.21	"	
T6	1109	B 0.15	0.23	5.40	"	
T7	1113	B 1.0	8.31	5.40	"	
T8	1116	B 1.0	8.31	5.50	"	
T9	1155	B 1.0	8.31	5.76	"	
T10	1156	D 0.25	0.59	5.50	"	Ni Cell Interrupted
T11	1179	B 1.0	8.31	4.75	"	
T12	1185	B 0.5	1.43	5.43	"	
T13	1181	B 1.0	8.31	5.55	"	
T14	1181	B 0.5	1.43	5.68	"	
T15	1176	B 1.0	8.31	5.40	"	Oxygen
T16	1180	A 2.0	39.00	0.56	Ventron	
T17	1187	B 0.25	0.34	8.33	"	
T18	1210	C 0.5	1.32	1.27	"	
T19	1210	A 1.0	7.6	0.56	"	
T20	1200	D 0.25	0.59	6.00	This Lab	Ni Cell

*Metal hydrides magnesium nitride from particulate material sampler.

with an error that was probably less than 10%.

One important question about these data is whether the peaks in the pressure curves were produced by outgassing. Blank[3] observed that when magnesium nitride was heated at 1130K the vapor pressure was initially high, but decreased over a period of 600 minutes to a steady lower value. She attributed this behavior to the evolution of water vapor from the hydrolysis product on the surface and to carbon monoxide from the reaction of magnesium oxide with the graphite effusion cell. But thermodynamic calculations for the reaction MgO + C = Mg(g) + CO(g) showed that the equilibrium pressure at 1110K was only 1% of the lowest pressures observed in our experiments and at 1210K was about 15% of the pressure measured in the Al.O effusion cell at 2000 minutes (see Fig. 18). Because the interfacial contact between the magnesium oxide and the graphite of the cell was low, it was doubtful that equilibrium pressures would be achieved for the reaction and this source of outgassing was probably negligible.

The quadrapole mass filter results--see Table VI--bear on the question of water vapor outgassing as the source of the peak. It was found that when hydrolysed magnesium nitride was heated, ammonia vapor was evolved along with the water vapor; however at temperatures above 950K ammonia was not detected indicating the completion of water vapor outgassing before 1130K was reached.

Additionally, when a sample was heated to 1110K without first being outgassed at 950K, the results were almost identical to those of an experiment that included outgassing--compare experiments T1 and T2 in

Figs. 11 and 12. The main difference in the two experiments was that when outgassing at 950K was omitted, the deflections of the effusion cell in the first few minutes were very large. But subsequently the pressures in the two experiments agree within 15%. This result, the thermodynamical argument and the quadrapole results provide strong evidence that the peak in each pressure versus time curve for magnesium nitride was due to vaporization of the nitride.

Another question about the peak is whether the time to reach the maximum--25 minutes for run T5 in Fig. 12 which was heated from 310K--was due to the slowness of heating or to some other factor. This question was answered in an experiment in which a B cell was charged with 5.4 grams of aluminum oxide powder in which a thermocouple was imbedded; Fig. 19 shows the temperature of the probe thermocouple and the thermocouple in the B cell as a function of time and also shows the difference in temperature of the two. It is seen in the figure that after 10 minutes the two thermocouples agree and the temperature of the powder was correctly measured by the probe thermocouple; thus, the slow rise to a maximum in pressure could not be attributed entirely to slow heating.

An examination of Fig. 11 shows that for experiments where the conditions--amount of charge and effusion temperature*--were the same, the vapor pressure varied inversely with the orifice area. For the experimental situation when the charge in the effusion cell was the

---

*In these experiments three different sizes of effusion cells were used and the same charge was always used in a cell of the same size. Thus a change in the amount of charge was accompanied by a change in the cross-sectional area of the effusion cell and in the internal geometry of the cell. Internal geometry is thought to be of secondary importance; however, cell cross-sectional area might be more important that the amount of charge; this question will be discussed in the Discussion section.

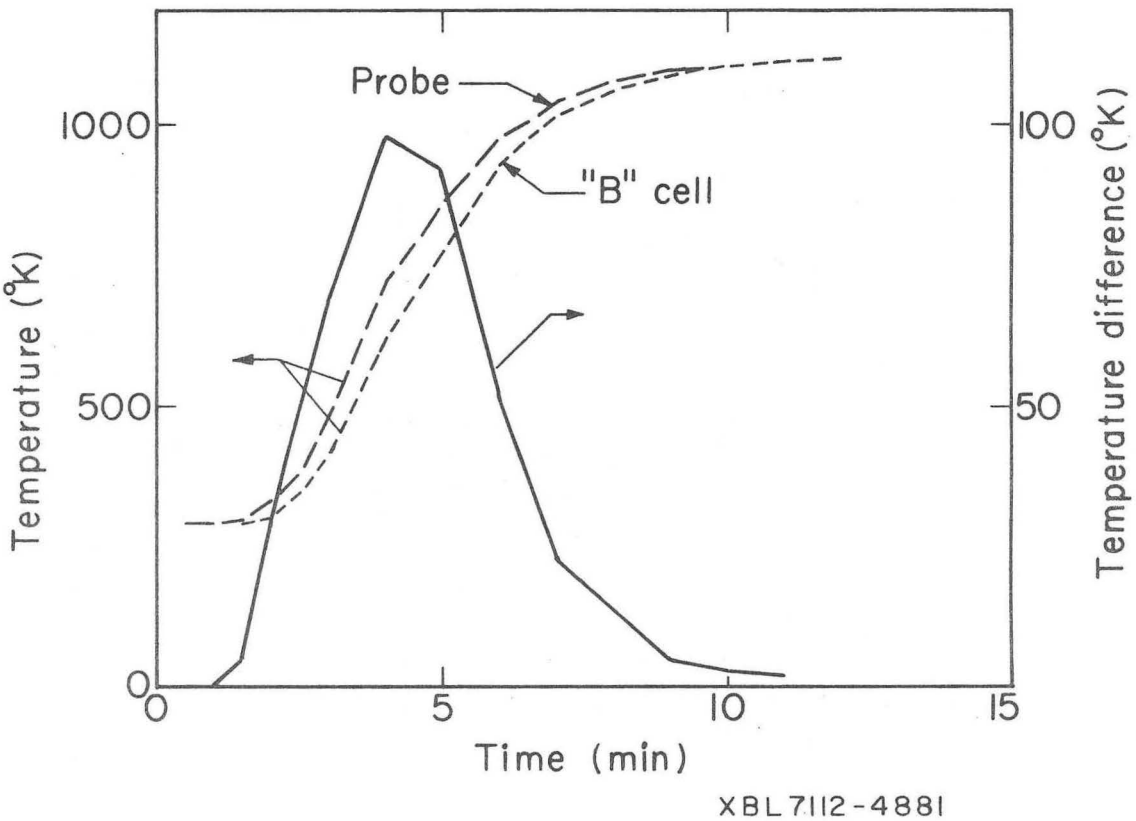

Fig. 19 Rate of heating from 298K for a "B" cell and the probe thermocouple in the torsion effusion furnace.

variable, Fig. 13 shows that the pressures observed in the large cell, B0.5 which contained 5.5 grams of magnesium nitride, was greater than that in the smaller cell, C0.5 which contained 1.4 grams of magnesium nitride. Higher pressures were observed for small orifices and for large charges of magnesium nitride in most of the experiments.

An exception is shown in Fig. 17 where the large effusion cell (run T20) contained 6.0 grams of magnesium nitride that was prepared in this laboratory and the small cell (run T18) contained 1.26 grams of Ventron magnesium nitride. The pressures in the two experiments were in fair agreement although the other results would lead to the expectation of higher pressures in run T20. This discrepancy probably arose because the specific surface area for the magnesium nitride that was prepared in this laboratory was exceptionally low (see Section III-F).

The results in Fig. 4 show that vapor pressures measured after an interruption in the vaporization process--the temperature was reduced to 940K for about 10 minutes-- resumed dropping in pressure near the point of interruption. However, it takes 7 minutes to reheat to 1150K but 15 minutes elapsed before the maximum pressure was attained--apparently an induction process was encountered on reheating after the delay of 10 minutes. That experiment T10 in the figure was made in a nickel effusion cell while the vapor pressure measurements were consistent with those in a graphite cell was a strong indication that side reactions were not interferring with the experiments.

In Fig. 15 the interesting feature is that run T15 was made at an oxygen pressure of 1×10^{-7} atm compared to run T11 where the oxygen pressure was 2×10^{-10} atm. It is seen that the initial vaporization

pressures during the oxygen run were higher but that the rate of pressure drop was unchanged (this is more obvious from the reciprocal pressure versus logarithm of time treatment of the data that is introduced in the Discussion).

The results of an experiment in an "A" effusion cell where the magnesium nitride vapor was exhausted at 1210K is presented in Fig. 18. The last two datum points were lower in pressure than would be expected from the trend of the preceeding points; this change was attributed to a substantial reduction in the amount of nitride left in the cell--approximately 70% had been exhausted at 2200 minutes when the accelerated drop in pressure began.

Since the vapor pressure above the magnesium nitride was nearer to equilibrium at higher temperature and appeared to be in equilibrium at temperatures above 1350K (see the transpiration data in the Introduction and Section III-D); an experiment to measure the equilibrium pressure at 1110K (see Section IV-B3) was conducted by rapidly cooling the effusion cell from 1390K to 1110K and monitoring the pressure--this was done after run T6 in Fig. 11 using the same cell and nitride. The results are shown in Fig. 20; the inflection point in the curve was at 27 minutes which can be compared to 20 minutes required for cooling to 1110K and indicated that the equilibrium pressure was about 5.2×10^{-4} atmospheres at 1110K. It was also noted that the lowest pressure observed in run T6 was 1×10^{-4} atmospheres compared to the leveling off pressure of 1.9×10^{-4} atmospheres for this experiment; this indicated that preheating to 1390K raised the steady state pressure.

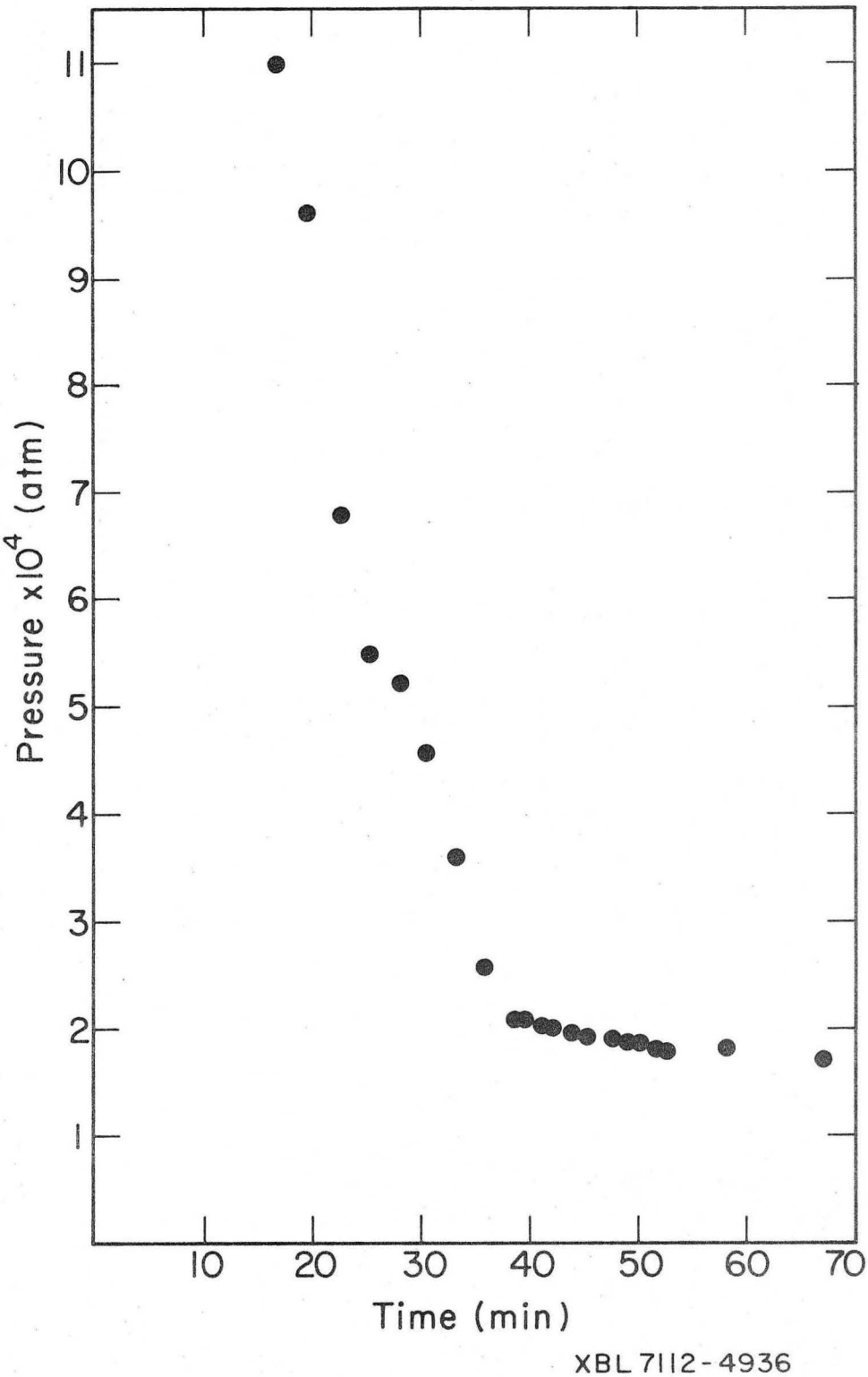

Fig. 20 Inflection in vapor pressure vs time curve for B0.15 effusion cell cooled from 1390K, inflection gives equilibrium at 1110K.

D. Pressure Versus Temperature Experiments

Measurements of the vapor pressure as a function of the temperature repeated to see if the anomalous results obtained by eariler workers[1-3] (Fig. 1) could be duplicated and to provide additional data for understanding the vaporization of the nitride. Experiments were made with charge ratios, the ratio of the sample weight in grams to the effective orifice area in cm^2, ranging from 15.0 in the A2.0 cell to 28,000 in the B0.15a* cell. The enthalpy of vaporization was calculated by using pressures for which λ/D** was greater than one--Blair and Munir[48] found a change from molecular flow to transition flow[41] at this value in their effusion study of calcium nitride.

The results of experiments conducted in the D0.25 cell are shown in Figs. 21 and 22. Metal Hydrides and Ventron magnesium nitride were used after outgassing to remove Mg(g) and H_2O(g); the charge ratio, was 12,000 for both. Each data point is numbered in the order that it was taken. Figure 21 shows the first and last series of points in the Metal Hydrides experiment to give an overall indication of how the magnesium nitride behaved during this type of experiment.

The first points were measured about 10 minutes after the samples reached the temperatures of appreciable vaporization. It is seen by following points one to six that the pressure approached the calculated equilibrium line in the middle of the temperature range while at the

---

*This cell differs from the B0.15 cell in Table III because of an 2L/D ratio of 16.7 and an effective orifice area of 1.9×10^{-4} cm^2.

**λ/D is the ratio of the mean free path of the vapor to the orifice diameter; it is calculated by using the hard sphere approximation[41] and the molecular diameter of nitrogen.[47]

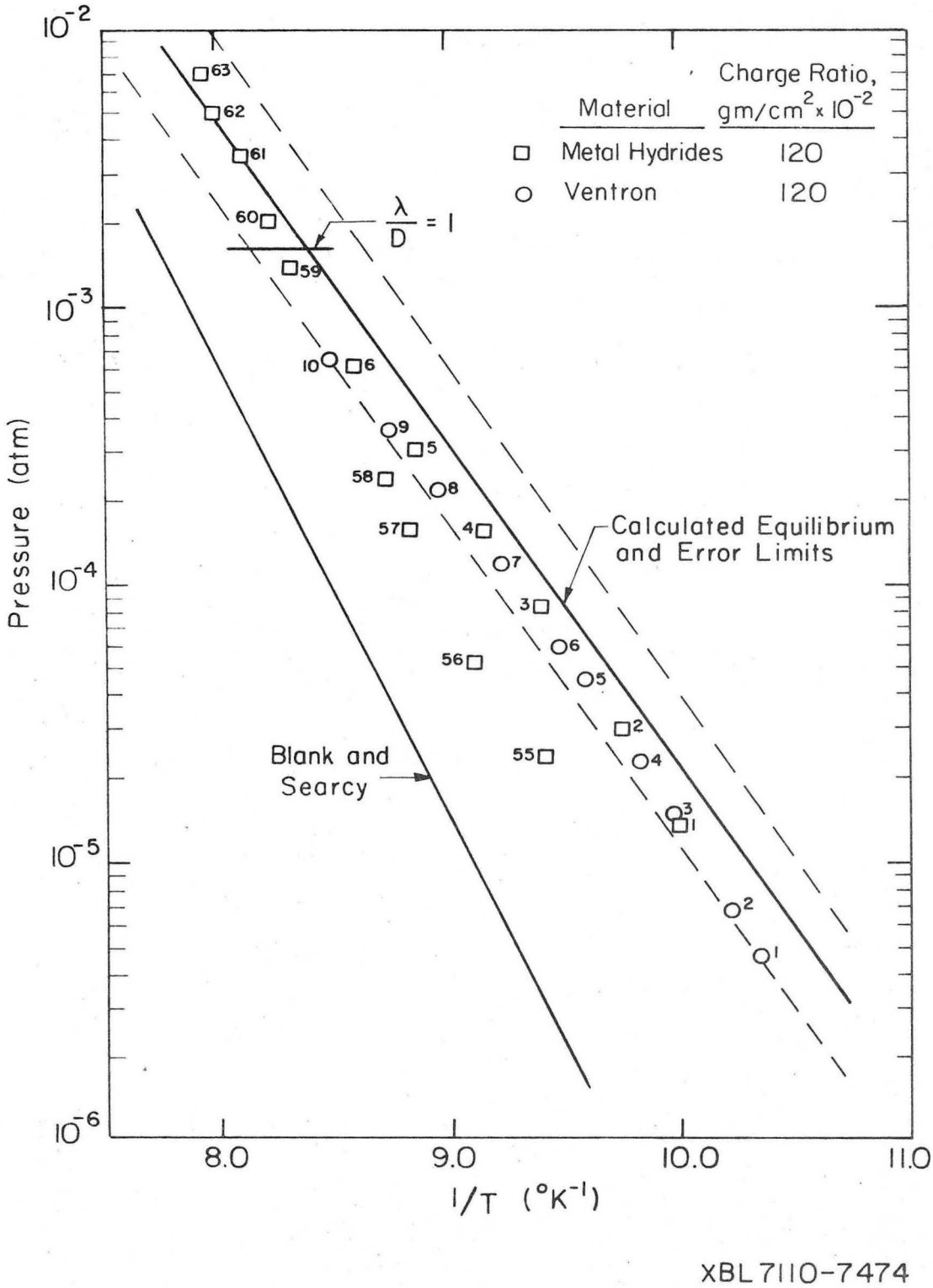

Fig. 21 Vapor pressure of magnesium nitride in a D0.25 effusion cell using 7 gm charges.

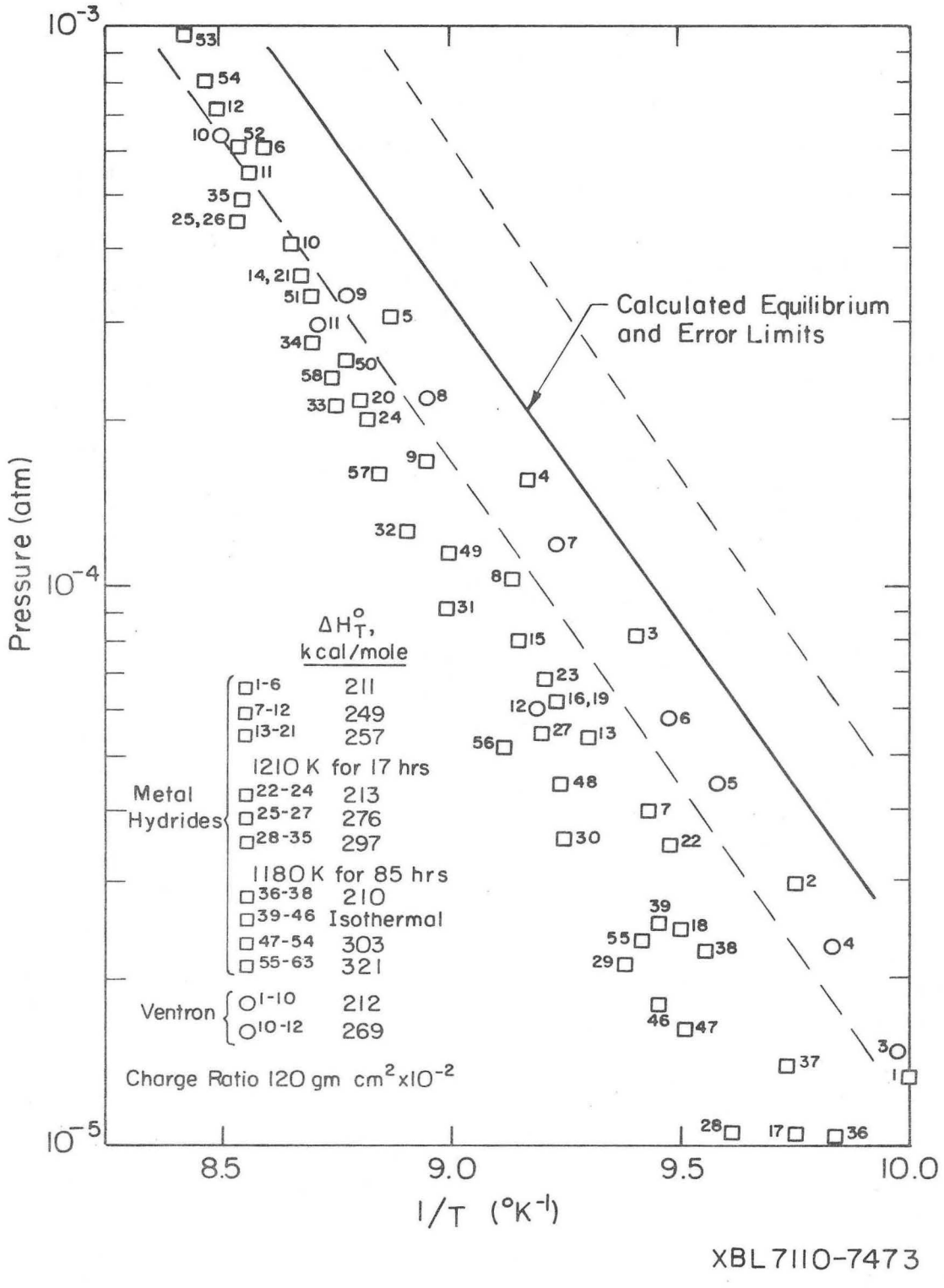

Fig. 22 Vapor pressure of magnesium nitride in a D0.25 effusion cell using 7 gm charges.

ends of the temperature range the pressure bent away from equilibrium; this was also the case for the Ventron material in points 1 through 10. After many intervening measurements points 55 through 63 were taken; it is seen that they had a steeper slope and that at higher temperatures the pressure approached equilibrium.

The points in the pressure range of 10^{-5} atm to 10^{-3} atm in Fig. 21 along with all of the other data points that were taken are shown in Fig. 22. It was seen that at the highest temperatures the ratio of the highest to the lowest pressures was about 1.4, while at the lowest temperatures the ratio was 3.5. It was also observed that the enthalpy of vaporization calculated from each successive series of points has a greater value with the exception that heating at a temperature above 1180K prior to determining the slope resulted in a near equilibrium slope--the enthalpy of vaporization at 1100K is 210 kcal/mole. Thus for the Metal Hydrides material the first series of points had a near equilibrium slope of 211 kcal/mole and the last series had a slope of 321 kcal/mole; the Ventron material behaved similarly.

Another feature of interest in Fig. 22 was that the pressure could be raised by 50% at low temperature as a result of heating at high temperatures (see Material Hydrides points 28 and 38). The isothermal experiment involving points 39 through 46 showed that 1000 minutes were required for the pressures to fall to their former level when the temperature was 1050K.

The pressures of Fig. 22 averaged a factor of 5 greater than the pressures of Blank and Searcy; however, when the charge ratio was increased by two order of magnitude to charge ratios similar to theirs,

close agreement with their data was obtained, as shown in Fig. 23. The Ventron material was heated for 2000 minutes at 1210K prior to making the measurements (see Fig. 17 for the first part of this period) which was on a par with Blank and Searcy's procedure of heating at 1280K for 1200 minutes; while the purified material was merely outgassed at low temperature. As with the previous experiment it was observed here that heating at a high temperature (on the order of 1250K) followed by a pressure measurement at around 1100K gave rise to a datum point that was much higher in pressure than points not taken in this way--datum point 15 was a result of this procedure.

When the charge ratio was reduced again by almost two orders of magnitude by using an A2.0 effusion cell the vapor pressures fell considerably below the data of Blank and Searcy as shown in Fig. 24. These samples were outgassed at low temperatures to drive off $H_2O(g)$ and $Mg(g)$. Here it is again noted that the apparent enthalpy of vaporization increased as vaporization progressed and data points for the Metal Hydrides material used by Blank and Searcy curved away from equilibrium on the ends of this temperature range. Also, the pressures decreased as the vaporization progressed as was observed in the experiments with higher charge ratios.

Figure 25 shows the results of experiments in a B0.15a effusion cell and a B0.25 effusion cell for which the charge ratios were 280 and 220, about twice that used in the D0.25 experiments described above. The Metal Hydrides material was heated for 40 minutes at 1200K and the Ventron material was heated for 20 minutes at 1200K prior to making vapor pressure measurements. The main feature of interest in this figure was that pressures

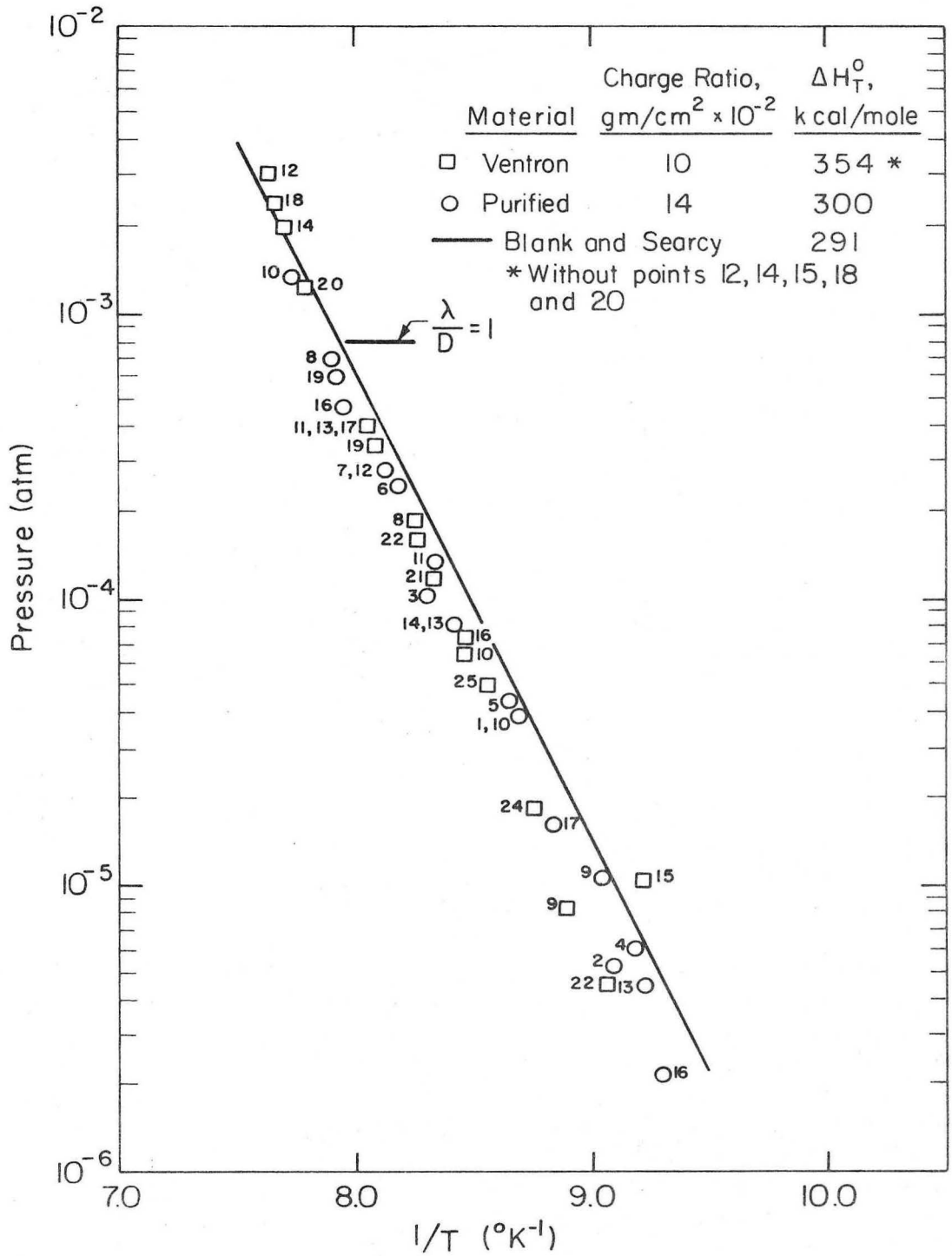

Fig. 23 Vapor pressure of magnesium nitride in a C0.5 effusion cell with a 1.3 gm charge of Ventron magnesium nitride and in a B0.5 effusion cell with a 2.0 gm charge of purified magnesium nitride.

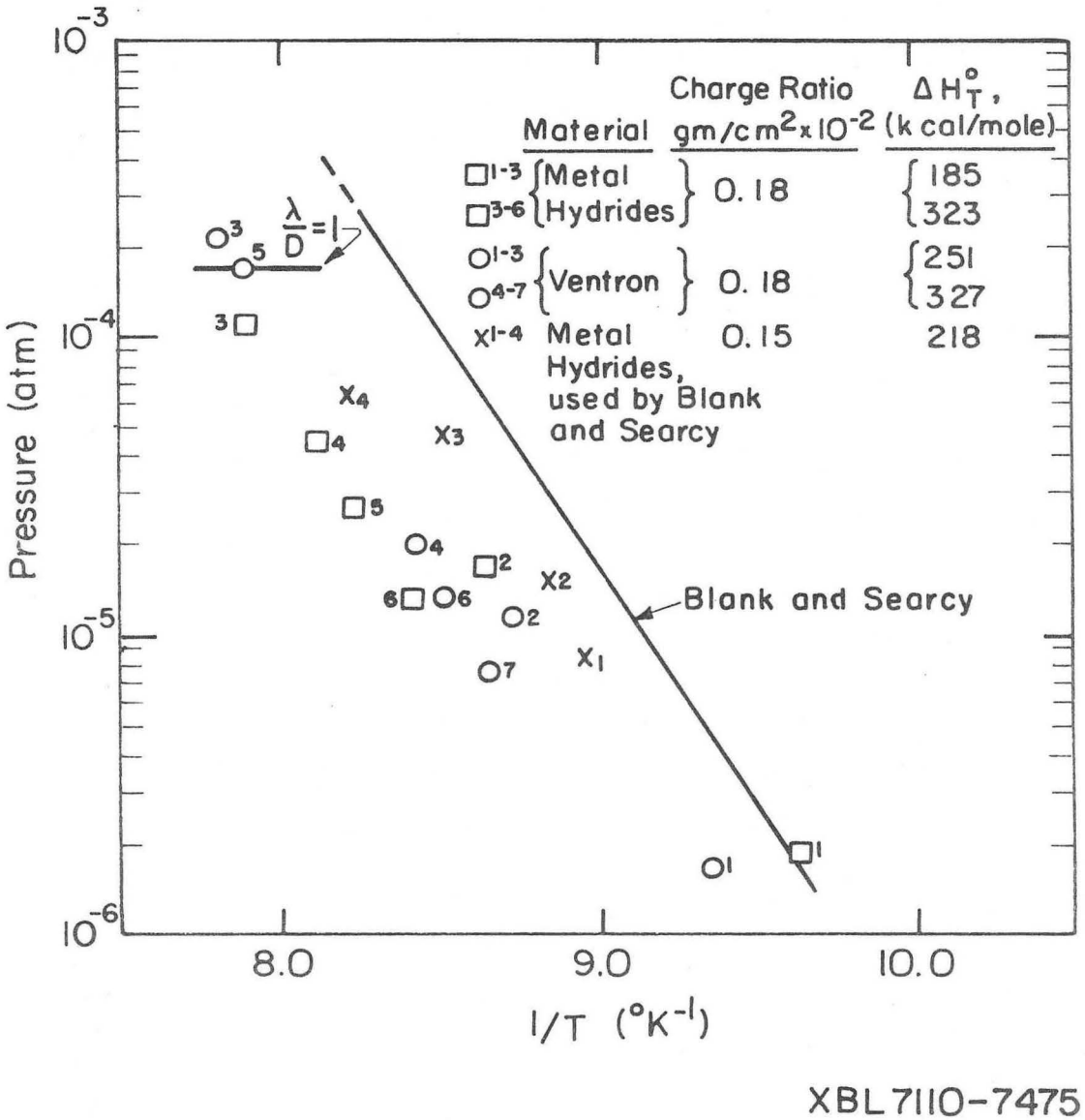

Fig. 24 Vapor pressure of magnesium nitride in a A2.0 effusion cell with 0.7 gm charges.

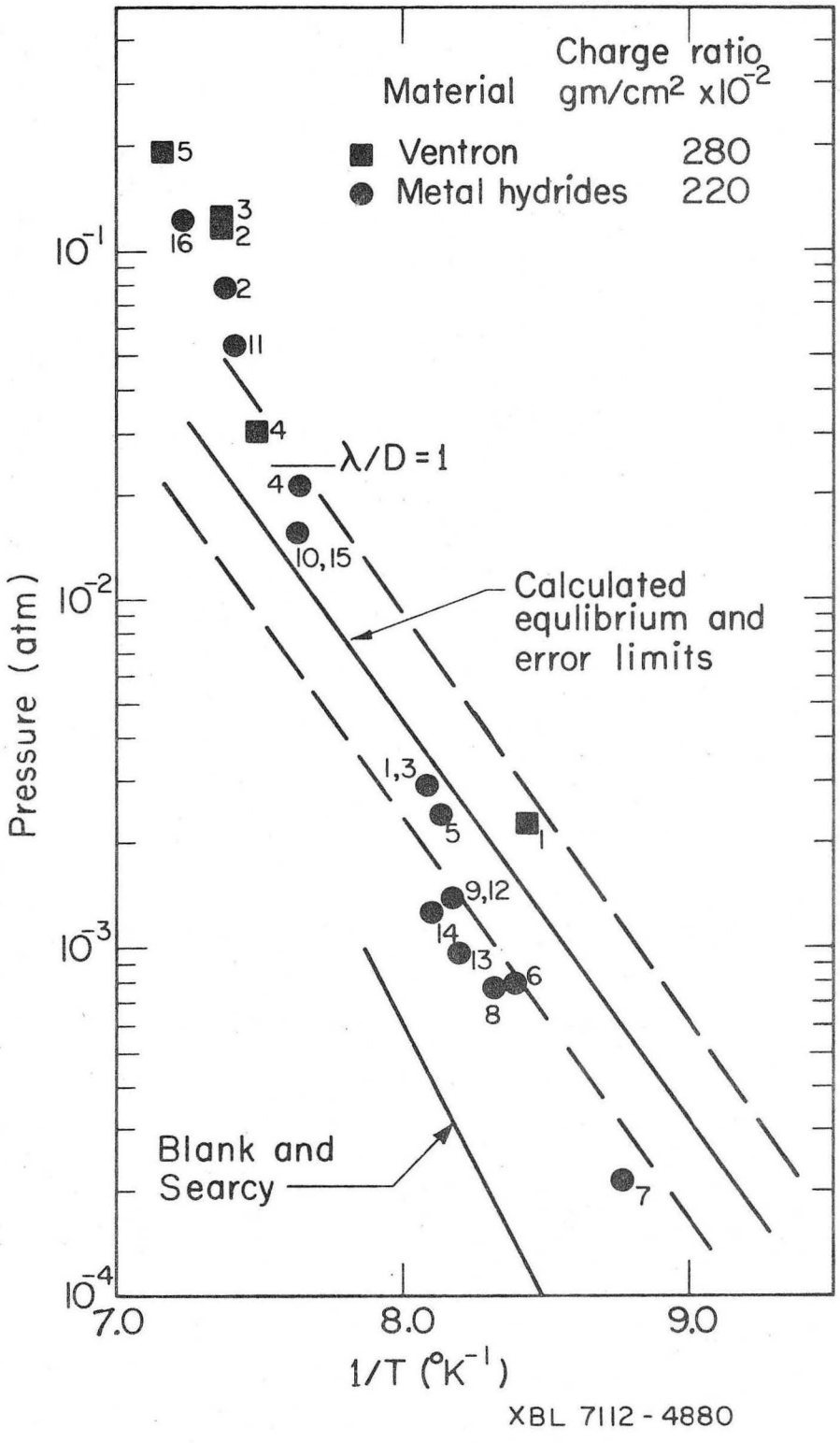

Fig. 25 Vapor pressure of magnesium nitride in a B0.25a effusion cell with a 5.5 gm charge of Ventron magnesium nitride and in a B0.25 effusion cell with a 7.4 gm charge of Metal Hydrides magnesium nitride.

above the calculated equilibrium line were obtained for λ/D ratios greater than and less than one.

With $\lambda/D < 1$ the measured pressures were a factor of four greater than the calculated equilibrium pressures at $T^{-1} = 7.25 \times 10^{-4}$ K^{-1}; however, Carlson[62,63] has shown that for the effusion of mercury, the change from molecular flow to hydrodynamical flow[41] caused an increase in the apparent vapor pressure by a factor of two. Using this factor to correct the vapor pressure at $T^{-1} = 7.25 \times 10^{-4}$ K^{-1} gave an estimate of the equilibrium pressure of 7×10^{-2} atm; this was near the upper error limit of the calculated vapor pressure. Several points with $\lambda/D < 1$--point 1 for the Ventron run and points 4, 10, and 15 for the Metal Hydride run--also had pressures near the upper limit suggesting that the equilibrium vapor pressure is near the upper limit.

E. Langmuir Experiments

The results of experiments using the Langmuir technique are shown in Fig. 26 with the results of Blank and Searcy shown for comparison. It is seen that there was order of magnitude agreement between the two studies; however, the present results were erratic. The datum points in the figure are numbered to give the order in which they were taken. The erratic behavior was most apparent in experiments 2 through 5 where it was observed that the pressure increased at constant temperature and that the increase often came as an instantaneous jump.

Microscopy of the Langmuir surface identified two reasons for the pressure rise--surface roughening and rupture of a magnesium oxide protective film. In experiment number 2 all of the nitride was vaporized

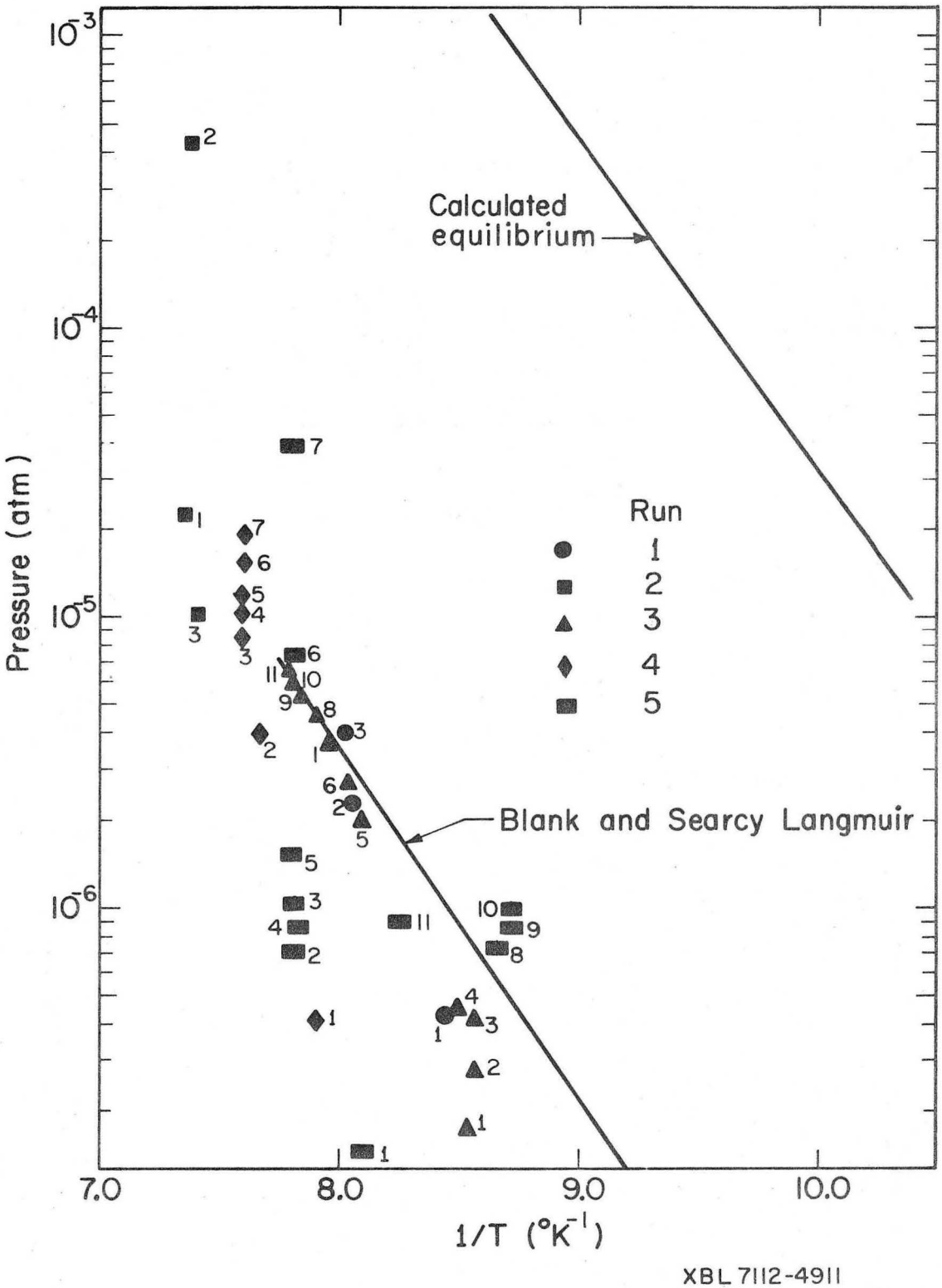

Fig. 26 Langmuir vapor pressure of polycrystalline magnesium nitride and results of Blank and Searcy's Langmuir work.

and the film shown in Fig. 27 remained. The increases in pressure in this experiment can be explained by the rupture and removal of parts of this film and its pealing away from the surface. Figure 28 shows the surface of a magnesium nitride Langmuir sample that had not been vaporized and Fig. 29 shows a sample for which the surface has been abraded to show the pore structure; the lower micrograph is a close-up of the "T" shaped pore. Figure 30 shows the Langmuir sample after evaporation experiment number 3 where it is seen that deep pits were beginning to form in the sample and there was a coarsening of the surface; the lower micrograph is a close-up of the pore in the center. Figure 31 shows the Langmuir sample after experiment number 5; here the deep pitting has been carried further and part of the film can be seen covering an area where the underlining magnesium nitride has evaporated. Figure 32 shows a magnesium oxide film partially covering the nitride after experiment number 4; it was estimated that this greyish film covered approximately 25% of the surface.

The presence of the magnesium oxide film obscured the vapor pressure measurements since it was not certain what percentage of the surface of the Langmuir sample was covered. However, the pressures were of the same order of magnitude as those measured by Blank and Searcy at 1250K.

F. Microscopy of Magnesium Nitride Powders

The pressure versus time studies reported in Section III-C indicated that the highest vapor pressures are observed in effusion cells that contain the most magnesium nitride, all other factors being equal. An exception was seen in Fig. 17; the D0.25 effusion cell contained 6 grams

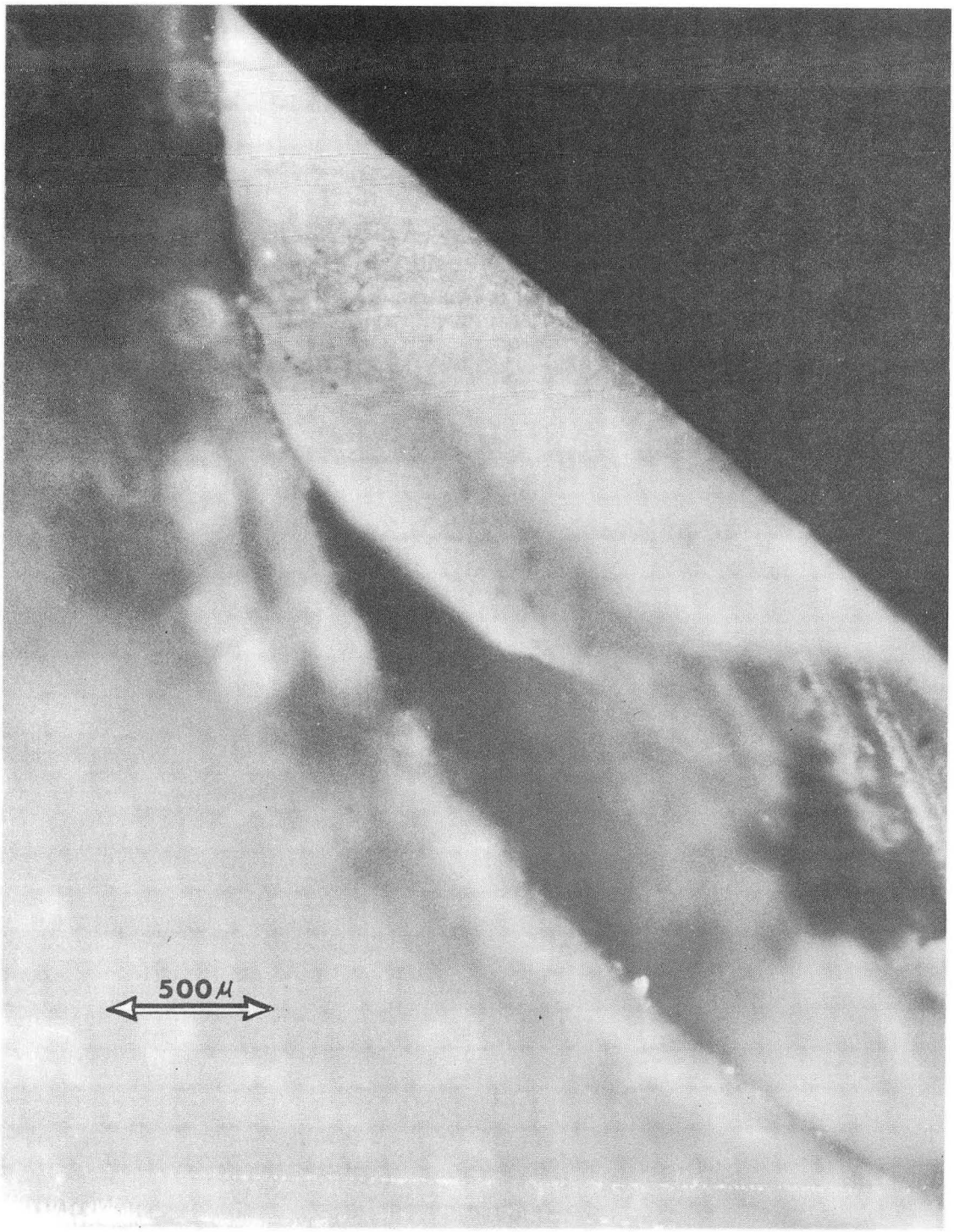

XBB 7112-5897

Fig. 27 Optical micrograph of the magnesium oxide film that remained after complete evaporation of a magnesium nitride Langmuir sample. Part of the Langmuir orifice is also shown in the photograph.

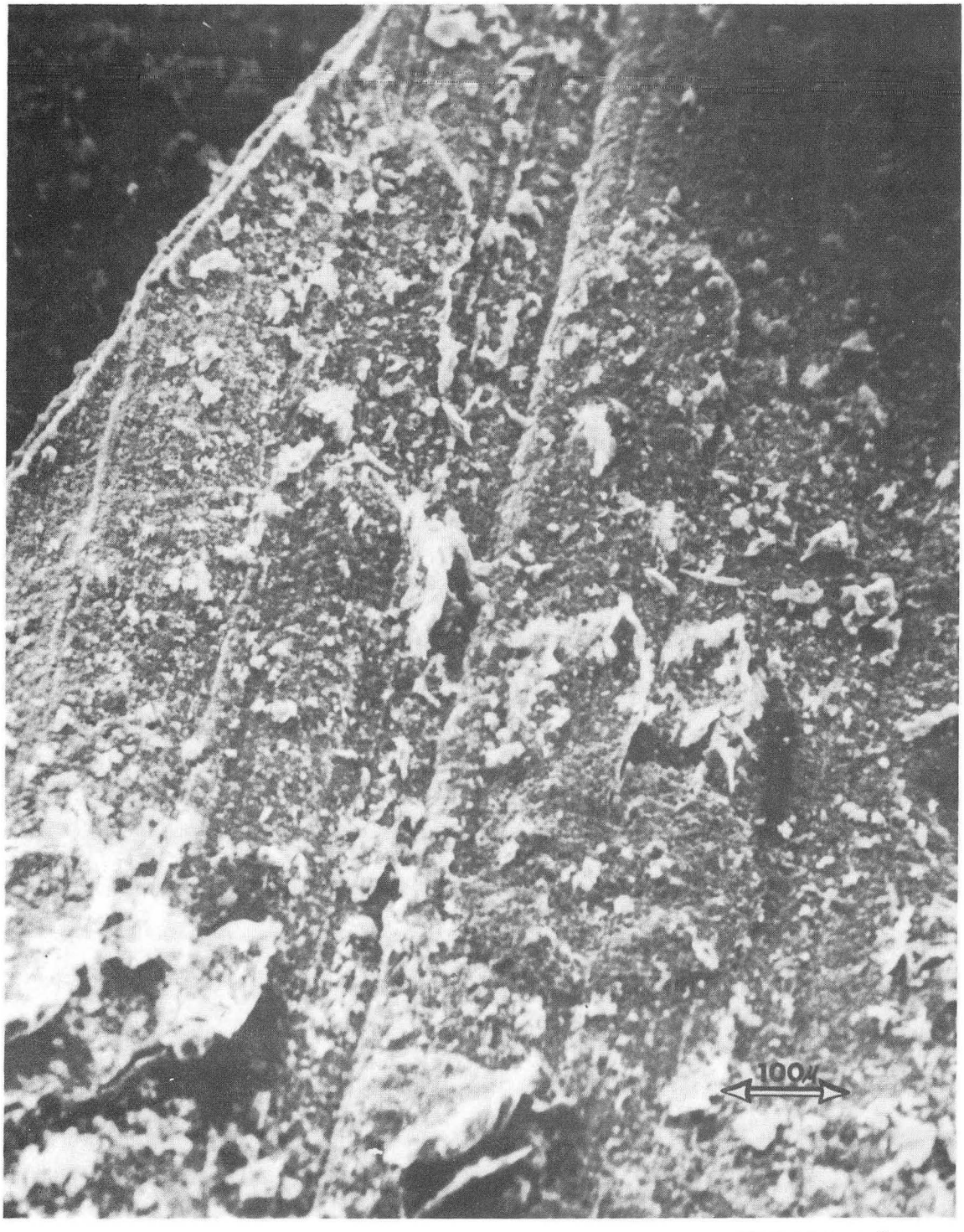

XBB 7112-5893

Fig. 28 Scanning electron micrograph of the surface of a magnesium nitride Langmuir sample before vaporization.

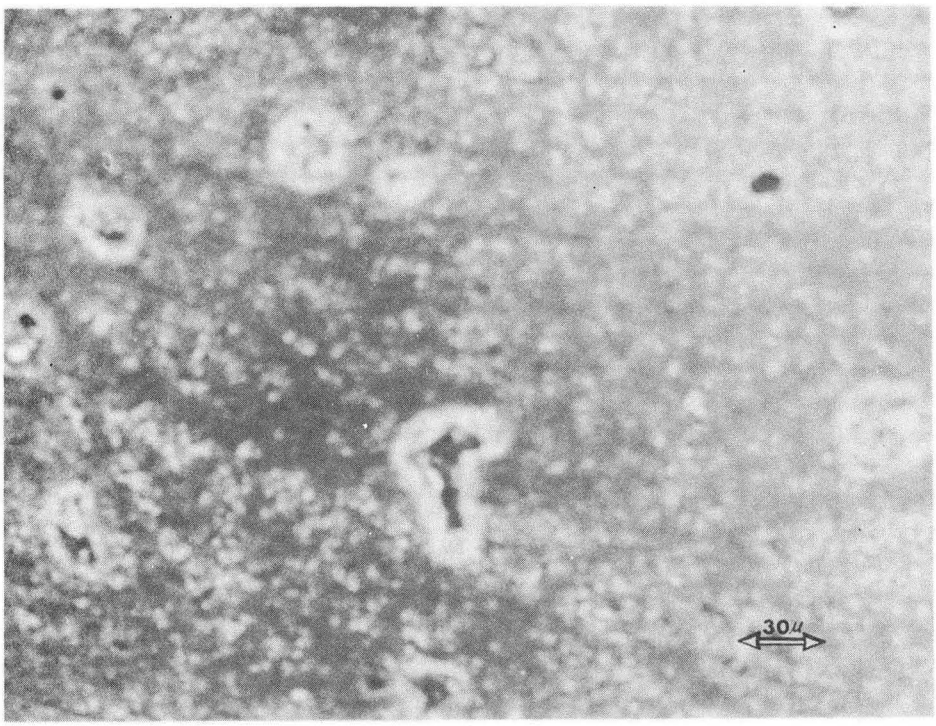

(a)

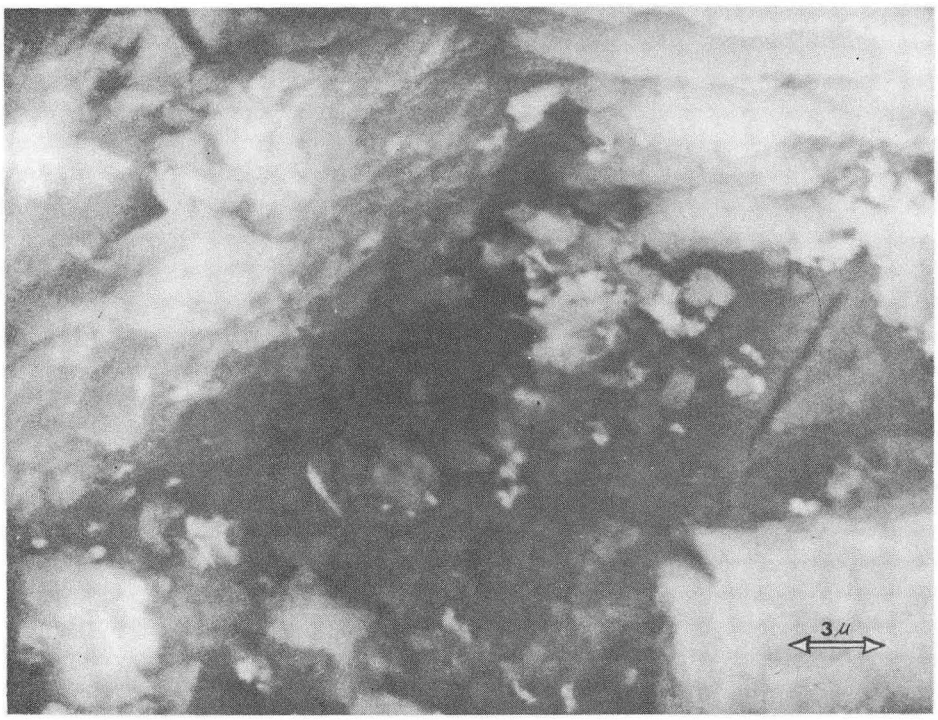

(b) XBB 7112-5899

Fig. 29 Scanning electron micrograph of a magnesium nitride Langmuir sample after polishing to show the pores. At bottom an enlargement of the "T" shaped pore shown above.

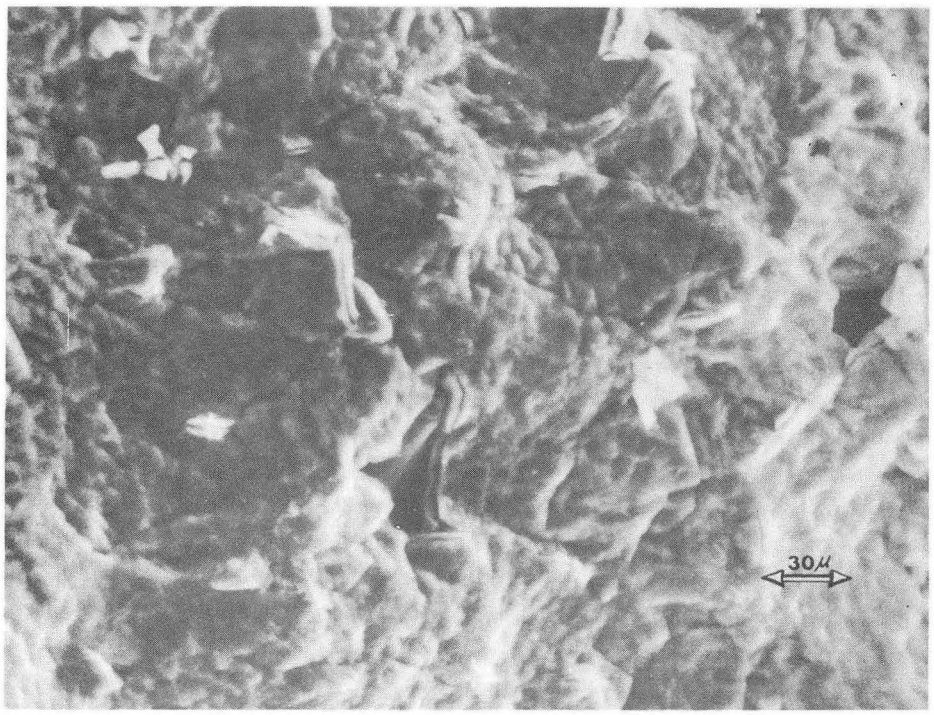

(a)

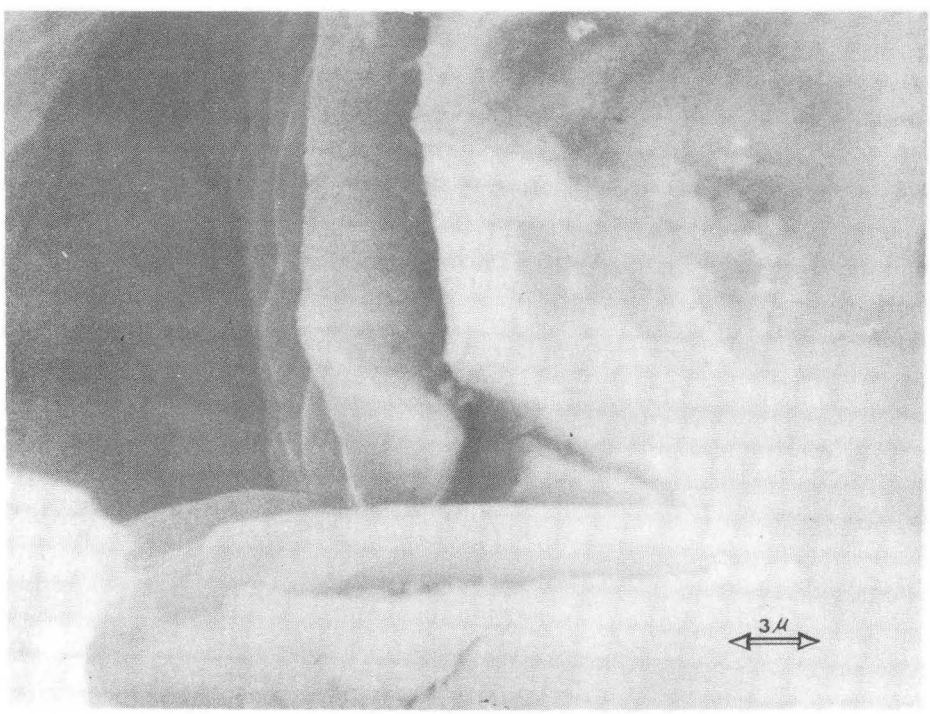

(b) XBB 7112-5896

Fig. 30 Scanning electron micrograph of a vaporized magnesium nitride Langmuir sample. At bottom an enlargement of the large pore in the middle of upper micrograph.

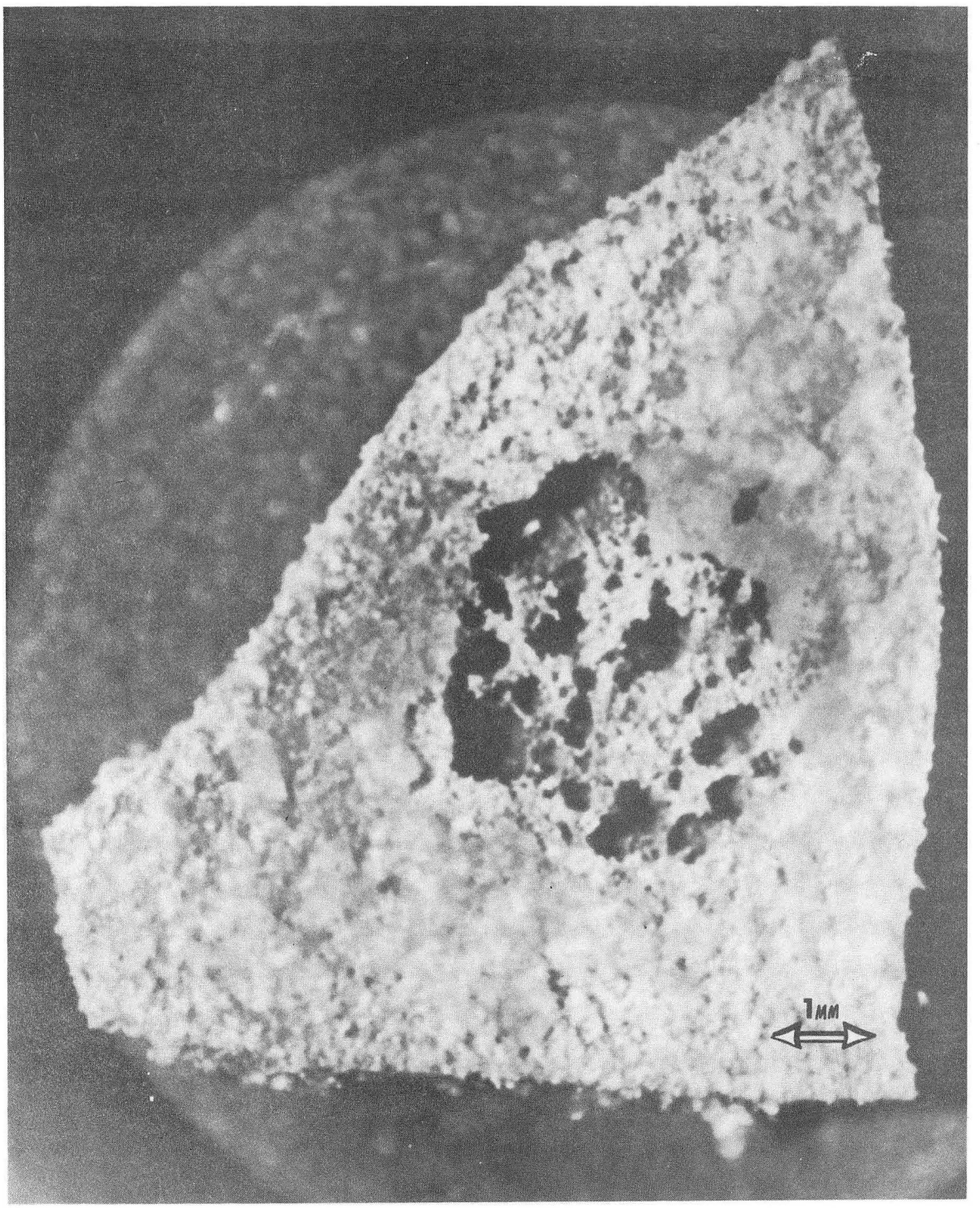

XBB 7112-5900

Fig. 31 Optical micrograph of a Langmuir sample after vaporization.

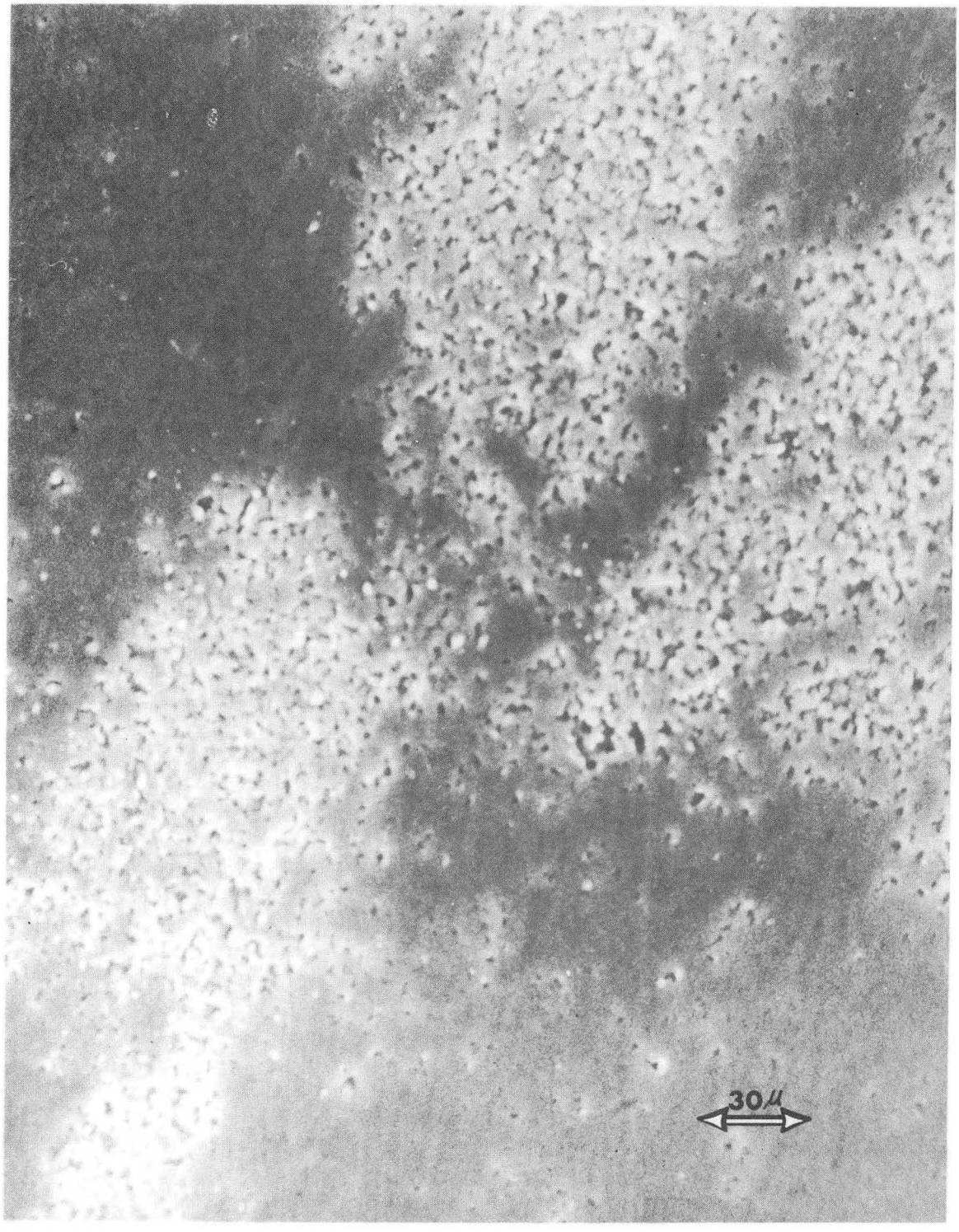

XBB 7112-5895

Fig. 32 Scanning electron micrograph of a Langmuir sample after vaporization, showing partial coverage by a magnesium oxide film.

of nitride and the C0.5 effusion cell contained 1.27 grams, but the pressures measured in the two cells were equal. The difference in these two experiments that accounted for the result was the specific surface area of the two samples.

Ventron magnesium nitride was used in the C0.5 effusion cell while nitride prepared in this laboratory was used in the D0.25 cell. The Ventron material had the same type of structure as the Metal Hydrides material that was studied here. Figure 33 is a light micrograph of Metal Hydrides material showing fibers and fuzzy looking spherical particles. Figures 34 and 35 show scanning electron micrographs of some of the spherical particles. At the top of Fig. 34 a broken particle of magnesium nitride shows that it consists of fibers; the bottom part of the figure shows a particle that has a part of its outer shell broken indicating that it is porous. Figure 35 shows two other particles that are fiberous and porous.

A light micrograph of the magnesium nitride powder prepared in this laboratory is shown in Fig. 36. The particles are larger and more angular than the Metal Hydrides particles. Figure 37 is a close-up of one of the particles; it appeared to have high density--probably 90% as measured for the Langmuir samples. The average particle was roughly equivalent to a sphere with a diameter of 70 microns while the Metal Hydrides material was made of fibers that were about 10 microns long and about 0.5 micron across. The ratio of specific surface areas for the two was calculated from these dimensions; it was about 30.

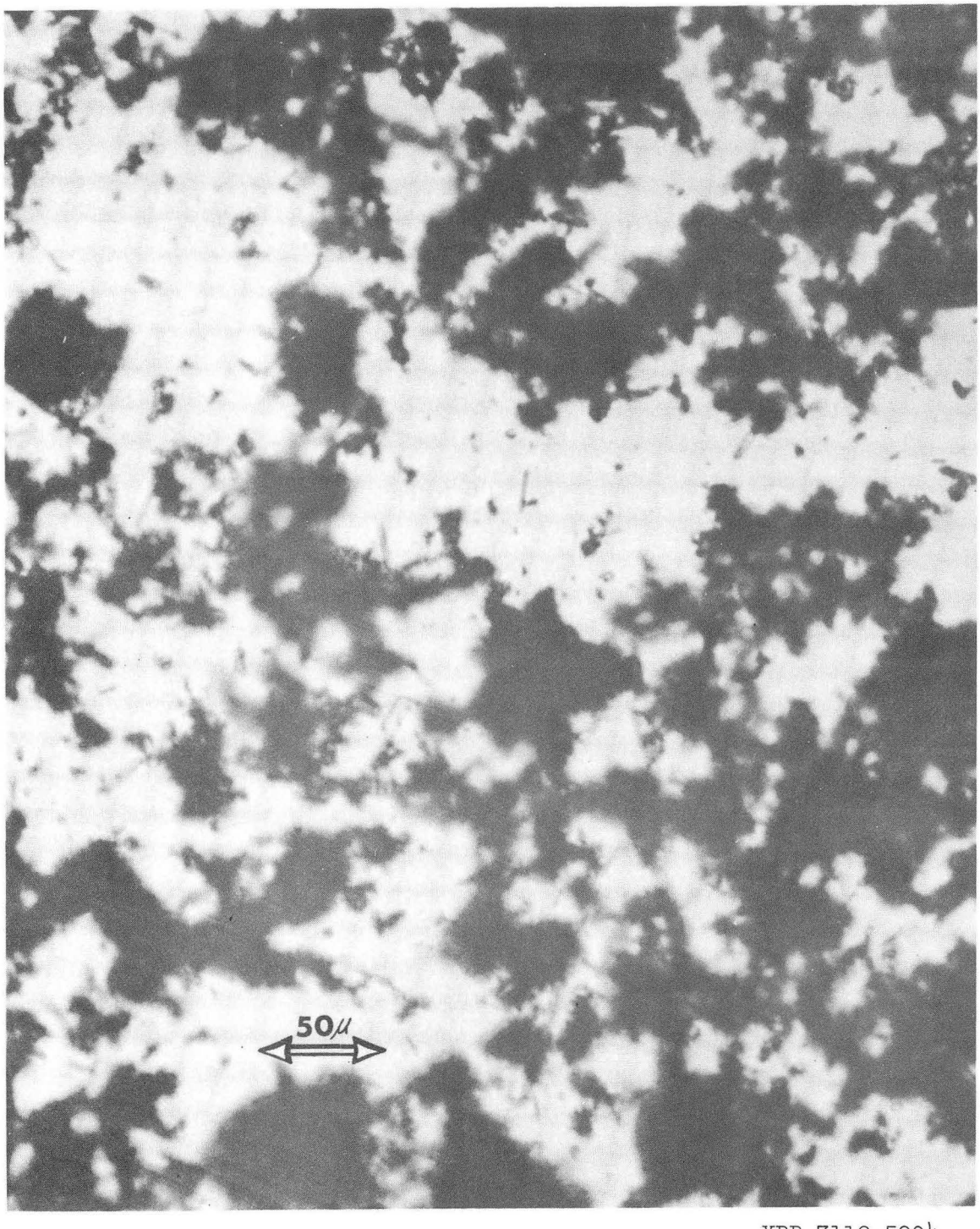

XBB 7112-5904

Fig. 33 Light micrograph of Metal Hydrides magnesium nitride powder.

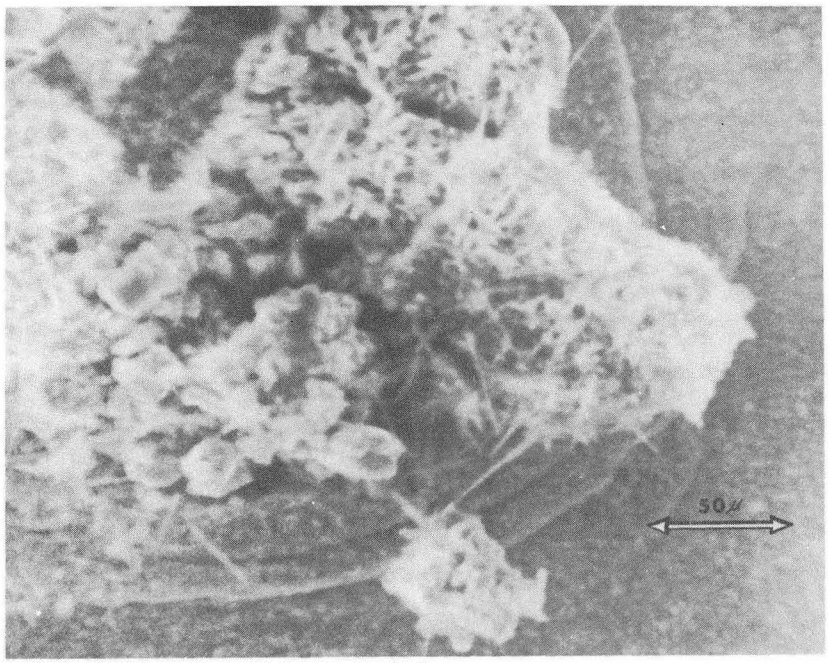

(a)

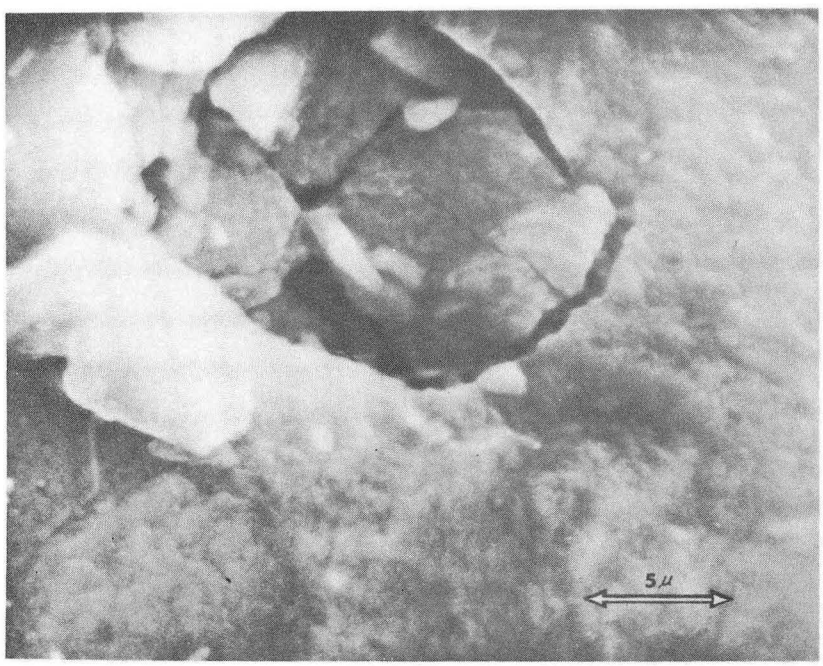

(b) XBB 7112-5901

Fig. 34 Scanning electron micrograph of particles from Metal Hydrides magnesium nitride.

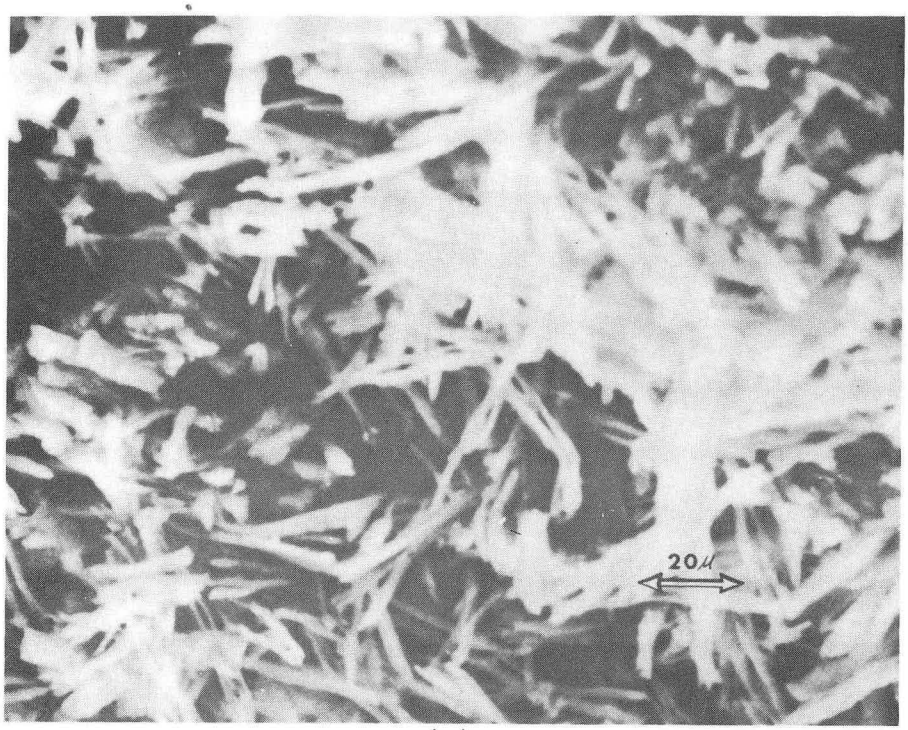

(a)

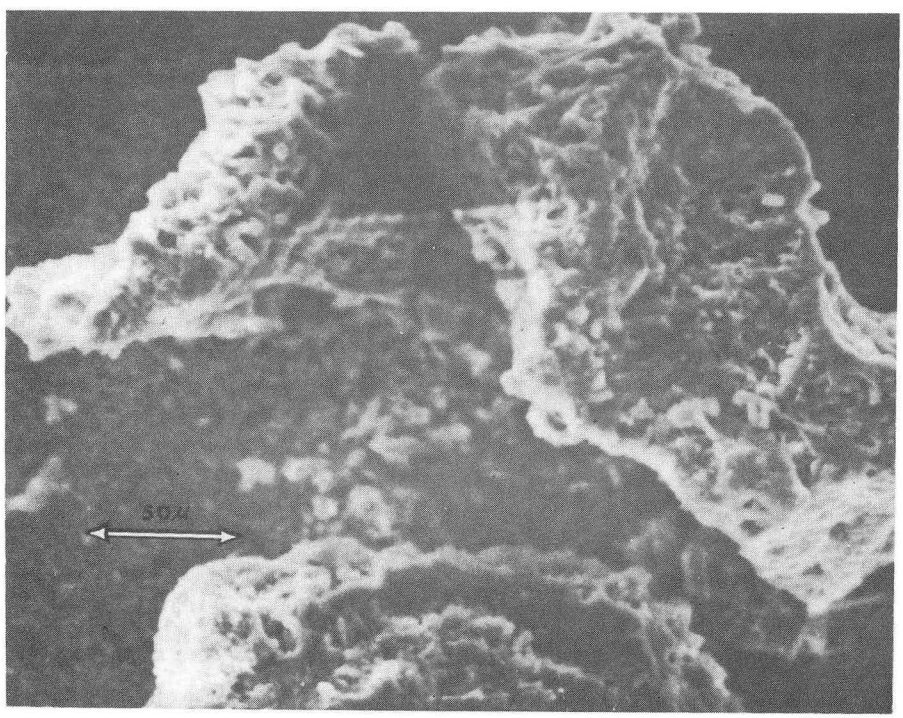

(b) XBB 7112-5902

Fig. 35 Scanning electron micrograph of particles from Metal Hydrides magnesium nitride.

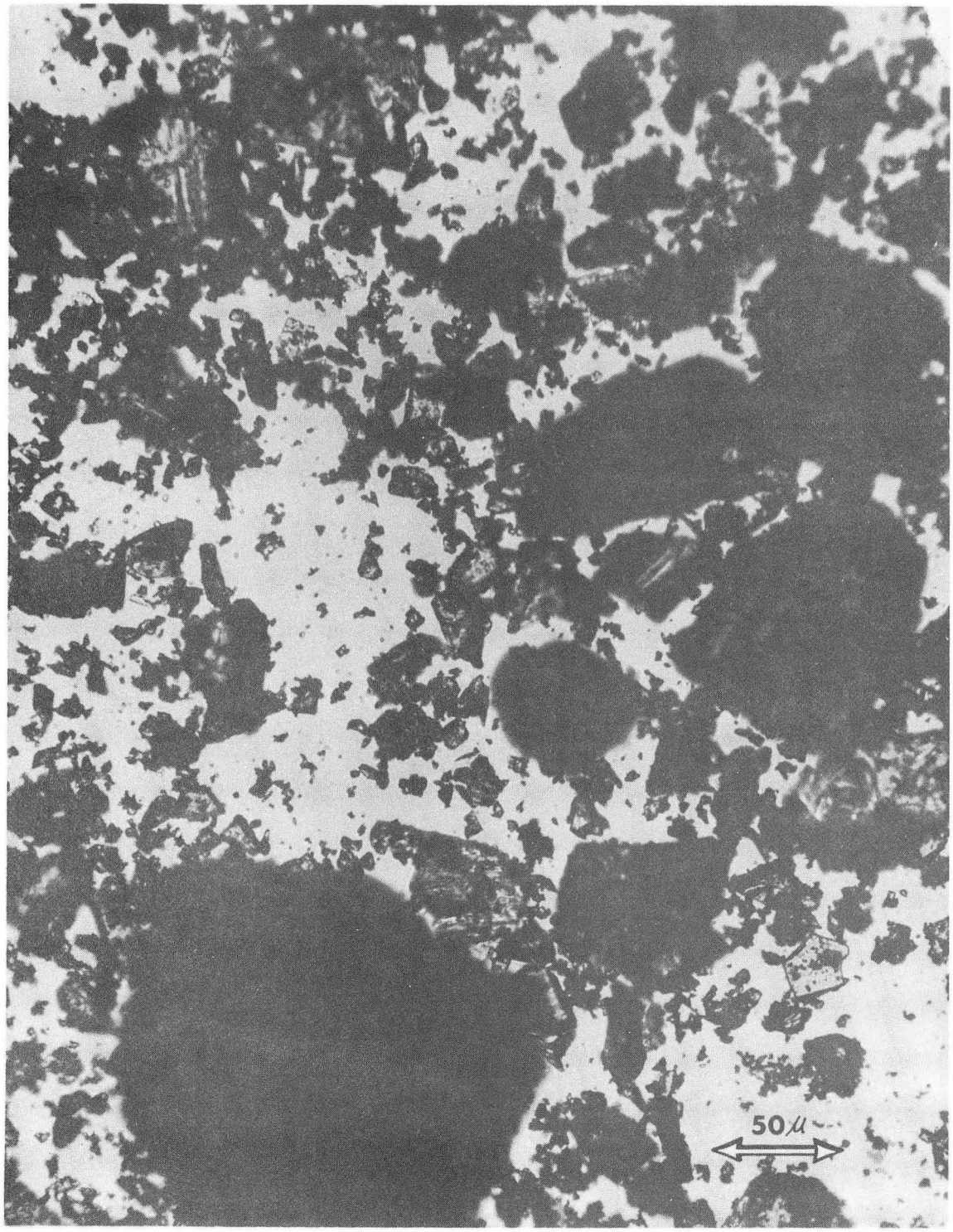

XBB 7112-5903

Fig. 36 Light micrograph of magnesium nitride particles prepared in this laboratory.

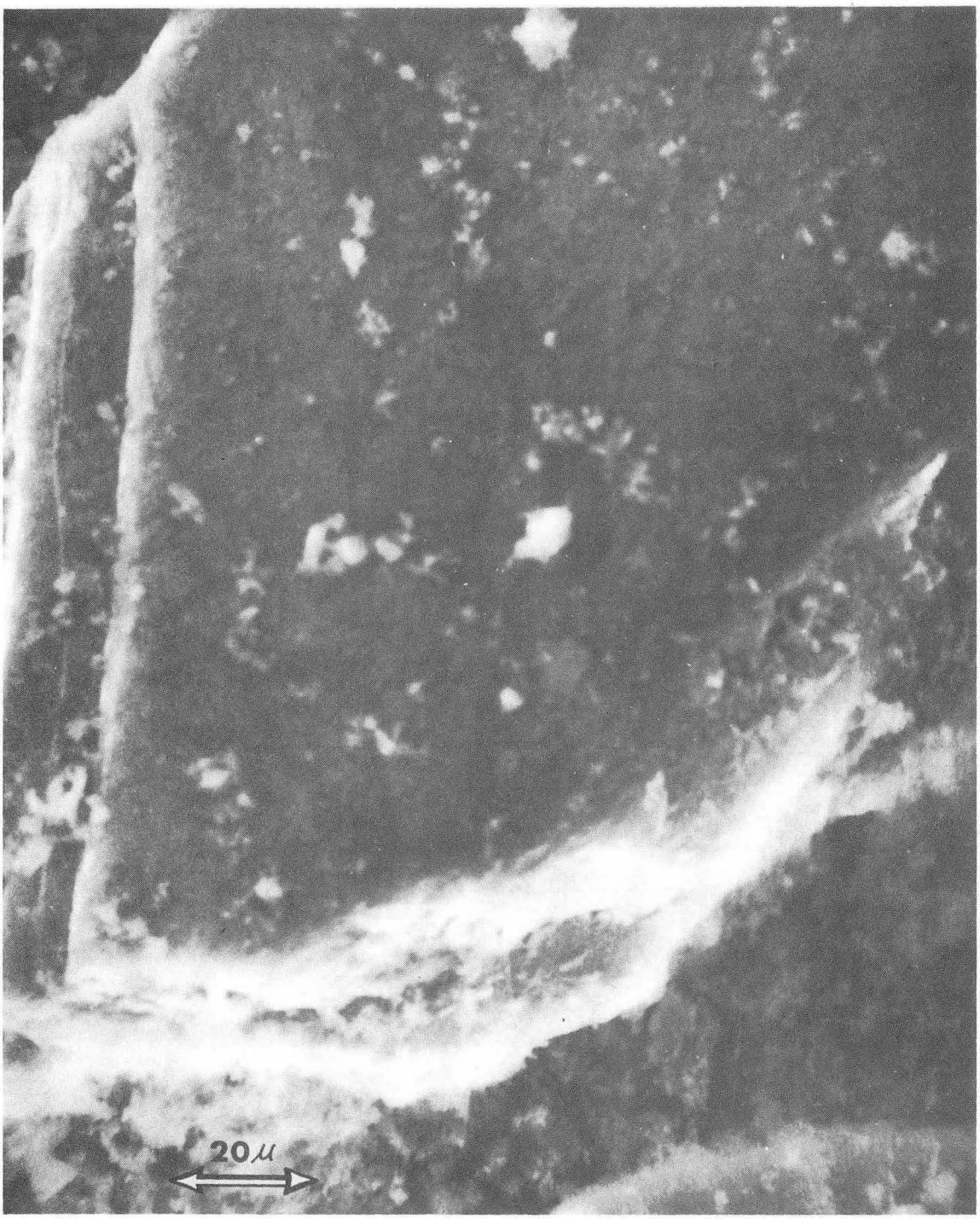

XBB 7112-5905

Fig. 37 Scanning electron micrograph of magnesium nitride particle from material prepared in this laboratory.

IV. DISCUSSION

In the Introduction the vapor pressures for magnesium nitride measured prior to this work were discussed; those pressures were lower than pressures predicted from independent thermochemical data, their temperature dependency was much greater than expected, the pressures measured by different workers were widely different and the Motzfeldt-Whitman[22,23] treatment of the data failed to give the expected equilibrium pressures. Our pressure versus temperature results--see Section III-D--were consistent with these observations and our pressure versus time results--see Section III-C--showed that the vapor pressure of magnesium nitride is strongly time dependent at the start of vaporization and weakly time dependent during the later stages of vaporization.

In many Knudsen effusion measurements[33-35] the vapor in the effusion cell is at the equilibrium vapor pressure and in some studies[49-51] the only difficulty is that the evaporation coefficient is small; this results in measurements that are below the equilibrium vapor pressure. But, by conducting experiments with several different orifice areas and by using the Motzfeldt-Whitman extrapolation[22,51,52] technique (see Section IV-B) equilibrium pressures can be determined. The temperature dependencies for systems of this type give the enthalpy of vaporization.

In two systems[27,28,53] in addition to magnesium nitride (magnesium hydroxide and gallium nitride) there have been observed time dependent vapor pressure measurements, measurements that were much lower than expected, a temperature dependency for the vapor pressures that was much greater than expected and for magnesium hydroxide and magnesium nitride the Motzfeldt-Whitman extrapolation failed (it was not tried for gallium

nitride). For all three of these systems the suggestion has been made[2,3,27,52] that a surface phenomenon was causing the discrepancies.

Blank and Searcy[3] suggested a mechanism for magnesium nitride vaporization in which surface sublimation sites were covered by the adsorption of water vapor or oxygen, and Schoonmaker, et al.[53] suggested a mechanism for gallium nitride vaporization in which a layer of gallium built up on the surface of the gallium nitride and acted as a diffusion barrier; but neither could provide further details to explain the discrepancies mentioned above. By resolving these discrepancies for magnesium nitride it is hoped that insights will be provided for these and other systems with unusual vaporization characteristics.

To see if some of the discrepancies are related to an incorrect identification of the vaporization reaction, we studied the vapor phase above magnesium nitride with a mass spectrometer and made an x-ray diffraction study of the solid phase. The evidence (reported in Section III-A) showed Eq. (1) to be the vaporization reaction (as previous workers had assumed) and afforded no explanation.

No reactions between the effusion cell and the magnesium nitride were observed, and effusion cells made of nickel and of graphite gave the same vaporization behavior. Thus, it is unlikely that interaction with the effusion cell can be used as an explanation for the discrepancies.

To explore other possible explanations for the behavior of magnesium nitride it will be helpful to examine the theory that relates the vapor pressure with other variables in Knudsen effusion measurements.

A. Motzfeldt-Whitman Equation

Motzfeldt[22] and Whitman[23] have derived an expression which predicts the relationships among the equilibrium vapor pressure, P_E; the evaporation coefficient, α; the cross-sectional area of the effusion cell, A, and its Clausing factor, W_A; the orifice area of the cell, B, and its Clausing factor, W_B; and the Knudsen effusion pressure, P_K, that is measured in an experiment. A refinement by Rosenblatt[21] accounts for the effective vaporization area of porous powder, A', which he defined as the area of plane sample surface which would give rise to the same gross rate of vaporization as the powder. The refined equation is

$$P_E = P_K \left[1 + \frac{BW_B}{A} \left(\frac{A}{A'\alpha} + \frac{1}{W_A} - 2 \right) \right] ; \qquad (5)$$

it assumes that the evaporation coefficient and condensation coefficient are equal.

The equation was derived by considering a mass balance at steady state in an effusion cell such as the one known in Fig. 38. A simplified derivation showing the important features of the equation can be made by neglecting the cell Clausing factor and using the reference plane shown in Fig. 38; in this case the upward flux, u, and the downward flux, d, are independent of the positioning of the reference plane.

At steady state the flow through the orifice in moles per unit time must be equal to the net flow across the reference plane,

$$W_B Bu = \frac{\alpha A' P_E}{G} - \alpha A' d \qquad (6)$$

where G is the factor $(2\pi MRT)^{1/2}$ in the Hertz-Langmuir-Knudsen equation.[15-20]

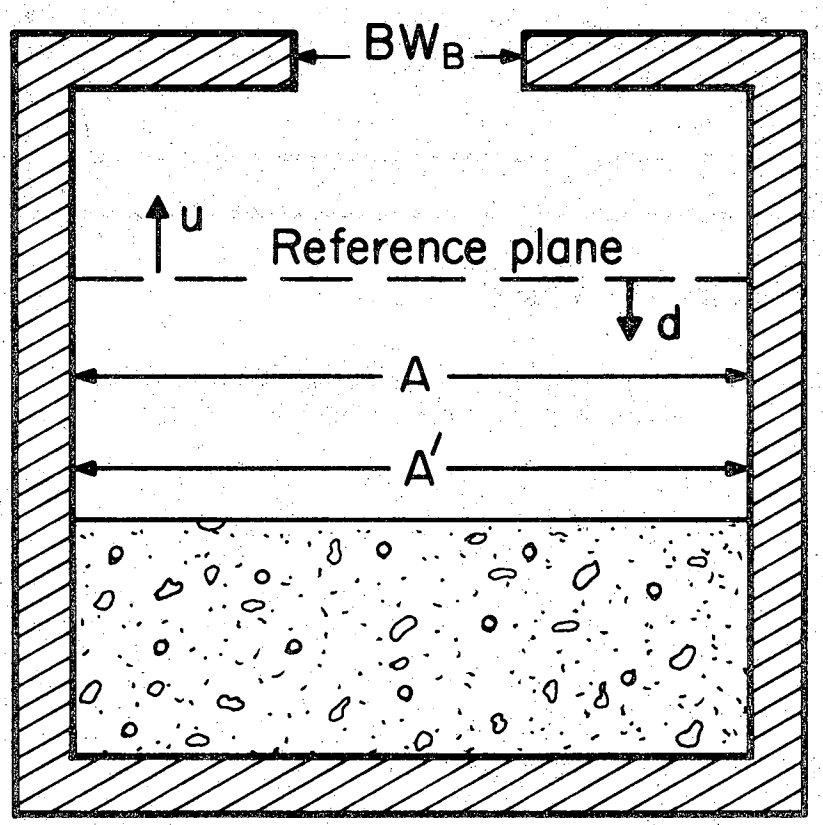

Fig. 38 Knudsen effusion cell, A' represents the effective vaporization area of the porous powder.

The downward flow can be written

$$Ad = Au - W_B Bu \tag{7}$$

and from the Hertz-Langmuir-Knudsen equation the upward flux, u, can be expressed as

$$u = \frac{P_K}{G} \tag{8}$$

By using Eq. (7) and (8), d and u in Eq. (6) can be eliminated with the results:

$$\alpha A' P_E = P_K \left[W_B B + \alpha A' \left(1 - \frac{W_B B}{A} \right) \right] , \tag{9}$$

which can be reduced to

$$P_E = P_K \left[1 + \frac{W_B B}{A} \left(\frac{A}{\alpha A'} - 1 \right) \right] . \tag{10}$$

It is seen that Eqs. (5) and (10) differ in the content of the parenthetical factor; however, for most Knudsen effusion experiments this factor reduces to $\frac{A}{\alpha A'}$ and the equations can be written

$$P_E = P_K \left(1 + \frac{W_B B}{\alpha A'} \right) \tag{11}$$

This is the case because $\frac{W_B B}{A}$ is usually less than 10^{-2} which requires that the parenthetical factor have a value of greater than 10 before a detectable difference--10%--arises between P_E and P_K; thus, in Eq. (10) omission of the 1 in the parenthetical factor causes a small error. In the more accurate Eq. (5), when $(\frac{1}{W_A} - 2)$ is omitted there is much less error since $\frac{1}{W_A}$ is about 2 for most effusion cells and the term is reduced to nearly zero.

Since the equilibrium vapor pressure, P_E, for magnesium nitride was

known and the Knudsen pressures, P_K, measured in this work were reliable (as evidenced by the good agreement of our vapor pressure measurements on silver with the values of other workers), the explanation for the discrepancies in magnesium nitride vapor pressures must be related to the term $W_B B/\alpha A'$ in Eq. (11).

One possible explanation is that $W_B B$ the reduced orifice area used in Eq. (11) is incorrect. To explain the drop in measured vapor pressure with time would require that the orifice be diminished in area by a factor of about 4 (see Fig. 11) as the experiment progressed; this was not observed, thus a mechanism of this type is unlikely.

The discrepancies in magnesium nitride vaporization would appear by process of elimination to be related to the evaporation coefficient, α, and the effective vaporization area, A', in Eq. (11). These factors could cause the drop in vapor pressure with time by reducing the flux of vapor from the powder. This could be accomplished by having a diminishing amount of the surface area exposed and liable to vaporization or by having a diffusion barrier that grows thicker with time and thereby reduces the flux from the powder.

B. Vaporization of Magnesium Nitride

1. Motzfeldt-Whitman Extrapolation

It was seen in the Introduction that the measured vapor pressure of magnesium nitride was much lower--a factor of 3.5 for Sthapitanonda[1] and a factor of 100 for Hildenbrand and Theard[2] at 1180K from Fig. 1--than the equilibrium vapor pressure. This by itself is not unusual; Blank[3] has observed lower than equilibrium Knudsen pressures for aluminum nitride, as have Hoenig and Searcy[53] for beryllium nitride, Coyle[50] for

cadmium oxide, and Hildenbrand and Hall[51] for aluminum nitride and boron nitride. However, in all of these studies the Motzfeldt-Whitman extrapolation technique[22,51,52] was used to find the equilibrium pressure while for magnesium nitride it failed to give equilibrium pressures. The technique uses Eq. (11) in the form

$$\frac{1}{P_K} = \frac{1}{P_E} + \frac{W_B B}{P_E \alpha A'} \quad ; \tag{12}$$

the vapor pressure is then measured for several orifice sizes taking care that the amount of material in the effusion cell is the same for each experiment. Plotting $1/P_K$ versus $W_B B$ and extrapolating the curve to zero orifice area then gives $1/P_E$.

Hildenbrand and Theard[2] used this technique for their magnesium nitride data and obtained an extrapolation that was a factor of 30 below the equilibrium pressure at 1110K. To understand the reason for this failure of the Motzfeldt-Whitman extrapolation, Figs. 39 and 40 were prepared. These figures present reciprocal pressures versus orifice area data at constant weight loss of magnesium nitride from the effusion cell. The pressure versus time data in Section III-C were numerically intergrated[54] and treated by the Hertz-Langmuir-Knudsen equation[15-20] to give the weight loss of nitride as a function of time. The vapor pressures at weight losses of 5 mg, 10 mg, etc., are presented in the figures.

All of the experiments were made with 5.4 grams of Metal Hydrides magnesium nitride in a "B" effusion cell and to assure the uniformity of each sample, all of the material was seperated by the particulate

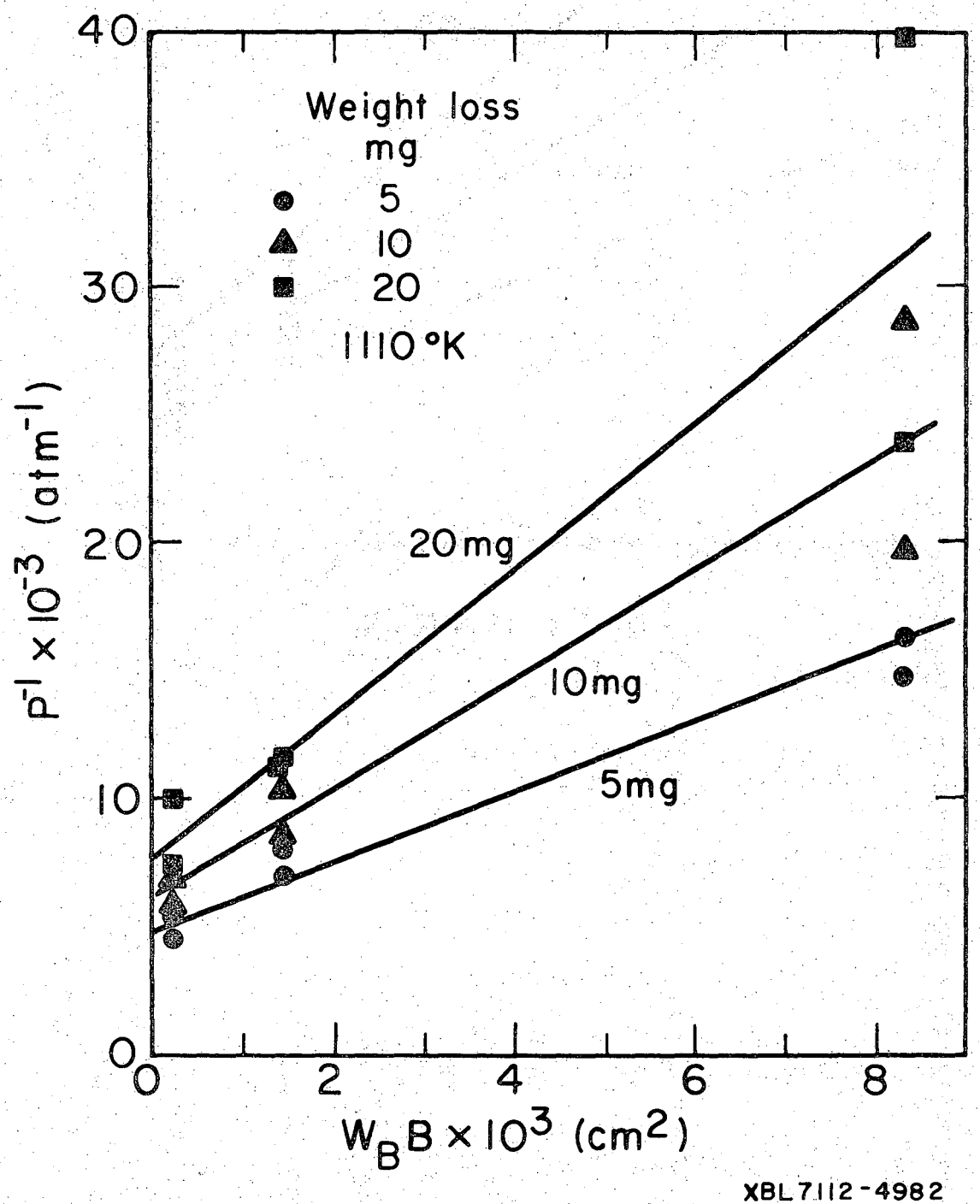

Fig. 39 Motzfeldt-Whitman extrapolation at constant weight loss for runs T1, T2, T5, T6, T7, and T8 at 1110K.

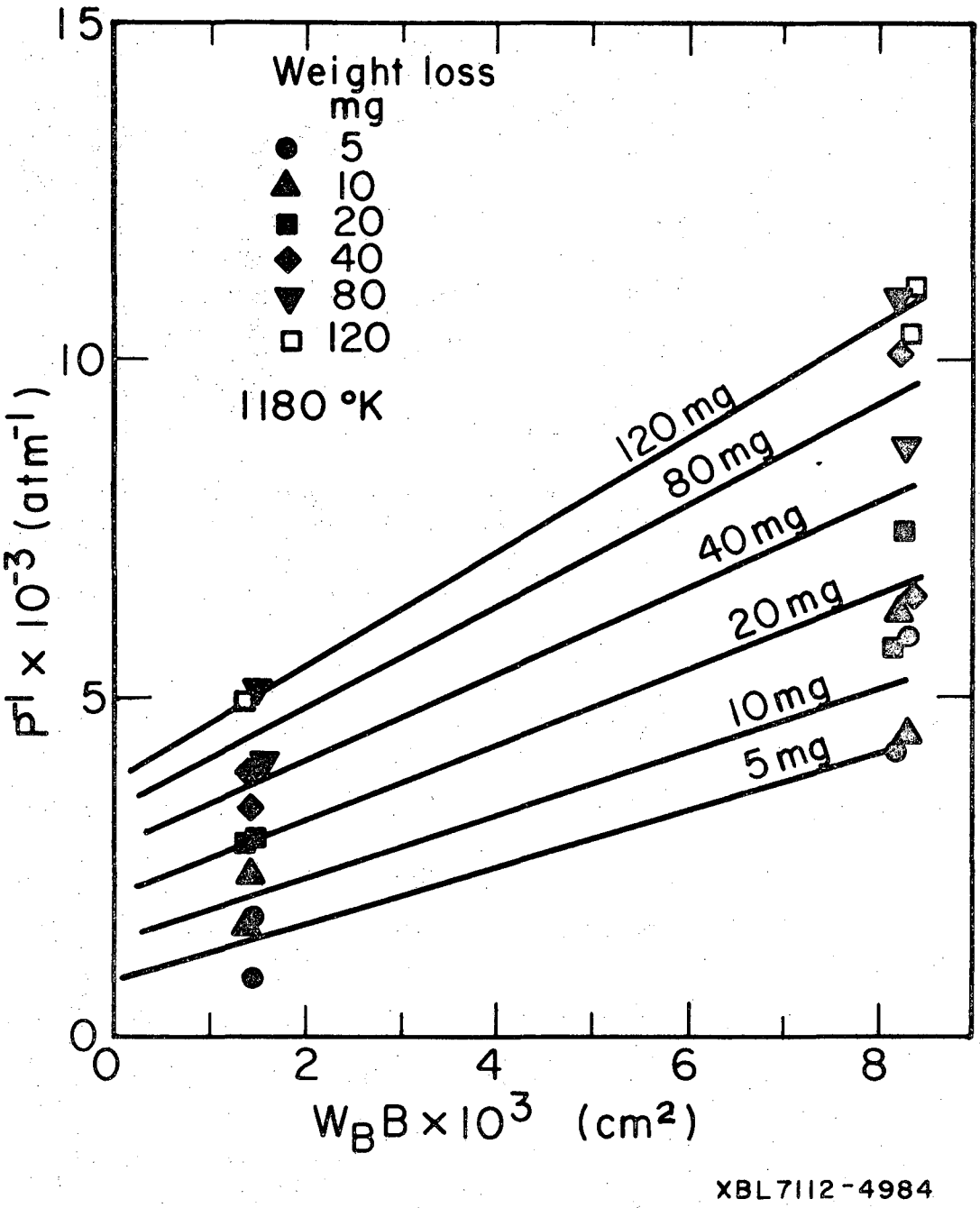

Fig. 40 Motzfeldt-Whitman extrapolation at constant weight loss for runs T11, T12, T13 and T14 at 1180K.

material sampler shown in Fig. 9.

It is seen in both figures that the reciprocal of the apparent equilibrium pressure, which from Eq. (12) is given by the intercept at zero orifice area, increased (the pressure lower) for larger weight losses. From this fact it would appear likely that Hildenbrand and Theard extrapolated under conditions of large weight loss and under conditions in which the weight losses for the different orifice areas were approximately equal. The fact that they failed to observe the time dependency of the Knudsen pressures (reported in Section III-C) also indicated that large weight losses had occurred when they took their data since the slowly changing part of the pressure-time curve occurs after large weight losses.

Another feature of magnesium nitride vaporization that is seen in these figures (also in the pressure-time curves in Figs. 11-18) is the increase in $1/P_K$ with an increase in weight loss. This increase must be more for smaller orifice areas (at constant weight loss) to cause the extrapolation to progressively move away from the equilibrium pressure.

These results indicated that because the pressure changed with time there was no unique Motzfeldt-Whitman extrapolation. To obtain a valid extrapolation one must know the cause of the decrease in $\alpha A'$ with time and must make extrapolations at constant $\alpha A'$ as required for this use of Eq. (12). Except when measurements are made at very short times, after vaporization becomes significant an extrapolation fails because the value of $\alpha A'$ varies with orifice area as well as with weight loss.

2. Scatter in Previous Vapor Pressure Measurements

Examination of Fig. 1--the vapor pressure measurements in previous studies of magnesium nitride--shows Knudsen pressures ranging over a factor of 30 at 1180K. In our study Knudsen pressures ranged over a factor of 170 at 1180K depending on the ratio of the orifice area to the surface area of magnesium nitride and on the time of vaporization (see Section III-D). Since previous measurements were made after relatively long times of heating when the variation with time was relatively low, the wide scatter in the data was primarily a consequence of differences in the amounts of nitride and to differences in the specific surface area of the magnesium nitride (i.e., in Fig. 17 it was seen that the magnesium nitride prepared in this laboratory had a lower vapor pressure than expected because of its low specific surface area).

3. Equilibrium Vapor Pressure of Magnesium Nitride

In Fig. 2 Sthapitanonda's[1] measurements of the vapor pressure of magnesium nitride by the transpiration technique showed values near the upper error limit of the calculated equilibrium pressure. He expressed uncertainty about the reliability of the data, however, because of a reaction between the oxygen impurity in the nitrogen flow gas and the magnesium vapor. This would give high pressure measurements, however, the pressures are probably correct within a factor of three and they indicate that equilibrium is near the upper error limit of the pressures calculated from thermochemical data.

There were several indications in the present experiments that the equilibrium vapor pressure was near the upper error limit; these are shown in Fig. 41. The peak in the pressure versus time curves for the

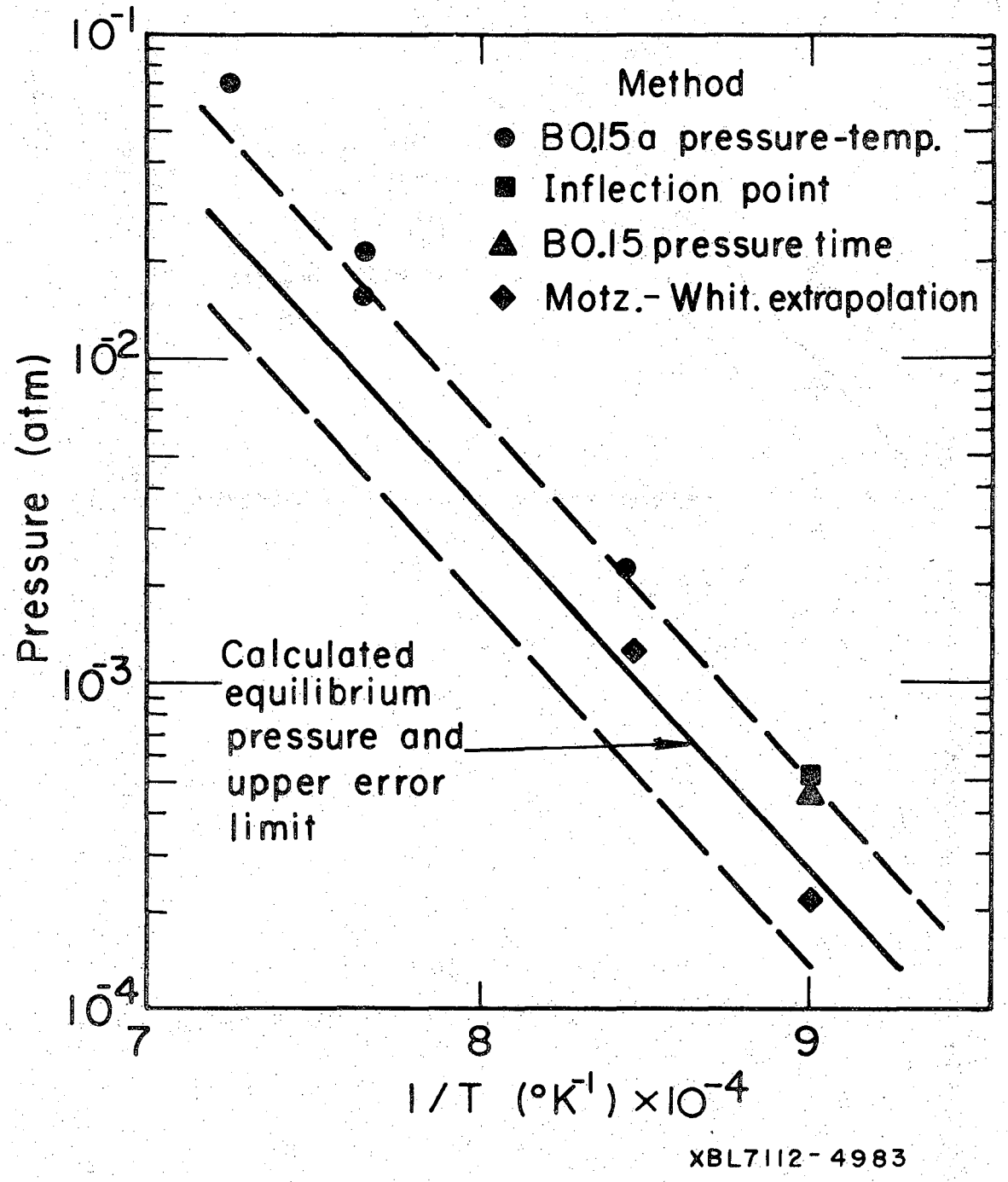

Fig. 41 Data points giving an indication that the equilibrium vapor pressure is near the upper error limit of the calculated value.

B0.15 effusion cells--these runs had the largest charge ratios, see Figs. 11 and 12--indicated that the equilibrium vapor pressure was above 4.5×10^{-4} atm at 1110K.

The results of the pressure versus temperature experiments in the B0.15a effusion cell and in the B0.25 effusion cell (see Fig. 25) gave several points that appeared to be close to equilibrium. The points at 1/T of 8.45×10^{-4} K^{-1} and 7.65×10^{-4} K^{-1} were taken with $\lambda/D > 1$; the point at 7.25×10^{-4} K^{-1} was in the hydrodynamical flow range[41] and was corrected by using Carlson's[62,63] factor of two for the apparent difference in pressure for change from molecular flow to hydrodynamical flow.

The Motzfeldt-Whitman extrapolations at 1110K and 1180K for a 5 mg weight loss provided a lower limit to the equilibrium vapor pressure; these points are shown in the figure. Another indication of the equilibrium vapor pressure was obtained from Fig. 20; in this experiment a B0.15 effusion cell was heated to 1390K to establish equilibrium conditions in the cell and the drop in pressure was monitored as the temperature was abruptly brought to 1110K. An inflection point in the pressure drop curve was seen at a pressure of 5.2×10^{-4} atm. This was taken to be a leveling off in the curve at the equilibrium pressure before the pressure continued to drop.

All of these data points suggest that the equilibrium pressure is near the upper error limit of the calculated pressure. Assuming that Mitchell's data for the enthalpy of formation of magnesium nitride[5] and that the data of Hultgren, et al.[13] for the enthalpy of vaporization of magnesium are correct, and that the entropy for magnesium vapor from Hultgren, et al.[13] and for nitrogen from Stull and Sinke[14] are correct

leaves the entropy of magnesium nitride to be adjusted in accounting for the difference in the calculated pressures and the observed pressures. Mitchell estimated a value of 22.4 eu for the entropy of magnesium nitride at 298K and the JANAF tables[55] list a value of 21 eu. The position of the measured vapor pressures in Fig. 41 near the upper error limit indicate a value of 17.5 eu for the entropy of magnesium nitride at 298K.

4. Temperature Dependency of the Vapor Pressure

The temperature dependency of the vapor pressure is commonly used to determine the enthalpy of vaporization for a compound;[29,30] however, for magnesium nitride the enthalpy calculated from the slope was 354 kcal/mole in Fig. 23 as opposed to the correct value of 210 kcal/mole at 1100K. The correct value is well established; it was calculated by summing the enthalpy of formation of magnesium nitride[4-10] and the enthalpy of vaporization of magnesium.[13] Another striking feature of the magnesium nitride temperature dependency was seen in Fig. 22 where the slope increased from 211 kcal/mole to 321 kcal/mole as the vaporization progressed.

This behavior suggests that a diffusion barrier was present on the surface of the nitride and that the barrier increased in thickness as the experiment progressed.

C. Logarithmic Rate Law for Magnesium Nitride Vaporization

The pressure versus time results in Section III-C can be fitted with the equation

$$\frac{1}{P_K} = k_1 + k_2 \log t \qquad (13)$$

after an induction period where P_K is the Knudsen pressure, t is the time measured from the start of heating at 950K, and k_1 and k_2 are constants. Figures 42 through 44 show the results of plotting the reciprocal of the pressure versus the logarithm of the time for some of the pressure versus time data; plots for the runs not shown in the figures were also linear.

Figure 42 shows the logarithmic rate law treatment of three pressure versus time experiments at 1110K in each of which 5.4 grams of Metal Hydrides magnesium nitride was used; it was observed that the slopes of the curves increased with increasing orifice area. In Fig. 43 data at 1180K are presented where again 5.4 grams of Metal Hydrides magnesium nitride was used. These runs, too, showed a dependence on orifice area; but when the oxygen pressure was changed from 4×10^{-10} atm in run T11 to 1×10^{-7} atm in run T15 there was no significant change in the logarithmic plot.

In one experiment the vaporization was continued until the effusion cell was exausted of vapor; the result of the logarithmic rate law treatment of these data is shown in Fig. 44. Here the logrithmic law is followed until the sample is 70% vaporized; at longer times the pressure decreased much more rapidly, probably because changes in particle surface area with time were then large enough to have significant influence on the total flux.

The results of the logarithmic rate law treatment for other pressure versus time experiments are presented in Table IX. Most of the experiments presented in the table were made in "B" effusion cell containing 5.4 grams of Metal Hydrides magnesium nitride. Some of the experiments, T3, T16

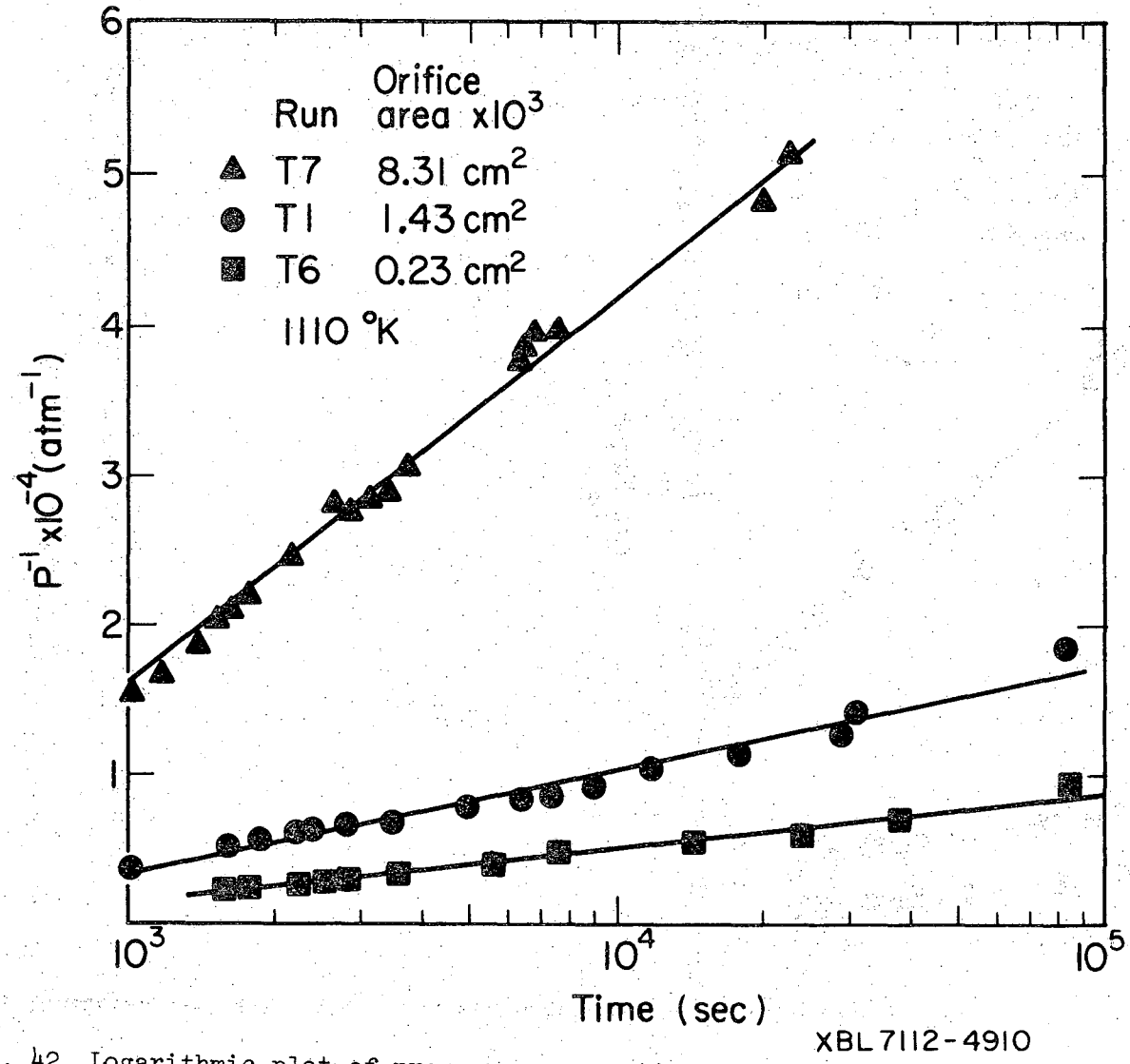

Fig. 42 Logarithmic plot of pressure versus time data at 1110K for three different orifice areas. All cells contained 5.4 grams of Metal Hydrides magnesium nitride.

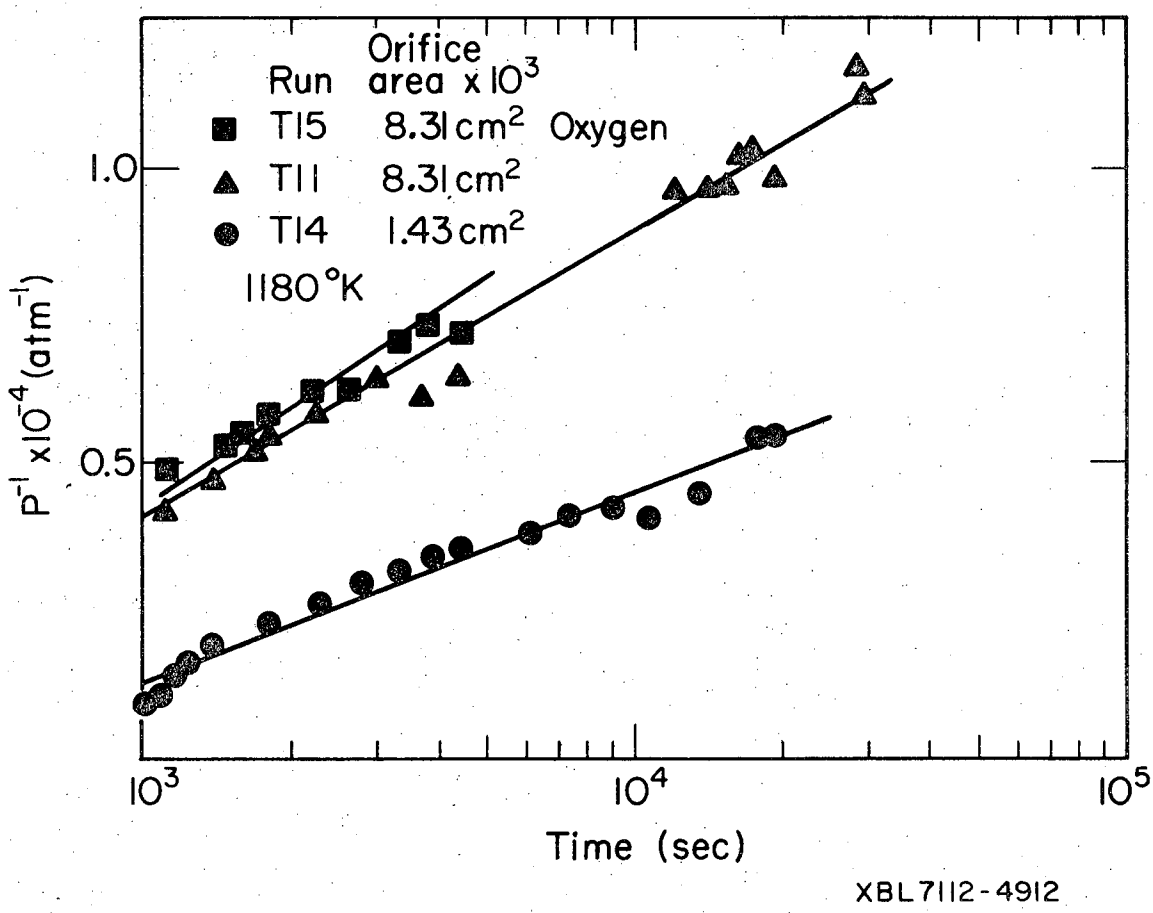

Fig. 43 Logarithmic plot of pressure versus time data at 1180K for two different orifice areas; all cell contained 5.4 grams of Metal Hydrides magnesium nitride and run T15 was made under 1×10^{-7} atm pressure of oxygen.

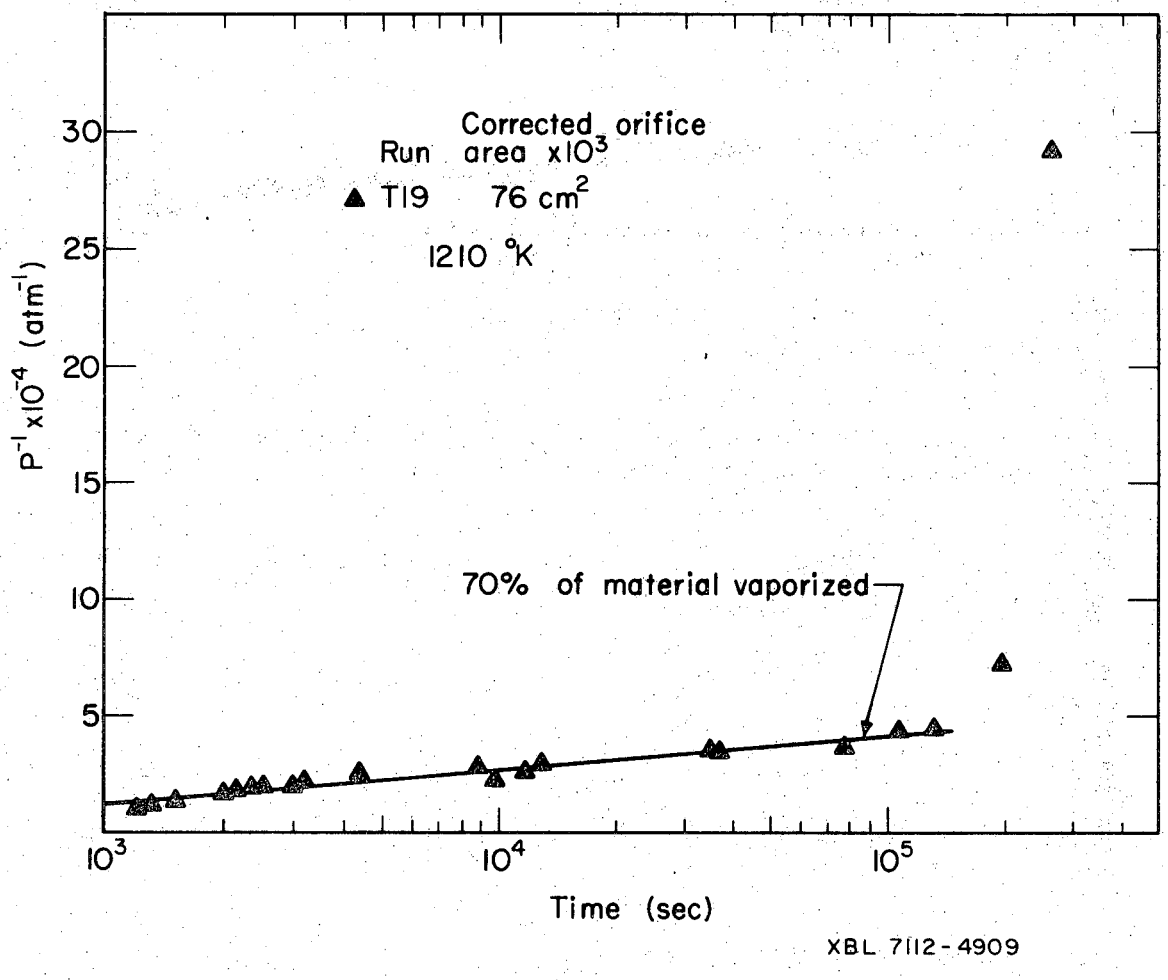

Fig. 44 Logarithmic plot of pressure versus time data at 1210K showing change in rate law after 70% vaporization.

Table IX. Results of the logarithmic rate law treatment of magnesium nitride vaporization.

Run No.	Temp. °K	Eff. Orif. Area $cm^2 \times 10^{-3}$	Charge gm	Corr. Orif. Area* $cm^2 \times 10^3$	k_2 atm^{-1}
T1	1110	1.43	5.29	EOA†	0.69
T2	1110	1.43	5.36	EOA	0.58
T3	1110	1.32	1.4	5.3	1.72
T4	1110	1.43	5.5	EOA	1.66
T5	1110	0.23	5.21		0.27
T6	1110	0.23	5.40		0.36
T7	1110	8.3	5.40		1.75
T8	1110	8.31	5.50		2.59
T9	1150	8.31	5.76	EOA	0.47
T10	1150	0.59	5.5	EOA	0.333
T11	1180	8.31	4.75	EOA	0.48
T12	1180	1.43	5.43	EOA	0.18
T13	1180	8.31	5.55	EOA	0.51
T14	1180	1.43	5.68	EOA	0.32
T15	1180	8.31	5.40	EOA	0.56
T16	1180	39	0.56	390	6.83
T17	1180	0.34	8.33	0.22	0.048
T18	1210	1.32	1.27	5.3	0.27
T19	1210	7.6	0.56	76	1.42
T20	1210	0.59	6.0**	17.7	0.52
T21	1210	39	0.56	390	1.31

*Using 5.4 gm of Metal Hydrides magnesium as a reference.

**Magnesium nitride prepared in this laboratory having 0.03 times the specific surface area of Metal Hydrides material.

†Same as effective orifice area.

through T19, and T21 contained a different amount of nitride and were conducted in "B", "C", and "A" effusion cells, and experiment T20 was made in a "B" cell using the magnesium nitride prepared in this laboratory. In order to normalize the different experiments for comparison one must decide whether the cell cross sectional area or the total surface area is important for replenishing the vapor that escapes through the orifice.

When the evaporation coefficient is unity the cross sectional area of the effusion cell is the important parameter; but when the evaporation coefficient is sufficiently low, the total surface area of the powder can contribute to replenishing the flux that is lost through the orifice. In the systems ZnO[56] and CdO[50] the evaporation coefficient was about 10^{-2} and the cell sectional area appeared to limit the flux from the powder; however, for magnesium nitride, which has a lower evaporation coefficient, the total surface area of the powder appears to be the limiting factor. This is indicated by the behavior seen in Fig. 17 where the cell having the larger cell cross sectional area exhibited the same Knudsen pressure as a sample of higher specific surface area in a cell of lesser cross sectional area.

Thus to compare experiments in which different amounts of magnesium nitride were used, one can use Eq. (11) to see that an increase in the effective vaporizing area, A', which is proportional to the charge in grams, is equivalent to a decrease in the orifice area. The equation

$$A_C = A_E \frac{M}{5.4} \tag{14}$$

places all experiments on the normalized basis of comparison, where A_C is the corrected orifice area, A_E is the effective orifice area, and M is the mass of magnesium nitride used--variations of less than 15% from

the 5.4 grams were ignored. For run T20 the corrected orifice area was increased by a factor of 30 to account for the difference in specific surface area of powder from Metal Hydrides and from this laboratory.

D. Model and Activation Enthalpy for Magnesium Nitride Vaporization

There were three stages in the vaporization of magnesium nitride from an effusion cell: 1) the pressure rose to a maximum at a rate that lagged behind temperature equilibration; 2) the pressure decreased according to a logarithmic law; and 3) after 70% vaporization the pressure decreased more rapidly than the prediction of the logarithmic law.

The measurements with the mass filter proved that the maximum is not a degassing of impurities, as has probably been assumed by all previous investigators. The first stage is thought to be associated with the rupturing of a protective film of magnesium oxide on the particles. A film was observed microscopically on the Langmuir samples (see Fig. 27, 31, and 32) and during the Langmuir measurements the vapor pressure was observed to rise in abrupt steps suggestive of the stages in the rupture and pealing back of the film. For the Knudsen experiments there were no abrupt steps during the rise in pressure, but none would be expected because the large number of particles in the powder should cause a smoothing of the rupturing process. The third stage in the vaporization of magnesium nitride is thought to be associated with a decrease in the surface area of magnesium nitride particles since this stage started after 70% of the powder has vaporized. The second stage which obeys the empirical rate law in Eq. (13) is of most interest here.

The logrithmic law for this stage, Eq. (13), can be derived by assuming that vaporization is limited by a growing diffusion barrier

(see Fig. 45). At a given time, the mass flow in moles per unit time through the orifice is equal to the mass flow through the diffusion barrier; this mass balance can be written

$$J_1 A = J_2 B W_B \tag{15}$$

where J_1 is the flux through the diffusion barrier, J_2 is the flux at the inside of the orifice, B is the orifice area, and W_B is the orifice Clausing factor.

An expression for the flux through the diffusion barrier can be obtained from Ficks' first law of diffusion.[57] The concentration gradient in the equation is calculated from the difference between the equilibrium pressure, P_E, which characterizes the activity of Mg or N_2 at the magnesium nitride side of the duffusion barrier, and the Knudsen pressure, P_K, which characterizes the activity on the vapor side, divided by the thickness, L, of the barrier; this is written

$$J_1 = D \frac{P_E - P_K}{L} \tag{16}$$

where D is the diffusion coefficient. It is assumed that L is independent of the mass loss through the diffusion barrier, and that the rate of increase of L is small compared to the velocity of diffusion through the layer.[58,59] The flux of Mg(g) or N_2(g) through the orifice is given by the Hertz-Langmuir-Knudsen equation

$$J_2 = P_K G^{-1} \tag{17}$$

where G is the factor $(2\pi MRT)^{1/2}$; M is the molecular weight, R is the gas constant, and T is the absolute temperature.

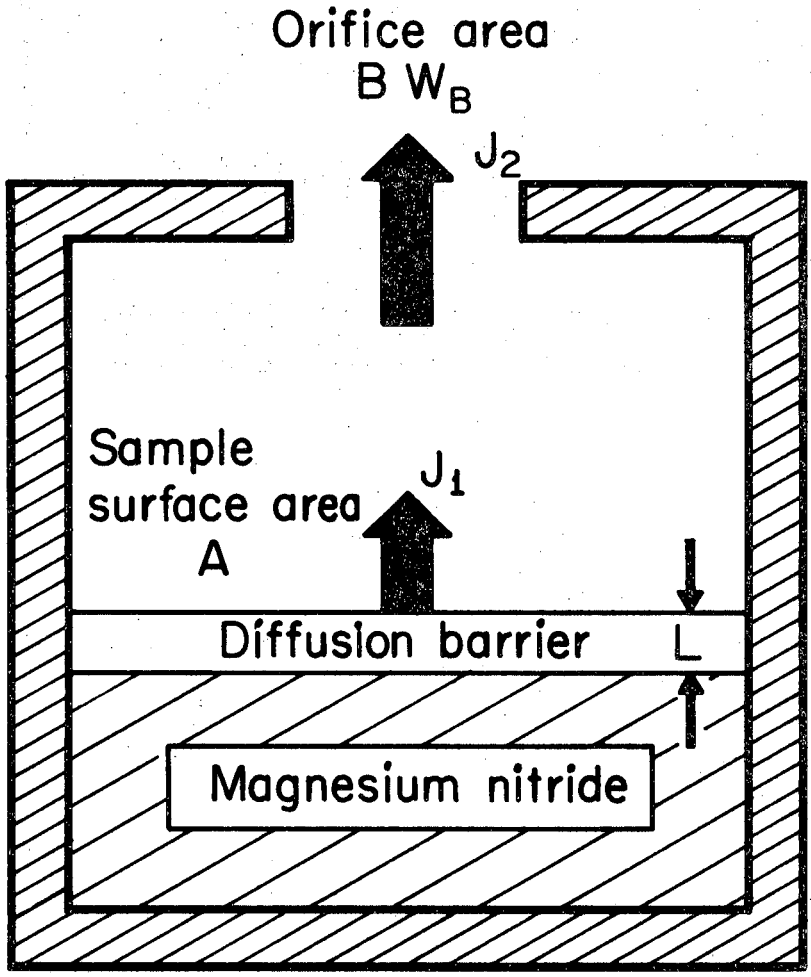

XBL7112-4906

Fig. 45 Model for Knudsen effusion experiment where the vaporization of magnesium nitride is inhibited by a diffusion barrier.

Substituting Eqs (16) and (17) into (15)

$$\left(\frac{P_K}{G}\right)\frac{BW_B}{A} = D\,\frac{P_E - P_K}{L} \tag{18}$$

which can be written

$$\frac{1}{P_K} = \frac{1}{P_E} + \frac{BL}{P_E GAD} \tag{19}$$

For a logarithmic growth of the barrier layer the thickness can be written[60]

$$L = k_L \,\mathrm{Log}\,(1 + t/t_o) \tag{20}$$

substituting this into (19) gives

$$\frac{1}{P_K} = \frac{1}{P_E} + \left(\frac{BW_B}{GA}\right)\left(\frac{k_L}{P_E D}\right)\mathrm{Log}\,[1 + t/t_o] \tag{21}$$

Thus if a mechanism of this type is correct for magnesium nitride k_1 in Eq. (13) would be associated with the reciprocal of the equilibrium pressure and k_2 in that equation would be associated with the two parenthesized factors in Eq. (21). The data in Figs. 42 through 44 were plotted using t instead of $(1 + t/t_o)$ in Eq. (21); this would indicate that t_o is small compared to t. Also, the intercept was not $1/P_E$ as predicted by Eq. (21), but this is not unexpected since the first stage of vaporization was dominated by the rupturing of magnesium oxide films.

By comparing Eq. (13) and Eq. (21)

$$k_2 = \frac{BW_B}{GA}\left(\frac{k_L}{P_E D}\right) \tag{22}$$

where the parenthesized factors are the ones with strong temperature dependence. These terms can be written[20]

$$\frac{k_L}{P_E D} = \frac{A_L}{A_E A_D} \exp\left[\frac{-\left(\Delta H_L^{\ddagger} - \frac{\Delta H_V^{\circ}}{4} - \Delta H_D^{\ddagger}\right)}{RT}\right] \qquad (23)$$

where the A's are the pre-exponential terms for the respective rate constants and the ΔH's are the activation enthalpies.

The slope of a plot of the logarithm of the constant k_2 versus the reciprocal temperature thus should give the combination of these three enthalpy terms. To make a plot of this sort, the data in Table IX was used in Fig. 46 (the datum points for runs T16, T19, and T21 were moved to fit on the graph by dividing k_2 and the corrected orifice area by a common factor). The curves for the four temperatures were drawn through the origin as required by Eq. (22).

Data at a constant orifice area of 10^{-2} cm^2 was then taken from this figure and used in Fig. 47 to evaluate the enthalpy terms in Eq. (23); an enthalpy of activation of 90 kcal/mole was obtained. The equilibrium enthalpy of vaporization at these 1100K was 210 kcal/mole of solid; when this was combined with the other enthalpy terms in Eq. (23) one can calculate for $\Delta H_L^{\ddagger} - \Delta H_D^{\ddagger}$ a value of 37.5 kcal/mole. This is the activation enthalpy per mole of vapor for forming the film and for diffusion through it.

E. Mechanism of Magnesium Nitride Vaporization

Owing to the presence of magnesium oxide in the magnesium nitride as seen in Table IV and to the magnesium oxide film seen on the Langmuir samples, it is plausible to consider the possibility that a magnesium oxide protective layer is formed again at high temperature. The most obvious path for reforming this layer is by reaction of magnesium vapor with the residual water vapor or oxygen in the system--in keeping with

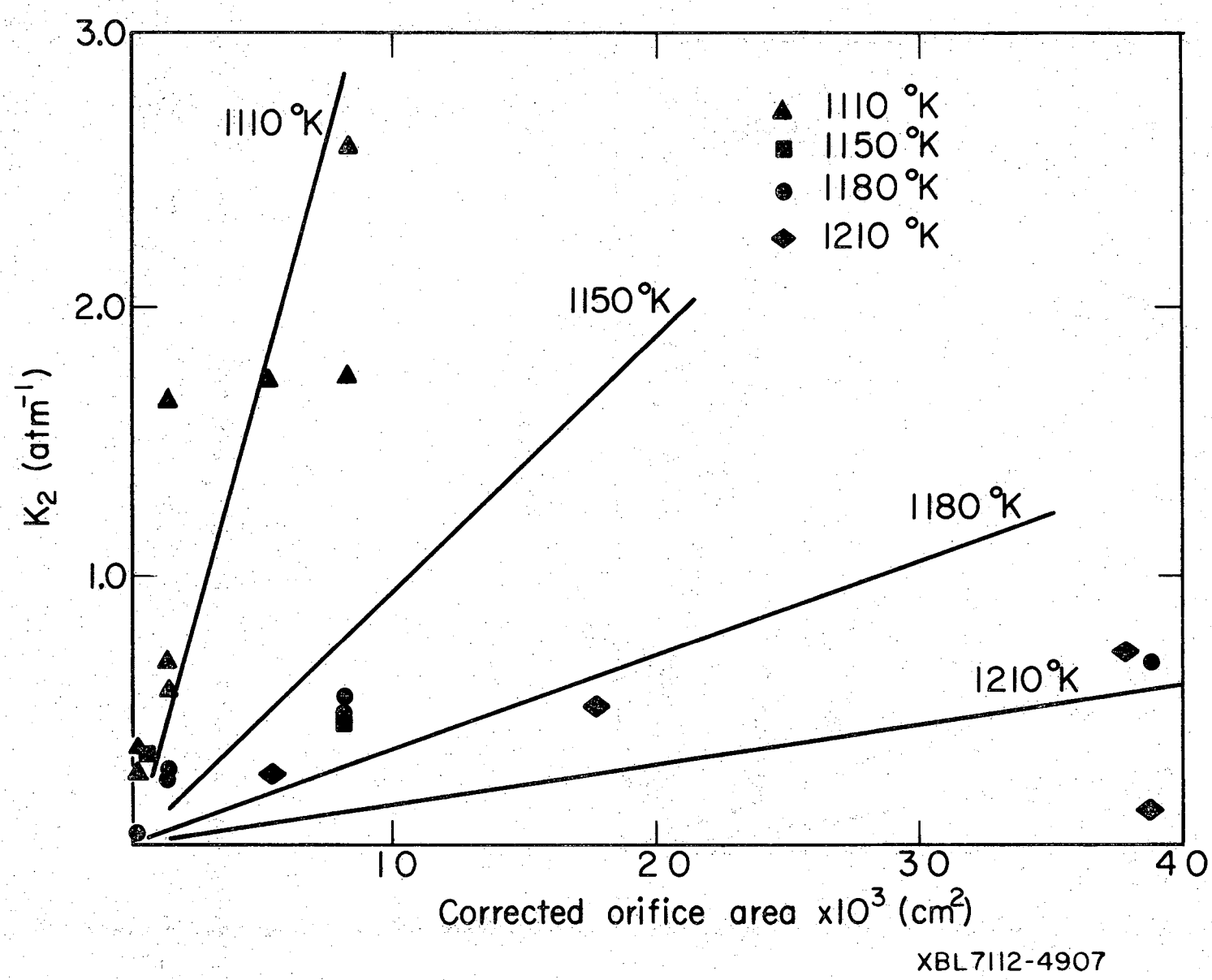

Fig. 46. Slope from logarithmic rate law versus orifice area for magnesium nitride Knudsen experiments.

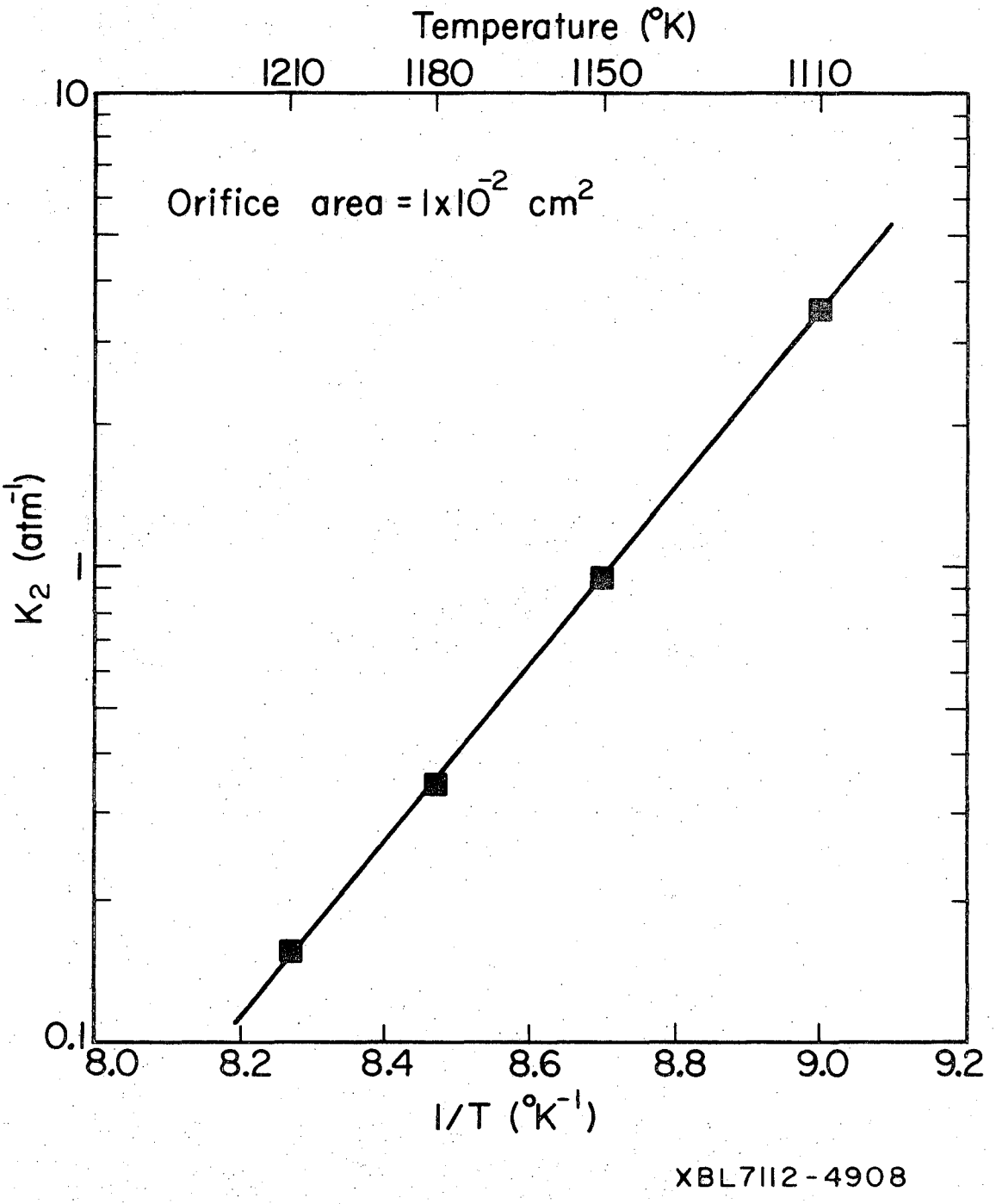

Fig. 47 Activation energy for logrithmic rate law vaporization of magnesium nitride.

the assumptions of the model the layer build-up would then be independent of weight loss. The layer would probably be relatively insensitive to temperature, but strongly dependent on the background gas pressure.

The fact that the increase of nearly three orders of magnitude in the oxygen pressure (see Fig. 43) has no influence on the slope of the logarithmic plot argues that a magnesium oxide layer reformed in this way is not responsible for the time and temperature dependent decrease in vaporization rates. Furthermore, the magnesium partial pressure was always greater than 1×10^{-5} atm in the pressure versus time experiments in Section III-C while the oxygen pressure was always less than 1×10^{-7} atm--for all except one experiment less than 10×10^{-10} atm. As a consequence it would be expected that if the availability of oxygen were rate limiting a linear time dependency would result. Because many more magnesium atoms escaped than were needed to react with all of the available oxygen, the rate of formation of the magnesium oxide layer would be proportional to the oxygen pressure and independent of time. The expression $L = k_{LIN}\, t$, were k_{LIN} is the linear rate constant, would replace Eq. (20), and Eq. (13) would become $1/P_K = k_3 + k_4 t$; however, this equation did not fit the data. Thus, it is unlikely that the barrier layer would form by this mechanism.

It is also plausible to consider the possibility that a magnesium oxide protective layer is formed by dissolution of small amounts of magnesium oxide from the mangesium nitride lattice as the vaporization proceeds (Section III-A admitted the possibility of up to 1% of dissolved magnesium oxide). The thickness of the layer would be proportional to the weight loss of the nitride; this violates one of the assumptions in

deriving the model and precludes its use in this case. However, one can reason that the layer thickness is proportional to the area under the pressure versus time curve and since it has been shown that the Knudsen pressure is nearly constant at times greater than 400 minutes, one can conclude that at long times the layer thickness would increase linearly. But a linear increase in thickness was shown above to be inconsistent with the data; thus this mechanism too would seem unlikely.

A dissolution mechanism in which the oxide protective layer is prevented from growing beyond a given thickness by a transformation to a porous product is consistent with the data. This has been observed by Beruto and Searcy[61] for $CaCO_3$ vaporization. The mechanism might also be associated with the intrinsic behavior of magnesium nitride (i.e. a competition between adjustment of the stoichiometry by diffusion into a particle and removal of magnesium vapor and nitrogen from the surface of a particle, both proceeding at approximately the same rate and causing a drop in the evaporation coefficient).

ACKNOWLEDGEMENTS

I thank Prof. Alan W. Searcy for his guidance in this work and for his interest in me both professionally and personally. I am indebted to Dr. David Meschi for opening many new worlds to me through his fine library and through his knowledge on many subjects. I also thank my fellow students, especially those in Prof. Searcy's group for stimulating discussions on many topics and for sharing their experiences and insights.

I salute the staff of IMRD and of the Lawrence Berkeley Laboratory for their outstanding support throughout this work. Special thanks go to Emery Kozak for his help with the quadrapole mass filter and the effusion cells, to Dick Holroyd for his help in assembling the torsion effusion furnace, and to Jean Wolslegel for her tireless work in preparing the manuscript.

I deeply appreciate my wife, Judith, for her love, for her encouragement, and for her help in many ways.

This work was done under the auspices of the U. S. Atomic Energy Commission.

APPENDIX A. DETERMINATION OF THE EFFECTIVE PORE AREA

The effective pore area for a B cell was calculated from the weight loss of the cell with no orifice by using the Hertz-Knudsen equation. Metal Hydrides magnesium nitride (5.1860 grams from the particlate material sampler) was outgassed at 690K for 180 minutes and 920K for 260 minutes before heating to 1110K for 280 minutes where a loss of 4.2 milligrams was measured. The weight loss from the graphite crucible under these conditions was 2.0 micrograms per minute; thus, 0.6 milligrams was subtracted and a net of 3.6 milligrams was determined for the weight loss of nitride. Assuming that the pressure in a cell with no orifice was equal to that in a B0.15 cell* an average pressure of 2.3×10^{-4} atm was determined for the 280 minute interval and the effective pore area calculated from these data was 1.4×10^{-4} cm^2. This parameter can also be calculated by measuring the weight loss of a cell with an orifice and calculating--from the measured pressures and the orifice area--the expected weight loss. The average weight loss measured for three B1.0 cells and two B0.5 cells at 1180K were respectively 1.9% and 8.9% greater than the calculated weight loss.** Using these precentages with the reduced orifice areas for these cells in Table III, the effective pore area is calculated to be 1.2×10^{-4} cm^2 for the B0.5 cell and 1.65×10^{-4} cm^2 for the B1.0 cell. Thus, for the "B" cells the effective pore area

---

*The calculated weight loss through the orifice--see next footnote--for a B0.15 cell for 280 minutes at 1110K is 2.4 milligrams compared to a 3.6 milligram loss for a closed cell. Thus, the effective orifice area of the B0.15 cell is only 40% greater and the two cells have nearly the same pressure.

**The weight loss through the orifice is calculated by using the Hertz-Knudsen equation for each point in the pressure vs time curve--Figs. 11 through 18--to calculate the mass loss rate and numerically integrating to determine the mass loss.

is probably within 20% of 1.4×10^{-4} cm^2. For the C0.5 and D0.25 effusion cells the same value is used in the absence of experimental data; this estimate was probably good for the C cell since it was made of graphite but may be in error for the D cell which was made of nickel. For the A cells, weight loss experiments were made at 1180K for 1300 minutes and effusion pressures were calculated to be 7.8×10^{-6} atm for the A2.0 cell and 2.7×10^{-5} atm for the A1.0 cell. These pressures compare with respective torsion effusion pressures at 600 minutes--the average pressure over the 1300 minute time interval--of 1.0×10^{-5} atm and 3.0×10^{-5} atm; the good agreement indicates that the effective pore area is negligible for the A cells.

REFERENCES

1. P. Sthapitanonda, Ph. D. Thesis, University of Wisconsin (1955). J. R. Soulan, P. Sthapitanonda, and J. L. Margrave, J. Phys. Chem. 59, 132 (1955).
2. D. L. Hildenbrand and L. P. Theard, ASTIA Unclassified Report 258410 Aeroneutronic Report U-1274 (1961).
3. B. Blank and A. W. Searcy, J. Phys. Chem. 72, 2241 (1968) and B. Blank, UCRL 16018 (1965).
4. Lebedov and Nefedova, Zhur. Fiz. Khim. 32, 819 (1958).
5. D. W. Mitchell, Ind. Engr. Chem. 41, 2027 (1949).
6. E. Neuman, C. Kroger, H. Kunz, Z. Anorg. Chem. 207, 133 (1932).
7. Brunner, Z. Elektrochem. 38, 67 (1932).
8. B. Neuman, C. Kroger, and H. Haebler, Z. Anorg, Chem. 304, 90 (1932).
9. C. Matignon, Comp. Rend. 154, 1351 (1912).
10. L. Moser and R. Herzner, Monatsh 44, 115 (1923).
11. F. R. Bichowski and F. D. Rossini, The Thermochemistry of the Chemical Substances (Reinhold Publishing Corp., New York, 1936) p. 341.
12. Shun-ichi Satoh, Sci. Papers Inst. Phys. Chem Research (Tokyo) 34, No. 1, 3992 (1938).
13. R. Hultgren, R. L. Orr, P. D. Anderson and K. K. Kelley, Selected Values of Thermodynamic Properties of Metals and Alloys (John Wiley & Sons, Inc., New York, 1963) (Supplement for Mg Oct. 1966).
14. D. R. Stull and G. C. Sinke, Thermodynamic Properties of the Elements (American Chemical Society, Washington, D. C., 1956).
15. I. Langmuir, Phys. Rev. 2, 329 (1913).

16. O. Knacke and I. N. Stranski, Prog. Met. Phys. 6, 181 (1956).

17. R. C. Paule and J. L. Margrave in J. L. Margrave (Ed.), The Characterization of High Temperature Vapors, (Wiley, New York, 1967) Ch. 6.

18. H. Hertz, Ann. Phys. (Leipzig) 17, 177 (1882).

19. M. Knudsen, Ann. Phys. (Leipzig) 47, 697 (1915).

20. A. W. Searcy in A. W. Searcy, et al. (Ed.) Chemical and Mechanical Behavior of Inorganic Materials, (Wiley-Interscience, New York, 1970) Ch. 6.

21. G. M. Rosenblatt, J. Electrochem. Soc. 110, 563 (1963).

22. K. Motzfeldt, J. Phys. Chem. 59, 139 (1955).

23. C. I. Whitman, J. Chem. Phys. 20, 161 (1952).

24. D. Clausing, Ann. Physik, 12 (5), 961 (1932).

25. D. A. Schulz and A. W. Searcy, J. Chem. Phys. 36, 3099 (1962).

26. D. A. Schultz, Ph. D. Thesis, University of California, Berkeley, 1962.

27. E. Kay and N. W. Gregory, J. Phys. Chem. 62, 1079 (1958).

28. Z. A. Munir and A. W. Searcy, J. Chem. Phys. 42, 4223 (1965).

29. J. R. McGreary and R. J. Thorn, J. Chem. Phys. 50, 3725 (1969).

30. G. N. Lewis, M. Randall, K. S. Pitzer and L. Brewer, Thermodynamics, 2nd Edition (McGraw-Hill Book Company, New York, 1961).

31. P. Teilhard de Chardin, Bernard Wall, Translator, The Phenomenon of Man, (Harper and Row, Pbulishers, 1955).

32. R. D. Freeman, J. L. Margrave (Ed.), The Characterization of High Temperature Vapors, (Wiley, New York, 1967) Ch. 7.

33. M. J. Lim and A. W. Searcy, J. Phys. Chem. 70, 1762 (1966).

34. R. W. Mar and A. W. Searcy, J. Phys. Chem. 71, 888 (1967).

35. H. B. Skinner and A. W. Searcy, J. Phys. Chem. 72, 3375 (1968).

36. R. D. Freeman and A. W. Searcy, J. Chem. Phys. 22, 762 (1954).

37. R. W. Freeman, ASD-TDR-63-734, 1967.

38. American Petroleum Institute Research Project Number 44.

39. J. W. Otvos and D. P. Stevenson, J. Am. Chem. Soc. 78, 564 (1956).

40. R. I. Reed, Ion Production by Electron Impact, (Acedemic Press, New York, 1962).

41. S. Dushman and J. M. Lafferty, Scientific Foundations of Vacuum Technique, 2nd Edition, (John Wiley and Sons, Inc., New York, 1962).

42. J. V. Smith, (Ed.) X-ray Powder Data File (Inorganic), (American Society for Testing Materials, Philadelphia, 1960).

43. B. D. Cullity, Elements of X-Ray Diffraction, (Addison-Wesley, Reading, Mass., 1956), p. 39.

44. C. W. Bunn, Chemical Crystallography, 2nd Edition, (Oxford Press, London, 1961).

45. P. Debye and P. Scherrer, Phys. Z. 17, 227 (1916).

46. M. E. Straumanis and A. Ievins, Z. Phys. 98, 461 (1936).

47. R. W. Weast, Editor in Cheif, Handbook of Chemistry and Physics, 46th Ed., (Chemical Ruber Co., Cleveland, 1965).

48. R. C. Blair and Z. A. Munir, J. Phys. Chem. 72, 2434 (1968).

49. G. Lewis and C. E. Myers, J. Phys. Chem. 67, 1289 (1963).

50. R. T. Coyle, M. S. Thesis, University of Missouri (Rolla), (1967).

51. D. L. Hildenbrand and W. F. Hall in E. Rutner, et al. (Ed.), Condensation and Evaporation of Solids, (Gordon and Breach, New York, 1964).

52. C. L. Hoenig and A. W. Searcy, J. Am. Cer. Soc. 59, 460 (1967).

53. R. C. Schoonmaker, A. Buhl, and J. Lemley, J. Phys. Chem. 69, 3455 (1965).

54. P. R. Bevington, Data Reduction and Error Analysis for the Physical Sciences, (McGraw-Hill, New York, 1969).

55. JANAF Thermochemical Tables, Dow Chemical Company, USAF Contract No. AF33(616)-6149, 1969.

56. R. J. Galluzo, UCRL 20528, (1971), AEC Contract No. W-7405-eng-48.

57. P. G. Shewmon, Diffusion in Solids, (McGraw-Hill, New York, 1963).

58. D. Beruto, Private Communication.

59. J. P. Hirth in Metal Surfaces: Structure, Energetics and Kinetics, (Am. Soc. for Metals, Metals Park, Ohio, 1963) p. 204.

60. W. W. Smeltzer and M. T. Simnad, Acta Met. 5, 328 (1957).

61. D. Beruto and A. W. Searcy, to be published.

62. K. D. Carlson, J. L. Margrave (Ed.), The Characterization of High Temperature Vapors, (Wiley, New York, 1967) Ch. 5.

63. K. D. Carlson, P. W. Gilles, and R. J. Thorn, J. Chem. Phys. 38 2725 (1963).

TECHNICAL INFORMATION DIVISION
LAWRENCE BERKELEY LABORATORY
UNIVERSITY OF CALIFORNIA
BERKELEY, CALIFORNIA 94720